Scuola Dottorale in Scienze Matematiche e Fisiche

Dottorato di Ricerca in Fisica
XXIV Ciclo

NLO QCD corrections to CP-even and CP-odd Higgs boson production via gluon fusion in the MSSM

Stefano Di Vita

Docente guida: Prof. Giuseppe Degrassi

Coordinatori: Prof. Guido Altarelli, Prof. Orlando Ragnisco

A mamma, papà e Marco
per aver sempre creduto in me

Acknowledgements

This work would never have been possible without the precious support, the endless patience and the continuous encouragement of my advisor, Prof. Giuseppe Degrassi.

I also wish to thank Pietro Slavich for his collaboration and precious advice.

I am especially grateful to Prof. Vittorio Lubicz for his constant, sincere support since I started my Master's thesis.

I would also like to thank Prof. Guido Altarelli, who guided my first steps in the field of supersymmetry.

I acknowledge the financial support of Istituto Nazionale di Fisica Nucleare, which funded my Ph.D. fellowship.

Special thanks go to all my friends. To the closest ones, who I have been fortunate to share joys and troubles with, every day. To the ones scattered around the world, who are close anyway, they know it.

Finally, I would like to thank my family for their endless love, support and trust in me. To them I dedicate this work.

Contents

Introduction

With the coming into operation of the Large Hadron Collider (LHC), a new era has begun in the search for the Higgs boson(s). During the first year of collisions at $\sqrt{s} = 7\,\text{TeV}$ the LHC has performed surprisingly well. By the end of 2012 (after only two years of collisions), it is expected to deliver about 10fb^{-1} of integrated luminosity, which is comparable to that delivered by the Tevatron Run II in its operation lifetime.

The main production mechanism at hadron colliders for the Standard Model (SM) Higgs boson, H_{SM}, is the loop-induced gluon fusion mechanism [1], $gg \to H_{\text{SM}}$, where the coupling of the gluons to the Higgs is mediated by loops of colored fermions, primarily the top quark. The knowledge of this process in the SM, which depends on the only unknown SM parameter $m_{H_{\text{SM}}}$, includes the full next-to-leading order (NLO) QCD corrections [2–5], the next-to-next-to-leading order (NNLO) QCD corrections [6–11] including finite top mass effects [12–19], soft-gluon resummation effects [20], an estimate of the next-to-next-to-next-to-leading order (NNNLO) QCD effects [21, 22] and also the first-order electroweak corrections [23–29].

The Minimal Supersymmetric extension of the Standard Model (MSSM) is an attractive New Physics (NP) scenario which typically implies a rich phenomenology at energies not far above the weak scale. The Higgs sector of MSSM consists of two $SU(2)$ doublets, H_1 and H_2, whose relative contribution to electroweak symmetry breaking is determined by the ratio of vacuum expectation values of their neutral components, $\tan\beta \equiv v_2/v_1$. The spectrum of physical Higgs bosons is more complex than in the SM, consisting of two neutral CP-even bosons, h and H, one neutral CP-odd boson, A, and two charged scalars, $H^{\pm}$. The couplings of the MSSM Higgs bosons to matter fermions differ from those of the SM Higgs, and they can be considerably enhanced (or suppressed) depending on $\tan\beta$. As in the SM case, the gluon-fusion process is one of the most important production mechanisms for the neutral Higgs bosons, whose couplings to the gluons are mediated by top and bottom quarks and their supersymmetric partners, the stop and sbottom squarks.

In the case of the CP-even bosons h and H the gluon-fusion cross section in the MSSM is known at the NLO in QCD.* The contributions arising from diagrams with quarks and gluons can be obtained from the corresponding SM results with an appropriate rescaling of the Higgs-quark couplings. The contributions arising from diagrams with squarks and gluons were first computed under the approximation of vanishing Higgs mass in ref. [31].

*First results for the NNLO contributions in the limit of degenerate superparticle masses were presented in ref. [30].

The complete top/stop contributions, including the effects of stop mixing and of the two-loop diagrams involving gluinos, were computed under the same approximation in ref. [32, 33], and the result was cast in a compact analytic form in ref. [34]. Later calculations aimed at the inclusion of the full Higgs-mass dependence in the squark-gluon contributions, which are now known in a closed analytic form [35–38].

The approximation of vanishing Higgs mass in the contributions of two-loop diagrams allows for compact analytic results that can be implemented in computer codes for a fast and efficient evaluation of the Higgs production cross section. For what concerns the top-gluon contributions, the effect of such approximation on the result for the cross section has been shown [37, 39] to be limited to a few percent, as long as the Higgs mass is below the threshold for creation of the massive particles running in the diagrams (in this case, the top quarks). This is typically the case for the light Higgs h, while such situation is realized for the heavy Higgs H only in specific regions of the MSSM parameter space. Concerning the two-loop diagrams with gluinos, this approximation has been shown [34] to work well for the contribution of top, stop and gluino to h boson production, while in the case of the H boson it is somehow less reliable and, again, not feasible for general values of the MSSM parameters. No approximate computation valid in the top-pair threshold region has ever been made available so far.

The Higgs mass cannot obviously be neglected in the corresponding diagrams involving the bottom quark, where the Higgs is always above threshold and whose contribution can be relevant for large values of $\tan\beta$. For the latter diagrams the dependence on the Higgs mass should in principle be retained, which has proved a rather daunting task. A calculation of the full quark-squark-gluino contributions via a combination of analytic and numerical methods was presented in ref. [40] (see also ref. [41]), but neither explicit analytic results nor a public computer code have been made available so far. However, ref. [42] presented an evaluation of the bottom-sbottom-gluino diagrams based on an asymptotic expansion in the large supersymmetric masses that is valid up to and including terms of $\mathcal{O}(m_b^2/m_\phi^2)$, $\mathcal{O}(m_b/M)$ and $\mathcal{O}(m_Z^2/M^2)$, where m_ϕ denotes a Higgs boson mass and M denotes a generic superparticle mass. This expansion should provide a good approximation to the full result, at least comparable to the one obtained for the top-stop-gluino diagrams, as long as the Higgs boson mass is below all the heavy-particle thresholds. An independent calculation of the bottom-sbottom-gluino contributions, restricted to the limit of a degenerate superparticle mass spectrum, was also presented in ref. [43], confirming the results of ref. [42].

In the case of the CP-odd boson A the calculation of the production cross section is somewhat less advanced. Due to the structure of the A-boson coupling to squarks, only loops of top and bottom quarks contribute to the cross section at LO, with the bottom loops being dominant for even moderately large values of $\tan\beta$. In the limit of vanishing A-boson mass, m_A, the contributions from diagrams with quarks and gluons were computed at NLO in ref. [44, 45] and at NNLO in ref. [46] (see also ref. [47–49]). The dominant two-loop electroweak contributions have been evaluated in ref. [50]. For arbitrary values of m_A the NLO contributions arising from two-loop diagrams with quarks and gluons, as well as from one-loop diagrams with emission of a real parton, were computed

in ref. [4]. Supersymmetric particles contribute to the cross section at NLO through two-loop diagrams involving quarks, squarks and gluinos. The top-stop-gluino contributions were computed in ref. [51] in the limit of vanishing m_A. The analytic result for generic values of the stop and gluino masses was deemed too voluminous to be explicitly displayed in ref. [51], and was instead made available in the fortran code `evalcsusy.f` [32, 33]. On the other hand, neither the two-loop bottom-sbottom-gluino contributions (which can be relevant for large values of $\tan\beta$) nor the two-loop top-sbottom-gluino contributions in the top-pair threshold region, have never been directly computed so far.

With the present work we aim at reducing the gap in accuracy between the available NLO calculations of the production cross sections for CP-odd and CP-even Higgs bosons of the MSSM, exploiting the techniques developed for computing the top-stop-gluino [34] and bottom-sbottom-gluino [42] contributions in the CP-even case. Moreover, we also aim at obtaining approximate formulae for the top-stop-gluino contributions to CP-even and CP-odd Higgs production valid when the Higgs mass is close to the top-pair threshold and an expansion in m_ϕ^2/m_t^2 is not feasible ($\phi = h, H, A$).

In particular, we present an evaluation of the two-loop top-stop-gluino contributions to the CP-odd production cross section valid up to and including terms of $\mathcal{O}(m_A^2/m_t^2)$ and $\mathcal{O}(m_A^2/M^2)$. We show how the terms of order zero in m_A^2 can be cast in an extremely compact analytic form, fully equivalent to the result of ref. [51], and we investigate the effect of the first-order terms. We also evaluate the same contributions via an asymptotic expansion in the large superparticle masses, valid up to and including terms of $\mathcal{O}(m_A^2/M^2)$ and $\mathcal{O}(m_t^2/M^2)$. While the latter result is valid for $m_t, m_A \ll M$ but does not assume a hierarchy between m_t and m_A, the former is expected to provide a better approximation in the region with $m_A < m_t$ and relatively light superparticles, $M \simeq m_t$. As a byproduct, we also obtain a result for the bottom-sbottom-gluino contributions valid up to and including terms of $\mathcal{O}(m_b^2/m_A^2)$ and $\mathcal{O}(m_b/M)$. Finally, we compare our results for the bottom-sbottom-gluino contributions to both CP-even and CP-odd Higgs production cross sections with those obtained in the effective-Lagrangian approximation of refs. [52, 53]. The results on CP-odd Higgs production have been published in ref. [54].

We also apply the asymptotic expansion strategy to the evaluation of the two-loop top-stop-gluino contributions to the CP-even production cross section. We present original results which do not assume any hierarchy between the Higgs mass m_ϕ ($\phi = h, H$) and the top mass m_t and are valid up to and including terms of $\mathcal{O}(m_\phi^2/M^2)$, $\mathcal{O}(m_t^2/M^2)$ and $\mathcal{O}(m_Z^2/M^2)$. These results are expected to provide a better approximation of the full result if the Higgs mass is in the threshold region $m_\phi \simeq 2m_t$.

A non-trivial technical issue that arises in the calculation of the pseudoscalar production cross section is the treatment of the Dirac matrix γ_5 – an intrinsically four-dimensional object – within regularization methods defined in a number of dimensions $d = 4 - 2\epsilon$. The original calculation of the two-loop quark-gluon contributions of ref. [4] was performed in Dimensional Regularization (DREG), employing the 't Hooft-Veltman (HV) prescription [55] for the γ_5 matrix and introducing a finite multiplicative renormalization factor [56] to restore the Ward identities. In ref. [51] the calculation of the top-gluon and top-stop-gluino contributions to the Wilson coefficient in the relevant effective Lagrangian was performed

both in DREG and in Dimensional Reduction (DRED), which, differently from DREG, preserves supersymmetry (SUSY). The latter method does not require the introduction of finite renormalization factors, but it involves additional subtleties concerning the treatment of the Levi-Civita symbol $\varepsilon_{\mu\nu\rho\sigma}$.

In our calculation of the quark-squark-gluino contributions we avoided all problems related to the treatment of γ_5 by employing the Pauli-Villars regularization (PVREG) method. Being defined in four dimensions, the PVREG method respects both SUSY and the chiral symmetry, therefore no symmetry-restoring renormalization factors need to be introduced. We tested our implementation of PVREG by computing the top-gluon contributions via an asymptotic expansion in the top quark mass, and recovering the result obtained in DREG in refs. [4, 36]. As a further cross check, we also computed the quark-squark-gluino contributions using the DREG procedure outlined in ref. [56], and found agreement with the result that we obtained in PVREG.

We made extensive use of symbolic manipulation software in order to process the very large intermediate expressions entering the calculations. Our computations are fully automatized and require only little external input. In particular we generated the relevant two-loop diagrams with the help of the `Mathematica` [57] package `FeynArts` [58], using a modified version of the MSSM model file [59] which implements the Background Field Method [60–64]. The integrals are processed through a chain of `Mathematica` and/or `FORM` [65] programs optimized in order to perform Dirac algebra, color algebra, Taylor and asymptotic expansions and the actual integration (through reduction to Master Integrals). For the reduction in DREG of a class of integrals entering the asymptotic expansions we developed a `FORM` code which performs an Integration By Parts (IBP) reduction by efficiently importing and enforcing the IBP identities generated with the software `REDUZE` [66].

The present thesis is organized as follows: part I is devoted to reviewing useful Higgs phsyics concepts and defining the framework in which this work has been performed, in part II we discuss some technical aspects relevant for our calculation, while part III contains our original results. In chap. 1 we give an overview of the status of the experimental searches for the SM Higgs boson and we describe the main problems of the SM, thus motivating the statement that New Physics (NP) is actually "needed" at the TeV scale. In chap. 2 we introduce the Minimal Supersymmetric extension of the SM (MSSM) and discuss some aspects which are relevant to our work, namely the MSSM Higgs sector, the squark masses and the Higgs interactions with quarks and squarks. In chap. 3, after presenting a brief overview of the main MSSM Higgs production mechanisms at hadron colliders, we focus on the gluon fusion process and summarize some general results on the hadronic cross section for CP-even and CP-odd Higgs production. We also give the corresponding LO expression and discuss the origin of the NLO contributions. In chap. 4 we illustrate some issues related to the regularization of ultraviolet and infrared divergences in DREG and PVREG and discuss our renormalization procedure. In chap. 5 we give the details of our asymptotic expansion procedure and in chap. 6 we present our method for the exact evaluation of disconnected two-loop integrals which is needed in the asymptotic expansion approach. Chap. 7 and chap. 8 contain our two-loop results for, respectively, CP-even and CP-odd Higgs production, while in chap. 9 we give some concluding remarks. The

appendices contain some results or explicit formulae which we did not include in the main body of this work.

Part I

Physics

Chapter 1

Standard Model Higgs status and the "need" for New Physics

The Standard Model (SM) has proven to be impressively succesful in describing, with a rather modest number of free parameters, the vast phenomenology of particle interactions observed by the experiments in the last decades.

Quantum Chromodynamics (QCD) [67–70] is well established as the fundamental theory of strong interactions. Asymptotic freedom grants the possibility of describing and predicting, through perturbative computations, a series of high energy experimental results like the ones from Deep Inelastic Scattering or Drell-Yan processes, the spectrum of *quarkonium*, the production of hadrons in e^+e collisions. In the low energy regime, where QCD becomes non-perturbative and must be approached with different techniques (e.g. Lattice QCD or Sum Rules), the theory has proven capable of predicting from first principles many hadronic quantities, e.g. certain classes of weak decays hardonic matrix elements or the masses of several hadrons.

The Glashow-Weinberg-Salam [71–73] model of electroweak (EW) interactions is extremely well supported by the data. Nevertheless, there is still one particle predicted by such model (and actually crucial for its consistency) which has so far escaped detection, namely the Higgs boson, whose mass represent the only paramter of the SM which is still completely unknown. Then, even if the Higgs boson would be found, there would still remain several phenomenological and conceptual reasons why we believe the SM cannot be considered as a fundamental theory, valid up to arbitrarily high scales.

In sec. 1.1 we will first give an overview of the status of the experimental searches for the SM Higgs boson, then in sec. 1.2 we will describe the main problems of the SM and motivate the statement that New Physics (NP) is actually "needed" at the TeV scale.

1.1 Experimental Standard Model Higgs searches

Evidence for the SM Higgs boson has been seeked for in the past decades at collider experiments. We will focus on the most recent results about direct searches at LEP/LEP2,

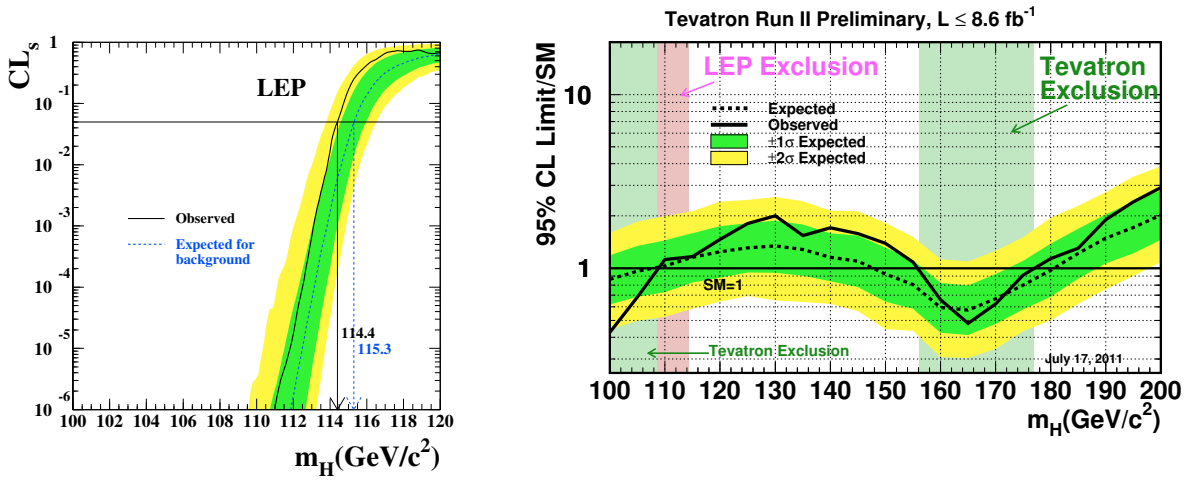

(a) (b)

Figure 1.1: (a) LEP combination (the green and yellow areas represent the 68% and 95% probability bands around the median background expectation, respectively); plot from ref. [74], (b) CDF-DØ combination; plot from ref. [75]

the Tevatron and the LHC, and then spend a few words about the indirect information provided by the electroweak precision measurements.

The LEP2 phase of the LEP e^+e^- collider at CERN consisted in a scan in the center of mass (c.o.m.) energy, up to $\sqrt{s} = 209\,\text{GeV}$, primarlily searching the SM Higgs boson H_{SM} in the *Higgsstrahlung* channel $e^+e^- \to Z^* \to ZH_{\text{SM}}$. Except for a slight 2.1σ fluctuation reported by one of the four detectors operating at LEP2, no signal has been observed. Given the Z boson mass, an on-shell Higgs as heavy as 118 GeV could in principle be produced, but due to sensitivity limits the final combined lower limit is [74]

$$m_{H_{\text{SM}}} < 114.4 \text{ GeV} \quad \text{excluded at 95\% Confidence Level (LEP2)}\,,$$

as it can be seen in fig. 1.1a, where the Confidence Level (CL) ratio $\text{CL}_s = \text{CL}_{s+b}/\text{CL}_b$ for the signal plus background hypothesis is plotted against the Higgs mass (the intersection of the horizontal line $\text{CL}_s = 0.05$ with the curve defines the 95% CL exclusion limit). Before the LHC started being operational, the $p\bar{p}$ collider Tevatron was the only hadron collider taking data. The Tevatron has been shut down at the time this thesis was being written (end 2011), and has had an impressive performance rise in its final years. The analysis of the whole amount of delivered integrated luminosity (around $10\,\text{fb}^{-1}$) has not yet been completed. The last CDF-DØ public combination for the SM Higgs searches results is shown in fig. 1.1b, where the 95% CL exclusion limit is plotted as a function of the Higgs mass in the range 100 GeV ÷ 200 GeV. The excluded regions are those where the solid

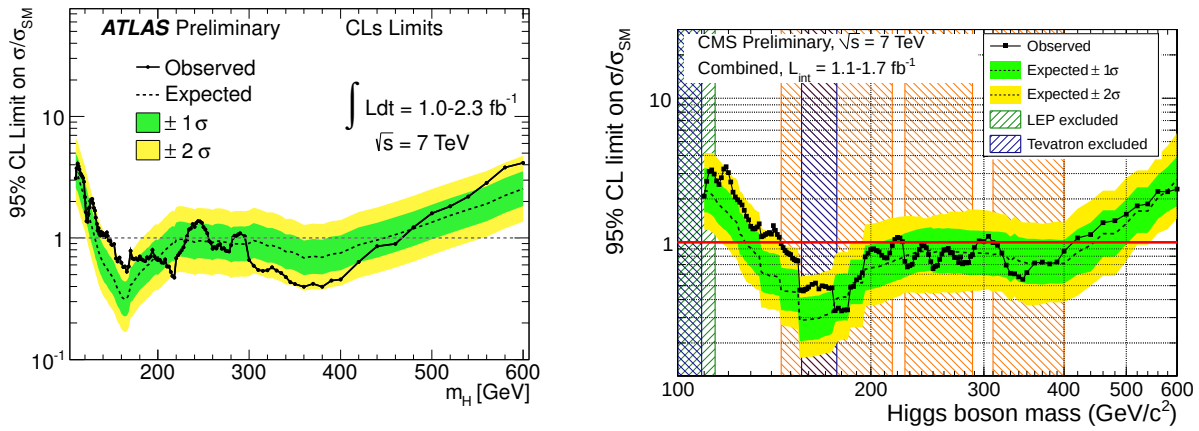

(a) **(b)**

Figure 1.2: (a) ATLAS Lepton-Photon 2011 combination for SM Higgs; plot from ref. [76] and (b) CMS Lepton-Photon 2011 combination for SM Higgs; plot from ref. [77]

black line dips below the horizontal dashed line at 1, that is

$$\left.\begin{array}{l} 100\,\text{GeV} < m_{H_{\text{SM}}} < 108\,\text{GeV} \\ 156\,\text{GeV} < m_{H_{\text{SM}}} < 177\,\text{GeV} \end{array}\right\} \quad \text{excluded at 95\% CL (Tevatron, Summer 2011)}\,.$$

The LHC (pp collider) is running at $\sqrt{s} = 7$ TeV, that is at an energy lower than its design value. It is expected to deliver around $10\,\text{fb}^{-1}$ of integrated luminosity by the end of 2012. This would be a remarkable performance, since only 2 years of collisions should be enough to deliver the same amount of integrated luminosity delivered by the Tevatron in its entire "lifetime". Such a result would allow combinations of Tevatron and LHC results to achieve a combined 5σ sensitivity for a SM-like Higgs boson for masses between 114 GeV and 600 GeV. The current 2011 LHC exclusions are based on the analyses of about $1\,\text{fb}^{-1}$ of integrated luminosity and the combinations of the different search channels are given separately by each experiment. The Atlas analysis (see fig. 1.2a) excludes at 95% CL the existence of a Standard Model Higgs boson in three Higgs mass ranges

$$\left.\begin{array}{l} 146\,\text{GeV} < m_{H_{\text{SM}}} < 232\,\text{GeV} \\ 256\,\text{GeV} < m_{H_{\text{SM}}} < 282\,\text{GeV} \\ 296\,\text{GeV} < m_{H_{\text{SM}}} < 466\,\text{GeV} \end{array}\right\} \quad \text{excluded at 95\% CL (ATLAS, Summer 2011)}\,.$$

Similarily, as shown in fig. 1.2b, the CMS analysis excludes at 95% CL the three Higgs mass ranges

$$\left.\begin{array}{l} 145\,\text{GeV} < m_{H_{\text{SM}}} < 216\,\text{GeV} \\ 226\,\text{GeV} < m_{H_{\text{SM}}} < 288\,\text{GeV} \\ 310\,\text{GeV} < m_{H_{\text{SM}}} < 400\,\text{GeV} \end{array}\right\} \quad \text{excluded at 95\% CL (CMS, Summer 2011)}\,.$$

All these limits arise from *direct searches*, where one seeks for the decay products of an on-shell Higgs and tries to reconstruct its mass. Another source of information about

the Higgs mass is represented by the many electroweak precision observables (EWPO) measured with remarkable precision in several experiments, like the various leptonic and hadronic asymmetries or the corrections to the relation $\rho = m_W^2/(m_Z^2 \cos^2\theta_W) = 1$. When loop effects are included in the theoretical predictions for such quantities, since in the SM the Higgs mass is the only free parameter, one can gain *indirect* information about it through combined fits of all the EWPO data available. At one-loop level the higher order predictions for many EWPO are typically dominated by terms proportional to m_t^2. Instead (due to the $SU(2)$ custodial symmetry) it is only the logarithm of the Higgs mass that enters the one-loop formulae, while quadratic terms appear at two-loops (thus being suppressed). On the one hand this allowed a quite accurate prediction for the top mass [78], by assuming $m_{H_{\rm SM}}$ to vary in a reasonably large range between 60 GeV and 1 TeV, a few months before its discovery was announced (actually after the first few candidate events and their plausible interpretation in terms of $t\bar{t}$ pairs were made public). On the other hand, the predictions one derives for the Higgs mass are bound to be less stringent and strongly depend on the value and the accuracy of the top mass measurements. Several analyses have been performed to date [79–81]. Without entering the details, they are all consistent with the statement that if no New Physics (NP) is assumed at the weak scale, all the available electroweak precision data require a light Higgs boson, excluding with a high confidence masses above ~ 200 GeV. It is peculiar that the expected value for its mass should actually be around 91 GeV, below the LEP2 limit. Anyway, by considering the fitting procedure uncertainties, the expected value is still consistent with the direct searches data. The general picture one obtains by consistently combining the information from direct searches and from precision fits, is that we expect the SM Higgs to be relatively light. Its discovery *could* be just around the corner.

1.2 SM issues and the "need" for New Physics

As already mentioned, there are still good reasons why we believe that the SM is not the full story. Here we will give an overview of the main arguments and motivate the need for New Physics, starting from the TeV scale.

Three observational motivations come from cosmology. First of all, there is strong astrophysical evidence for dark matter (DM) in the universe, which would explain structure formation, the observed anisotropies in cosmic microwave background radiation, the galactic rotation curves. DM properties can be inferred by cosmological considerations and it turns out that favourite candidates for DM are non-relativistic, TeV-scale, neutral weakly interacting massive particles (WIMP's). The SM cannot provide any candidate for dark matter but, surprisingly enough, it is quite easy to have DM candidates with the requested properties in many NP scenarios. Second, ordinary baryonic and dark matter contribute only with a small fraction (respectively $\sim 4\%$ and $\sim 23\%$) to the total cosmological energy density which is observed. The large remaining fraction of the total energy density, needed in order to account for the rate of expansion of the universe, is attributed to the so-called dark energy. Dark energy behaves like a negative pressure fluid, which can be included in

the Einstein equations in the form of a cosmological constant Λ. No fundamental explanation for the origin of such a term has been devised so far. The most direct interpretation of the cosmological constant as the energy of the vacuum in Quantum Field Theory (QFT) fails to reproduce the correct order of magnitude, e.g. $\Lambda_{\rm SM}/\Lambda_{\rm obs} \sim 10^{120}$. One last fact is that the SM has no explanation for the baryon-antibaryon density asymmetry observed in the universe. CP violation is a necessary condition for baryogenesis [82], but the SM fails to provide the right amount of CP violation.

Another obvious remark is that the gravitational force, which we believe becomes relevant at quantum level at energies of $\mathcal{O}(10^{19}\,\text{GeV})^*$, cannot be straightforwardly included in the SM. A QFT treatment of gravitation, just like the other particle interactions, gives rise to a non-renormalizable theory. After all, it is the very meaning of a quantum treatment of gravity which has to be investigated: QFT describes the quantum dynamics of fields *on* a spacetime, while gravitation is a theory of the dynamics of *the* spacetime. Different approaches like String Theory, Loop Quantum Gravity, Non-commutative Geometries are being studied. Without entering the details, the lesson is that we expect our SM to be just an effective theory, valid at most up the Planck scale, of a more fundamental theory including gravity.

A theoretical argument in favour of NP is based on the observation that the renormalization group running of the *three* SM gauge couplings is such that they almost reach the same value at a scale $\Lambda_{\rm GUT}$ of $\mathcal{O}(10^{16}\,\text{GeV})$. This may be much more than a coincidence, and reducing the number of fundamental parameters in our model by embedding the SM gauge group $SU(3)_c \otimes SU(2)_L \otimes U(1)_Y$ in a single Grand Unified gauge group G would be quite welcome. Moreover, Grand Unified Theories (GUT's) can predict quantities like the weak angle θ_W or the specific pattern of gauge quantum numbers assigned to matter fields, which is unexplained in the SM. Unification is not quantitatively perfect if one assumes that the SM is valid *as is* up to the unification scale, but one can always hope that NP contributions entering at some intermediate scale may improve such behaviour.

Concerning the flavor sector, one observes that the specific pattern of fermion masses and Cabibbo-Kobayashi-Maskawa matrix elements is very peculiar (e.g. all the fermion masses being much smaller than the typical EW scale $\Lambda_{\rm EW} \simeq 250\,\text{GeV}$ *but* the top mass, which is of the same order). This is the so-called SM flavor problem. The flavor sector is the least understood part of the SM, in which only a phenomenological description is given: indeed the majority of the SM free parameters (13 out of 19 if one assumes massless neutrinos) are needed in the flavor sector. Moreover, the observation of neutrino oscillations (which depend on the difference of the squared neutrino masses), requires at least two massive neutrinos. Cosmological considerations allow to set bounds on the sum of the neutrino masses, requiring it to be less than $\mathcal{O}(0.1\,\text{eV})$. Including in the SM right-handed, gauge singlet neutrinos represents a quite natural extension. Just as for the other SM particles, Dirac mass terms $m_\nu \bar{\nu}_L \nu_R + \text{h.c.}$ can be added, where m_ν is generated through EW spontaneous symmetry breaking. Then one would have to choose m_ν to be several orders of magnitude smaller than $\Lambda_{\rm EW}$, ending up with an even worse flavor problem.

*If there are no extra dimensions or other mechanisms bringing down the Planck scale.

More attractive scenarios can be devised, as the so-called type-I see-saw mechanism. A Majorana mass term $M\bar{\nu}_R^c\nu_R$ is actually gauge invariant and can be added as well, although it violates lepton number conservation (which anyway is only an accidental symmetry of the SM). By diagonalizing the neutrino mass matrix, the lightest eigenvalue turns out to be m_ν^2/M. If one assumes a natural value for the Dirac mass term, $m_\nu \sim \Lambda_{\rm EW}$, then one must actually require $M \sim \Lambda_{\rm GUT}$ in order to justify the smallness of neutrino masses. This seems to suggest that ν masses fit well in GUT scenarios, where lepton number violating interactions are expected at scales $\sim \Lambda_{\rm GUT}$. This is just an example of the fact that in general we expect that a theory that could dynamically explain the EW scale flavor sector in terms of a few parameters would probably involve NP at higher scales.

There are actually compelling reasons why NP is needed right at the EW scale. The Higgs potential is put by hand in the SM Lagrangian and in particular there is no explanation why the coefficient of the quadratic term develops a "wrong" sign, contributing to the potential as a negative mass term and thus triggering EW spontaneous symmetry breaking (EW SSB). The dynamics of the EW SSB is an *urgent* problem of particle physics and hints for its solution are expected to lie not too far above the EW scale. Indeed, if one considers the scattering of longitudinally polarized vector bosons (whose degrees of freedom actually come from the Goldstone bosons of the SSB sector, realized in the SM through the Higgs mechanism), an upper limit on the Higgs mass can be set by requiring that the theory remains perturbatively unitary. In the SM it is actually the Higgs scalar exchange that unitarizes the process. A thorough analysis of partial waves amplitudes [83] (where a precise unitarity constraint can be defined), shows that its mass cannot exceed $\mathcal{O}(700\,\text{GeV})$. Even if no SM Higgs boson is observed, we still believe that some sort of SSB mechanism is at work since gauge symmetry is observed in the couplings but is broken in the spectrum. On the other hand, NP around the TeV scale is needed in order to recover perturbation theory unitary. In this perspective the SM Higgs boson represents the minimal choice for an ultraviolet (UV) completion of the SM, while more involved solutions may be invoked in the form of weakly coupled NP (e.g. Supersymmetry) or strongly interacting sectors (e.g. Technicolor or Composite Higgs models). A discussion of all the NP scenarios is beyond the scope of this thesis, but in any case the general picture is that the scale of NP cannot be pushed too high if one wants to preserve perturbative unitarity.

Two more bounds, as functions of the NP scale, can be obtained by analyzing the Renormalization Group (RG) behaviour of the SM couplings. In particular, let us consider the running [84, 85] of the Higgs quartic coupling λ:

$$32\pi^2\frac{d\lambda}{d\ln Q/Q_0} = 24\lambda^2 - (3g' + 9g^2 - 24y_t^2)\lambda + \frac{3}{8}g'^4 + \frac{3}{4}g'^2g^2 + \frac{9}{8}g^4 - 24y_t^4 + \dots\,, \quad (1.1)$$

where g and g' are respectively the $SU(2)_L$ and the $U(1)_Y$ couplings and y_t is the top quark Yukawa coupling. We see that when $m_{H_{\rm SM}}^2 = 2\lambda v$ becomes large, the first term dominates. Then the RG equation reduces to

$$\lambda(Q) = \frac{\lambda(Q_0)}{1 - \frac{3}{2\pi^2}\lambda(Q_0)\ln Q/Q_0}, \quad (1.2)$$

which can be easily solved in order to show that λ has a Landau pole at some scale $Q = \Lambda$. If one requires that the theory is well behaved of any Λ, then λ must be zero in the low energy theory (*triviality problem*). Otherwise, one can require that the denominator never vanishes, that is $\lambda(Q)$ is always finite and $1/\lambda(Q) > 0$, obtaining an upper bound [86–89]

$$m_{H_{\rm SM}}^2 < \frac{8\pi^2 v^2}{3\ln \Lambda/v^2}\,, \tag{1.3}$$

where we have chosen $Q = \Lambda$ and $Q_0 = v$. Then if one insists that the theory can be extrapolated (*perturbative stability*) up to the Planck scale, the Higgs must be lighter than rougly 150 GeV. On the other hand, if NP is allowed around the TeV scale, the Higgs can be as heavy as $700 - 800$ GeV.

On the other hand, for a light Higgs the $-24y_t^4$ term dominates the RG equation. If we neglect all the other terms, the solution is given by ($Q = \Lambda$, $Q_0 = v$)

$$\lambda(\Lambda) = \lambda(v) - \frac{3}{4\pi^2} y_t^4 \ln \frac{\Lambda^2}{v^2}. \tag{1.4}$$

A lower bound on $m_{H_{\rm SM}}$ can then be obtained if one enforces the requirement of *vacuum stability* [86, 87, 89–92], by imposing that λ never becomes negative, so that the Higgs potential is always positive definite:

$$m_{H_{\rm SM}}^2 > \frac{3v^2}{2\pi^2} y_t^4 \ln \frac{\Lambda^2}{v^2}\,. \tag{1.5}$$

In particular, a Higgs boson heavier than 130 GeV is consistent with a SM that is valid all the way to the Planck scale. This lower bound on $m_{H_{\rm SM}}$ can be reduced to about 115 GeV if one allows for the electroweak vacuum to be metastable, with a lifetime greater than the age of the universe [93, 94].

Last, but not least, we discuss the *fine-tuning* or *hierarchy* problem (see e.g. ref. [95]). Contrarily to the SM fermion masses, which are protected by chiral symmetry from receiving large radiative corrections, the squared masses of the SM scalar particles are not protected by any symmetry and obtain arbitrarily large radiative corrections, quadratic in the cutoff at which we expect NP to enter. This has the consequence that, if the scale of NP is much higher than the typical EW scale $v \simeq 246$ GeV (e.g. the Planck scale if we insist the SM is the correct theory valid up to the scale where gravity must be taken into account) and $m_{H_{\rm SM}}$ is of the order of the EW scale (as it is plausible), the renormalized Higgs mass must result from an extremely fine-tuned cancellation between the bare mass and the counterterm. This raises the question whether there is some more natural mechanism which stabilizes the Higgs mass, i.e. either NP enters at much lower scales (roughly of order $1 \div 10$ TeV if one admits a "modest" amount of fine-tuning), or the scalar masses are protected by new symmetries.

In summary, we have discussed a number of reasons why the introduction of NP not too far above the EW scale seems plausible. Several different approaches have been studied and in this thesis we will focus on one of the most attractive possibilities, that is based on

the introducion of a new kind of symmetry known as Supersymmetry. In the next chapter we will discuss some general principles of Supersymmetry and introduce the Minimal Supersymmetric Standard Model, which is the framework in which the present work has been carried on.

Chapter 2

The Minimal Supersymmetric Standard Model (MSSM) and its Higgs sector

The Minimal Supersymmetric Standard Model (MSSM) is an attractive extension of the SM which allows to solve some of the issues discussed in the previous chapter and implies interesting phenomenological scenarios, including some peculiar features in its (extended) Higgs sector. In this chapter we give a brief overview of the concepts of the Minimal Supersymmetric Standard Model (MSSM) which will be needed in this thesis. A discussion of the status of the MSSM Higgs searches and of the parameter space exclusions, which are considerably more involved than those in the SM due to the many unknown parameters of the model and thus require more sophisticated analyses or the introduction of constraining assumptions, is beyond the scope of the present work.

In particular in sec. 2.1 we will recall some general ideas concerning supersymmetry. In sec. 2.2 we will introduce the MSSM field content. Then in sec. 2.3 we will discuss in more detail the MSSM Higgs sector, focusing on the way EW symmetry breaking arises and on the Higgs spectrum. Finally, in sec. 2.4 we will discuss the squarks spectrum and comment on the interactions arising in the model which are relevant for our computation.

2.1 Supersymmetry

A supersymmetry (SUSY) transformation turns a bosonic state into a fermionic state (and vice versa) and one can see that the operator that generates such a transformation must be an anticommuting spinor [96–100]. The attractive feature is that supersymmetry relates the couplings and masses of fermions and bosons, thus being very constraining on the structure of the interactions. The most phenomenologically interesting models are those in $d = 4$ spacetime dimensions in which there is only one SUSY generator ($\mathcal{N} = 1$). Irreducible representations of the SUSY algebra (*supermultiplet* or *superfield*) contain an equal number of fermionic and bosonic degrees of freedom (d.o.f.'s). More specifically,

$\mathcal{N} = 1$ SUSY supermultiplets contain two fermionic and two bosonic d.o.f.'s, their spins differing by one half. Moreover, SUSY generators commute with the Poicaré and internal symmetries, meaning that particles in a supermultiplet share the same mass (eigenstate of $p_\mu p^\mu$) and quantum numbers. In such theories, supersymmetry automatically tunes the couplings so that the quadratically divergent correction to the scalar masses coming from fermion and boson loops exactly cancel, thus solving (at least technically) the hierarchy problem.

No SUSY partners of the SM particles have been observed so far. If SUSY is a symmetry of nature, we should have already detected those particles, exactly degenerate in mass with the SM states. Thus we know that SUSY must be broken in such a way that the sparticles obtain large masses, which justifies the fact that they have escaped detection so far. After all, we have observed only particles whose masses are prohibited by (chiral) gauge invariance, namely vector bosons and matter fermions, and need to be generated through a SSB mechanism at the EW scale, which fixes their order of magnitude. On the contrary, scalars and adjoint fermions have no such a strict constraint and nothing prevents them from having mass terms. There is one subtlety. One should make sure that, by breaking SUSY, does not lose one of the interesting properties that make a SUSY extension of the SM appealing, namely the solution to the hierarchy problem. SUSY breaking may occur spontaneously or explicitly, through the introduction of non SUSY-invariant mass and interaction terms in the Lagrangian. The former case would automatically preserve the cancellation of quadratic divergences, while if explicit terms are introduced they must be chosen judiciously (operators of dimension strictly less than four, the so called *soft*-terms). Moreover, sparticle masses cannot be chosen too large since in a soft SUSY theory the quadratic divergences are reintroduced as terms proportional to the mass splitting between the partners in the same multiplet. In particular, if the superparticle spectrum lies around TeV scale (at least the top superpartners), naturalness can still be retained. This of course gives us hope that if SUSY is the NP scenario nature has chosen, the discovery of supersymmetric particles at colliders could be near.

Understanding the origin of SUSY breaking represents an important theoretical challenge and many models have been devised. These models typically consist in including new particles and interactions at high scales. Anyway, from a practical point of view, it is convenient to simply parametrize the breaking sector at low energy just adding the most general allowed terms with unknown parameters. The problem with such approach is that a very big number on unknown parameters and phases is introduced in the theory, which e.g. in general allow tree level FCNC processes, which we do not observe, and represent unwanted sources of CP-violation, which apparently is well described by the SM itself.

We have already seen that SUSY provides a natural mechanism for solving the hierarchy problem. Actually, considering a weak scale SUSY extension of the SM is phenomenologically and theoretically appealing for several other reasons. Let us just mention a few other. As we will see, SUSY can allow for a radiatively generated EW SSB. Another interesting fact is that the MSSM is able to quantitatively improve the Grand Unification of the SM gauge couplings. Another completely unexpected feature is that, by requiring R-parity symmetry to hold in order to forbid large contributions to (so far) unobserved processes

such as proton decay, one actually gets a WIMP candidate for Dark Matter. In fact, the lightest SUSY particle (LSP) cannot further decay because interaction vertices must always involve an even number of supersymmetric particles. Without entering the details, typical SUSY scenarios predict electrically neutral LSP's with properties compatible with the requirements derived from cosmological considerations. Supersymmetry is also an essential ingredients for Superstring theory, which is a possible approach to the problem of quantum gravity.

2.2 The MSSM field content and interactions

We will avoid introducting the formalism of superfields, which would allow to immediately write supersymmetric Lagrangians but at the same would demand a rather formal treatment. Let us just remark that a (left-handed) chiral superfield contains as physical d.o.f.'s a complex scalar φ and the left-handed component of a Majorana fermion $\psi_L = P_L\psi$, where P_L is the usual chirality projector and ψ is a four component spinor satisfying the Majorana condition $\psi = \psi^c$ (the superscript ^{c} denotes charge conjugation). Instead, a vector superfield contains a real vector boson V_μ and a Majorana spinor λ (in the Wess-Zumino gauge). All of these fields are described by two real d.o.f.'s when the equations of motion are enforced, so that the SUSY requirement that each bosonic d.o.f. is matched by a fermionic d.o.f. is satisfied. One actually needs auxiliary scalar fields when spinors and vectors are *off-shell*, but the equations of motion for those fields are actually just algebraic constraints and allow one to eliminate them in favour of the physical fields.

It can be shown that the most general Lagrangian (see e.g. ref. [101]) for a set of Majorana fermions ψ_i and complex scalars φ_i which is gauge invariant under a gauge group G, with generators T^a and gauge coupling g, renormalizable and invariant under supersymmetry transformations is given by (after the equations of motion for the auxiliary fields have been imposed)*

* When the gauge group G contains one or more $U(1)$ factors (as in the case of the SM gauge group), for each $U(1)_p$ factor of G one can actually add to the Lagrangian a so-called Fayet-Iliopoulos (FI) term, which upon enforcing the equations of motion for the auxiliary fields reads $\mathcal{L}_{\mathrm{FI},p} = -g_p\xi_p(\sum_i \varphi_i^* T_p \varphi_i + \xi_p)$. It can be shown (see e.g. [102]) that such terms can drive spontaneous SUSY breaking in the scalar sector, but a FI term for the SM $U(1)_Y$ is excluded or disfavoured because it would lead to electromagnetism and/or color breaking. The introduction of extra $U(1)$ factors (for extra gauge symmetries either broken at higher scales or decoupled from the SM) gives rise to other problems, so we will not discuss FI terms any further.

$$\begin{aligned}\mathcal{L}_{\text{SUSY}} = & -\frac{1}{4}\sum_a F^a_{\mu\nu}F^{a\mu\nu} + \sum_i \left[(D_\mu\varphi_i)^\dagger(D^\mu\varphi_i) + \frac{i}{2}\bar{\psi}_i D_\mu\gamma^\mu\psi_i\right] + \frac{i}{2}\sum_a \bar{\lambda}^a D_\mu\gamma^\mu\lambda^a \\ & - V(\varphi) \\ & - g\sqrt{2}\sum_{i,a}\left[\varphi_i\, T^a\bar{\lambda}^a\frac{1-\gamma_5}{2}\psi_i + \text{h.c.}\right] - \frac{1}{2}\sum_{i,j}\left[\left.\frac{\partial^2\mathcal{W}}{\partial\Phi_i\Phi_j}\right|_{\Phi=\varphi}\bar{\psi}_i\frac{1-\gamma_5}{2}\psi_j + \text{h.c.}\right],\end{aligned} \tag{2.1}$$

where the scalar potential $V(\varphi)$ is given by

$$V(\varphi) = \sum_i \left|\frac{\partial\mathcal{W}}{\partial\Phi_i}\right|^2_{\Phi=\varphi} + \frac{g^2}{2}\sum_a\left[\sum_i \varphi_i^* T^a\varphi_i\right]^2, \tag{2.2}$$

and $\mathcal{W}(\Phi_i)$ is the *superpotential*, which is required to be an analytic function of the (left chiral super-) fields Φ_i in order to guarantee invariance under supersymmetry. This observation will be crucial in the construction of the MSSM Higgs sector. The superpotential arises in the superfield formulation of supersymmetric theories but, as we have seen, it is only its functional form that determines the Lagrangian in terms of component fields. Thus we will interchangeably speak of fields and superfields when referring to $\mathcal{W}(\Phi_i)$. It can be shown that renormalizability of $\mathcal{L}_{\text{SUSY}}$ is enforced by requiring $\mathcal{W}(\Phi_i)$ to be a polynomial of degree three in the superfields.

Let us examine the content of the SUSY Lagrangian (2.1). The first line contains the kinetic terms for all the dynamical fields belonging to the chiral and vector supermultiplets ($F^a_{\mu\nu}$ is the standard field strenght tensor for the non-abelian gauge boson V^a_μ). Covariant derivatives are defined as usual, keeping in mind that the ψ_i and φ_i fields are in the fundamental representation of the gauge group, while the λ^a fields are in the adjoint representation, as the corresponding gauge bosons V^a_μ. The scalar potential in the second line is composed by two terms, see (2.2). The first addendum is completely determined by the superpotential $\mathcal{W}(\Phi_i)$ and is commonly referred to as F-term contribution. The second term contains the quartic scalar interactions, which are determined by their gauge quantum numbers, and is commonly referred to as D-term contribution. The third line contains the scalar-fermion Yukawa interactions, which once again are fixed by the functional form of the superpotential, and a new kind of interaction which is genuine to SUSY theories, namely the ψ_i-φ_j-λ^a interaction, whose coupling is constrained by SUSY and gauge invariance.

The MSSM is the minimal supersymmetric extension of the SM. The gauge group is the same as that of the SM, i.e. $SU(3)_c \otimes SU(2)_L \otimes U(1)_Y$. The SM spin-1 gauge bosons are identified to be the vector components V^a_μ of non-abelian vector supermultiplets, whose spin-1/2 fermionic components λ^a will be denoted as *gauginos*. The SM spin-1/2 fermions are taken to be the spinor component of left chiral superfields, implying that to each fermion ψ is associated a spin-0 complex scalar $\tilde{\psi}$ (*sfermion*). The SM is a chiral gauge theory, but

we choose to work with left-handed fields only[†], i.e. we trade each right-handed fermion ψ_R for the corresponding left-component of its charge conjugate $(\psi^c)_L$. In particular the MSSM supermultiplets corresponding to the SM fields q_L, $(u^c)_L$, $(d^c)_L$, l_L and $(e^c)_L$ [‡] will be denoted as Q, U^c, D^c, L and E^c. To be explicit, e.g. for the top superfields we have

$$T \ni \left(\tilde{t}_L, t_L\right) , \tag{2.3}$$

$$T^c \ni \left(\tilde{t}_R, (t^c)_L\right) \sim \left(\tilde{t}_R, t_R\right) , \tag{2.4}$$

where T is the up-type component of Q_3 and $T^c = U_3^c$. Since the SUSY generators commute with the generators of all the other symmetries of the theory, fields in the same supermultiplet are required to share the same quantum numbers. Thus each supermultiplet will be in the same representation as the corresponding SM field. Let us note that up to now we have effectively "doubled" the SM spectrum.

As already noted, the Higgs sector is quite delicate. The SM Higgs is a scalar field that shares the same quantum numbers as the leptons l_L. One could thus imagine identifying the Higgs as the scalar partner of the lepton doublet. When a non vanishing vacuum expectation value is assigned to the Higgs, one would end up with the spontaneous breaking of lepton number together with that of the EW gauge group. On the other hand, neither the corresponding (massless) Goldstone boson nor lepton number violating interactions have been observed so far, thus we seek for another strategy.

One could follow the same procedure adopted for the matter fields, simply promoting the SM Higgs field to a chiral superfield. The SM Yukawa terms are built by employing the Higgs doublet ϕ and its conjugate $\tilde{\phi} = i\sigma^2\phi^*$ (which has the opposite hypercharge as ϕ) in order to write gauge invariant terms that give mass to up-type quarks and down-type quarks. On the other hand, as shown in (2.1), fermion mass terms originate from the superpotential $\mathcal{W}(\Phi_i)$, which is required to be an analytic function of the Φ_i. In particular it cannot be a function of the conjugate Higgs superfield and we are thus forced to introduce two separate Higgs supermultiplets if we want them to have opposite $U(1)_Y$ charge,

$$H_1 = \begin{pmatrix} H_1^0 \\ H_1^- \end{pmatrix}_{Y=-1/2} , \quad H_2 = \begin{pmatrix} H_2^+ \\ H_2^0 \end{pmatrix}_{Y=+1/2} , \tag{2.5}$$

composed by four complex Higgs scalars and four Majorana *higgsinos*. A further remark is in order. If only one Higgs doublet (say with $Y = -1/2$) were included, the higgsinos would give rise to a non vanishing contribution to chiral anomalies because no $Y = +1/2$ higgsino would compensate.

[†]In the superfield formalism this is necessary. In fact right-handed chiral superfields can always be written as the hermitian conjugate of a left-handed chiral superfield but, as we have already stated above, the superpotential $\mathcal{W}$ is restricted to be an analytic function of left-handed chiral superfields only.

[‡]Unless explicitly specified, all the fields have to be considered as vectors in flavor space. With a slight abuse of notation we have e.g. $(u^c)_L = \begin{pmatrix} u^c \\ c^c \\ t^c \end{pmatrix}_L$. The fields q_L and l_L are the $SU(2)_L$ doublets $q_L = \begin{pmatrix} u \\ d \end{pmatrix}_L$ and $l_L = \begin{pmatrix} \nu \\ l \end{pmatrix}_L$.

We are now ready to write down the most general gauge invariant renormalizable superpotential for the MSSM, which reads

$$\begin{aligned}\mathcal{W} = & \underbrace{(U^c h^U Q)H_2 + (D^c h^D Q)H_1 + (E^c h^E L)H_1}_{\text{Yukawa}} \\ & + \underbrace{\mu H_1 \cdot H_2}_{\mu-\text{term}} \qquad (2.6) \\ & + \underbrace{(D^c h'^D Q)L + (E^c h'^E L)L + \mu'_i L_i H_2 + Y_{ijk} D^c_i D^c_j U^c_k}_{\text{R-parity violating}}, \qquad (2.7)\end{aligned}$$

where the fields are vectors in the gauge and flavor spaces, the h^X are matrices in the flavor space and the sums in the last line run on the flavor indices (the last term is to be intended as a color singlet). The first line is the MSSM generalization of the SM Yukawa sector; the second line contains the only term quadratic in the Higgs superfields allowed by gauge invariance (the $SU(2)$ invariant $H_1 \cdot H_2 = \epsilon_{\alpha\beta} H_1^\alpha H_2^\beta$, where $\epsilon_{\beta\alpha} = -\epsilon_{\alpha\beta}$ and $\epsilon_{12} = 1$) and supersymmetry; the last line contains terms that are in principle allowed but are disastrous when it comes to phenomenology. Those terms generate lepton (L) and baryon (B) number violating interactions, leading to processes like the proton decay or $\mu \to e\gamma$ or other tree level Flavor Changing Neutral Currents (FCNC) processes, which have not been observed. It is interesting to note that B and L violating interactions are forbidden in the SM because of two $U(1)$ accidental symmetries, while it is not so in the MSSM. One can posit an additional symmetry of the Lagrangian, named R-parity, defined for each particle as

$$P_R = (-1)^{3(B-L)+2s}, \qquad (2.8)$$

where B and L are the baryon and lepton number and s denotes the spin. Particles in the same supermultiplet have opposite R-parities, in particular all the SM particles have even R-parity while all the superpartners have odd R-parity. If R-parity is to be conserved, sparticles must be always appear in an even number in each interaction vertex. Note that R-parity is defined in terms of $B - L$, which means that it can be consistently introduced regardless of the non-perturbative effects that break $U(1)_B \otimes U(1)_L$ down to $U(1)_{B-L}$. It can be shown that the terms in the last line all violate R-parity and must therefore be dropped from the superpotential if R-parity is assumed (as we will do):

$$\begin{aligned}\mathcal{W}_{\text{MSSM}} = & \underbrace{(U^c h^U Q)H_2 + (D^c h^D Q)H_1 + (E^c h^E L)H_1}_{\text{Yukawa}} \\ & + \underbrace{\mu H_1 \cdot H_2}_{\mu-\text{term}}. \qquad (2.9)\end{aligned}$$

The last MSSM ingredient is the soft SUSY-breaking Lagrangian, which contains mass terms for the supersymmetric particles making them heavy enough to have escaped detection. SUSY breaking should be explained in terms of some dynamical mechanism occuring

at higher scales and/or in different sectors of the theory. One can nevertheless parametrize in the most general way the soft Lagrangian at the weak scale, writing it as

$$\mathcal{L}_{\rm soft} = \mathcal{L}_{m,\rm sfermions} + \mathcal{L}_{m,\rm Higgs} + \mathcal{L}_{m,\rm gauginos} + \mathcal{L}_{\rm soft\text{-}trilinear}\,. \tag{2.10}$$

The first piece is a sum of mass terms for the scalars

$$-\mathcal{L}_{m,\rm sfermions} = \tilde{q}_L^\dagger m^2_{\tilde{q}_L} \tilde{q}_L + \tilde{u}_R^\dagger m^2_{\tilde{u}_R} \tilde{u}_R + \dots\,, \tag{2.11}$$

where $\tilde{q}_L$, $\tilde{u}_R$ etc. are again matrices in flavor space and $\tilde{q}_L, \tilde{l}_L$ are weak isospin doublets[§]. The second term contains mass bilinears for the Higgs doublets (note that here we are allowed to introduce $H^\dagger H$ terms since we are breaking explicitly SUSY)

$$-\mathcal{L}_{m,\rm Higgs} = m^2_{H_1}|H_1|^2 + m^2_{H_2}|H_2|^2 + 2{\rm Re}(BH_1\cdot H_2)\,, \tag{2.12}$$

where $m^2_{H_1}$ and $m^2_{H_2}$ are real parameters while B needs not (and again $H_1\cdot H_2 = \epsilon_{\alpha\beta}H_1^\alpha H_2^\beta$). One phase in the Higgs sector can be redefined and this phase is usually taken to be that of B, which is chosen real and positive. The third contribution contains mass terms for the gauginos ($\tilde{g}$ is the Majorana gluino etc. and M_i, M_i' are real)

$$\begin{aligned} -\mathcal{L}_{m,\rm gaugino} = {} & \frac{1}{2}\left(M_3\bar{\tilde{g}}\tilde{g} + M_1\bar{\tilde{b}}\tilde{b} + M_2\bar{\tilde{w}}_i\tilde{w}_i\right) \\ & + \frac{1}{2}\left(M_3'\bar{\tilde{g}}\gamma_5\tilde{g} + M_1'\bar{\tilde{b}}\gamma_5\tilde{b} + M_2'\bar{\tilde{w}}_i\gamma_5\tilde{w}_i\right)\,, \end{aligned} \tag{2.13}$$

where summation on non-abelian gauge indices is understood. We note that the terms with M_i' violate CP. One of such masses may be removed by performing a chirality transformation on the gaugino field, and we take this to be M_3'. The last term of the soft-Lagrangian contains trilinear SUSY-breaking interactions between the sfermions and the Higgs bosons ("A-terms"), analogous to those in the superpotential

$$-\mathcal{L}_{\rm soft\text{-}trilinear} = \tilde{u}_R^\dagger\, \underline{A}^U \tilde{q}_L\, H_2 + \tilde{d}_R^\dagger\, \underline{A}^D \tilde{q}_L\, H_1 + \tilde{e}_R^\dagger\, \underline{A}^E \tilde{l}_L\, H_1 + {\rm h.c.}\,, \tag{2.14}$$

where A^E, A^U etc are matrices in flavor space and each trilinear coupling can be expressed in terms of the superpotential Yukawas ($X = U, D, E$ and no summation on i, j)

$$\underline{A}^X_{ij} = A^X_{ij} h^X_{ij}\,. \tag{2.15}$$

In summary, the MSSM Lagrangian is then given by

$$\mathcal{L}_{\rm MSSM} = \mathcal{L}_{\rm SUSY} + \mathcal{L}_{\rm soft}\,, \tag{2.16}$$

where $\mathcal{L}_{\rm SUSY}$ is (2.1) with gauge group $G = SU(3)_c \otimes SU(2)_L \otimes U(1)_Y$, the above discussed field content and the superpotential (2.9), while $\mathcal{L}_{\rm soft}$ is the soft SUSY-breaking part,

[§]Note that the $_{L,R}$ subscripts on the sfermion fields do not indicate any chirality, since they are scalar fields. Such labels are just a reminder of the fact that e.g. $\tilde{q}_L$ and $\tilde{u}_R$ are the scalar partners of the chiral fermions q_L and $(u^c)_L \sim u_R$.

defined by (2.10) and the equations below. By carefully counting the masses, the phases and the mixing angles introduced in the MSSM (removing those that can be eliminated by field redefinitions), one can see that the MSSM parameter space cosists of 124 (105 more than the SM) free parameters [103]. One has 9 parameters in the gauge/gaugino sector, 5 parameters in the Higgs sector, while the remaining 110 parameters are all needed in the flavor sector. It is plausible that once the SUSY breaking mechanism is understood, a large number of those parameters could be expressed in terms of a few fundamental parameters.

Note that the Lagrangian contains many quadratic terms for the MSSM fields, excluding the gauge bosons of the unbroken $SU(3)_c \otimes U(1)_Q$ which remain massless after EW SSB. Such terms can in general be put in diagonal form just as in the case of the SM Yukawa couplings. For given spin, the mass eigenstates of the SUSY particles will then be given by combinations of the interaction eigenstates, respecting all the Lagrangian symmetries. We refer to this phenomenon as *mixing*. For instance, $SU(2)_L \otimes U(1)_Y$ gauginos (winos and binos) will separately mix into charged and neutral mass eigenstates, while no gluino mixing is allowed. The scalar partners of the SM fermions represent the most complicated sector, since in general up-type and down-type sfermions will be obtained by diagonalizing two 6×6 matrices (two sfermion "chiralities", L and R, for each flavor).

In order to allow for efficient, manageble low energy phenomenological studies, one often makes certain assumptions on the MSSM parameters. Let us recall that the scale of the dimensionful parameters in the soft SUSY-breaking sector is required not to exceed a few TeV. This has to be done if one does not want to re-introduce large quadratic corrections to the scalar squared masses, e.g. in the form of terms proportional to the coupling times the splitting between the particle and sparticle masses squared. This justifies the assumption that at least the third generation fermions, which have large Yukawa couplings with the Higgs(es), have not too heavy supersymmetric partners. On the other hand, we can also rely on the many experimental results in the flavor sector that actually provide stringent constraints on those couplings. For instance, there are strong upper bounds on the flavor violating processes (like $\mu \to e\gamma$) that would be induced at tree-level by the MSSM if the off-diagonal (in flavor space) terms in the soft trilinear couplings $\underline{\mathrm{A}}$ were comparable to the diagonal terms. Also, neutral meson mixing processes provide constraints on the structure of squark masses, at least for the first two generations. Other constraints derive from the limits on the CP violating processes which would be predicted if the many new CP violating phases were different from zero. Therefore, one often works in a simplified framework in which the soft trilinear couplings $\underline{\mathrm{A}}^X$ are proportional to the Yukawa matrices appearing in the superpotential. For our purposes we can safely consider the $\underline{\mathrm{A}}^X$ matrices as flavor diagonal and neglect the first two generations.

2.3 The MSSM Higgs sector

We want now to discuss the Higgs sector of the MSSM. Let us proceed by assuming a vanishing vacuum expectation value for all the sfermions and considering the scalar potential for the Higgs fields. It is important to remark that the only dimensionless couplings en-

tering the MSSM Lagrangian (2.16) are the gauge couplings and the Yukawa couplings in the superpotential. This means that, at variance with the SM Higgs sector, no $\lambda\phi^4$ terms appear in the scalar potential. A consequence of this fact is that the Higgs mass(es) are not free parameters but satisfy some constraints. In particular, as we will see, a stringent upper bound on the lightest mass eigenstate can be derived.

The tree level Higgs potential of the MSSM is

$$\begin{aligned} V = & m_1^2|H_1|^2 + m_2^2|H_2|^2 - 2B\mathrm{Re}(H_1 \cdot H_2) \\ & + \frac{g^2}{8}\left(H_1^\dagger \vec{\sigma} H_1 + H_2^\dagger \vec{\sigma} H_2\right)^2 + \frac{g'^2}{8}\left(|H_1|^2 - |H_2|^2\right)^2 , \end{aligned} \tag{2.17}$$

where: $m_1^2 = m_{H_1}^2 + |\mu|^2$, $m_2^2 = m_{H_2}^2 + |\mu|^2$ (we remind the reader that $m_{H_i}^2$ and B are the soft supersymmetry-breaking masses (2.12), $m_{H_i}^2$ are real and B has been chosen real and positive as explained in sec. 2.2, μ comes from the only term allowed in the superpotential (2.9) and g and g' are the $SU(2)_L$ and $U(1)_Y$ gauge couplings.

A remark is in order: while m_Z is of the order of the EW scale and the parameters $m_{H_i}^2$ and B are of the order of the soft SUSY breaking scale, μ is a completely arbitrary parameter of the superpotential. If one does not want to re-introduce miraculos cancellations, the observed value of the scale of EW SSB breaking suggests that, although apparently unrelated, both μ and the scale of the soft parameters should not exceed a few hundreds of GeV or a few TeV (this is called the "μ-problem"). A solution to this puzzle is probably related to a precise understanding of the mechanism of SUSY breaking.

The parameters entering (2.17) must satisfy

$$m_1^2 + m_2^2 \geq 2B\,, \quad m_1^2 m_2^2 \leq B^2\,. \tag{2.18}$$

The first condition in (2.18) guarantees the potential is bounded from below: the D-term induced quartic interactions (whose coefficients in the MSSM are given in terms of the gauge coupling and quantum numbers) stabilize the potential for almost all arbitrarily large values of the fields, but it is easy to see that such quartic interactions vanish identically along the direction $H_1 = H_2$, so that a positivity condition must be imposed on the quadratic term. The second condition is necessary in order to make sure that the neutral components of the Higgs doublet acquire non-zero vacuum expectation values (VEV's) by allowing a combination of H_1^0 and H_2^0 to have the "wrong sign" mass term (close to $H_1^0 = H_2^0 = 0$), triggering SSB. Note that two conditions cannot be simultaneously satisfied if $m_1^2 = m_2^2$. Thus in order to break EW symmetry we must *also* break SUSY by introducing non zero, different mass terms for the two H_i in the soft breaking sector. In many popular models (such as minimal supergravity or gauge mediated SUSY breaking) the soft SUSY-breaking parameters are chosen to be equal at some high scale. It is their running to lower energies that removes this degeneracy, typically via the contribution of top/bottom quarks and their superpartners. In these models EW SSB is said to be *radiatively induced*. Note also that the B-term always favors EW SSB. We define the VEV's aquired by the neutral

components as[¶]

$$\langle H_1^0 \rangle = v_1 \,, \quad \langle H_2^0 \rangle = v_2 \,, \tag{2.19}$$

The neutral Higgs fields can then be written as fluctuations around the VEV's as follows:

$$H_1^0 = \frac{v_1 + S_1 + iP_1}{\sqrt{2}} \,, \quad H_2^0 = \frac{v_2 + S_2 + iP_2}{\sqrt{2}} \,. \tag{2.20}$$

After EW SSB, the gauge bosons obtain their masses in the usual way

$$m_W^2 = \frac{g^2}{4} v \,, \quad m_Z^2 = \frac{g^2 + g'^2}{4} v \,, \quad v \equiv \left(v_1^2 + v_2^2 \right) \,. \tag{2.21}$$

The important difference with respect to the SM is that the two Higgs doublets contain a total of eight scalar d.o.f.'s, of which only three are the Goldstone bosons $G^\pm$ and G^0 that are transferred to the W and Z gauge bosons, becoming their longitudinal d.o.f.'s. In the MSSM there remain thus *five* physical Higgses. If CP invariance is assumed in the Higgs sector (as we will do) the real and imaginary components of the Higgs fields do not mix, so the 4×4 mass matrix decomposes into two 2×2 blocks. The physical states are then two neutral CP-even bosons h and H, one neutral CP-odd[‖] boson A and a charged boson $H^\pm$, obtained as the eigenstates of the mass matrices of the corresponding sectors of the scalar potential. By imposing the minimum condition with respect to the fields in (2.17)

$$\left. \frac{\partial V}{\partial \phi_i} \right|_{\min} = 0 \,, \quad \left(\phi_i = P_1, P_2, S_1, S_2, H_1^-, H_2^+ \right) \,, \tag{2.22}$$

and taking the second derivatives

$$\left(M_P^2 \right)_{ij} = \left. \frac{\partial^2 V}{\partial P_i \partial P_j} \right|_{\min} = -B \frac{v_1 v_2}{v_i v_j} \,, \tag{2.23}$$

$$\left(M_S^2 \right)_{ij} = \left. \frac{\partial^2 V}{\partial S_i \partial S_j} \right|_{\min} = (-1)^{i+j} \left[-B \frac{v_1 v_2}{v_i v_j} + \frac{g^2 + g'^2}{4} v_i v_j \right] \,, \tag{2.24}$$

$$\left(M_\pm^2 \right)_{ij} = \left. \frac{\partial^2 V}{\partial H_i^+ \partial H_j^-} \right|_{\min} = \frac{v_1 v_2}{v_i v_j} \left[-B + \frac{g^2}{4} v_1 v_2 \right] \,, \tag{2.25}$$

one gets the mass matrices for the separate sectors. In terms of the original gauge eigentstates, the charged and CP-odd mass eigenstates are (we compactly write $c_\theta \equiv \cos\theta$ and $s_\theta \equiv \sin\theta$ for any angle θ)

$$\begin{pmatrix} G_0 \\ A \end{pmatrix} = \begin{pmatrix} s_\beta & -c_\beta \\ c_\beta & s_\beta \end{pmatrix} \begin{pmatrix} P_1 \\ P_2 \end{pmatrix} \,, \quad \begin{pmatrix} G^+ \\ H^+ \end{pmatrix} = \begin{pmatrix} s_\beta & -c_\beta \\ c_\beta & s_\beta \end{pmatrix} \begin{pmatrix} H_1^+ \\ H_2^+ \end{pmatrix} \,, \tag{2.26}$$

[¶]By an $SU(2)_L$ transformation it is always possible to rotate the charged Higgs fields in such a way that the minimum condition for the potential V reads $H_i^\pm = 0$. After all, we want to break the SM gauge group down to the subgroup $U(1)_Q$, leaving electromagnetic gauge invariance intact.

[‖]If CP-violation stems only from phases in the couplings, the CP-odd A boson couples only to the CP-odd fermion bilinears $\bar{\psi}_i \gamma_5 \psi_i$. Then one also deduces that it has also to be a Lorentz pseudoscalar. In the following, we will interchangeably speak of CP-even/odd and scalar/pseudoscalar Higgses.

where $\tan\beta \equiv v_2/v_1$ and $H_1^+ = \left(H_1^-\right)^*$. The corresponding eigenvalues for the physical states A and $H^\pm$ are

$$m_A^2 = -\frac{2B}{s_{2\beta}}\,, \quad m_{H^\pm}^2 = m_A^2 + m_W^2\,. \tag{2.27}$$

The mass matrix for the CP-even sector (2.24) can be rewritten in terms of m_A, m_Z and the angle β as

$$\left(M_S^2\right)_{ij} = \begin{pmatrix} m_Z^2 c_\beta^2 + m_A^2 s_\beta^2 & -\left(m_Z^2 + m_A^2\right) s_\beta c_\beta \\ -\left(m_Z^2 + m_A^2\right) s_\beta c_\beta & m_Z^2 s_\beta^2 + m_A^2 c_\beta^2 \end{pmatrix}\,, \tag{2.28}$$

so that its eigenvaules read

$$m_{H,h}^2 = \frac{1}{2}\left[m_A^2 + m_Z^2 \pm \sqrt{\left(m_A^2 + m_Z^2\right)^2 - 4 m_A^2 m_Z^2 c_{2\beta}^2}\right]\,. \tag{2.29}$$

The CP-even eigenstates h and H are connected to S_1 and S_2 through

$$\begin{pmatrix} H \\ h \end{pmatrix} = \begin{pmatrix} c_\alpha & s_\alpha \\ -s_\alpha & c_\alpha \end{pmatrix} \begin{pmatrix} S_1 \\ S_2 \end{pmatrix}\,, \tag{2.30}$$

where the angle α is determined by

$$\tan 2\alpha = \tan 2\beta \frac{m_A^2 + m_Z^2}{m_A^2 - m_Z^2}\,. \tag{2.31}$$

The angle α is traditionally chosen to be negative, so from this definition it follows that $-\pi/2 < \alpha < 0$ (provided $m_A > m_Z$). These (tree-level) relations show how the neutral Higgs masses are not independent parameters of the theory. In particular, from (2.29) one can actually derive an upper bound on the lightest Higgs mass:

$$m_h < |c_{2\beta}| m_Z\,, \tag{2.32}$$

which is of course already ruled out by LEP2 results. If the above relation were valid beyond tree-level, MSSM would be already excluded by direct searches. Fortunately, these tree-level relations receive sizable higher order corrections which allow this bound to be evaded, so that the MSSM can still be a candidate scenario for NP. An impressive theoretical effort has been devoted to precision loop computations of the MSSM Higgs sector masses, see [104] and references therein for more details on the status of two-loop calculations and their implementation in computer codes for numerical evaluation of the Higgs spectrum (see also ref. [105] for the first complete three-loop result in the limit of degenerate supersymmetric particles and ref. [106] for an asymptotic expansions based result valid for some specific hierarchies of the supersymmetric particle masses).

An interesting region of the MSSM parameter space is the one with $m_A \gg m_Z$ (actually even if $m_A \gtrsim 2m_Z$ only). Then one has the so-called "decoupling limit" in which,

as it can be seen from (2.29), m_h^2 can saturate the upper bound, with $m_h^2 \sim m_Z^2 c_{2\beta}^2 +$ radiative corrections. In this case $\alpha \sim \beta - \pi/2$, which in turn implies that h couples to the SM fields basically like a SM Higgs boson. The other Higgs particles $H, A, H^\pm$ substantially become heavy and degenerate, forming an isospin doublet that decouples from sufficiently low energy experiments. Note that a similar scenario is realized in the opposite regime $m_A \ll m_Z$, where it is the H boson that becomes SM-like ("anti-decoupling limit").

2.4 Squark masses and relevant MSSM interactions

A thorough discussion of the MSSM mass spectrum and interactions arising in the MSSM is well beyond the scope of this thesis and we refer the reader to more complete references, such as ref. [107], where also a complete set of the MSSM Feynman rules can be found. Instead, only a few more aspects of the MSSM will be relevant in the following. In the present work we consider the (SUSY) QCD corrections to CP-even and CP-odd Higgs boson production at hadron colliders through gluon fusion which, as we will discuss in the next chapter, proceeds at leading order through a quark or squark loop (since no Higgs-gluon-gluon coupling is present in the Lagrangian). We will therefore spend a few words about the squark mass matrices, the Higgs-(s)quark-(s)quark interactions and the quark-squark-gluino vertices which contribute a two-loop.

Squark masses

Ignoring intergenerational mixing according to the discussion at the end of sec. 2.2, squark mass-squared matrices decompose in a series of 2×2 blocks [108], one for each flavor, resulting in mass terms in the Lagrangian of the type ($\tilde{q}$ denotes here a generic up-type or down-type squark e.g. $\tilde{t}$ or $\tilde{b}$)

$$\mathcal{L}_{MSSM} \ni \left(\tilde{q}_L^\dagger, \tilde{q}_R^\dagger\right) \mathcal{M}_{\tilde{q}}^2 \begin{pmatrix} \tilde{q}_L \\ \tilde{q}_R \end{pmatrix} , \tag{2.33}$$

where the squared mass matrix (the upper part of $\left\{\right\}$ is for up-type quarks, the lower part for down-type quarks)

$$\mathcal{M}_{\tilde{q}}^2 = \begin{pmatrix} m_{\tilde{q}_L}^2 + m_q^2 + D_{q,L}\, m_Z^2 \cos 2\beta & -m_q \left(A_q + \mu \begin{Bmatrix} \cot\beta \\ \tan\beta \end{Bmatrix} \right) \\ -m_q \left(A_q + \mu \begin{Bmatrix} \cot\beta \\ \tan\beta \end{Bmatrix} \right) & m_{\tilde{q}_R}^2 + m_q^2 + D_{q,R}\, m_Z^2 \cos 2\beta \end{pmatrix} \tag{2.34}$$

receives several contributions, which we now discuss. The LL and RR entries contain the corresponding soft SUSY-breaking masses, the quark mass (which is generated through EW SSB as in the SM) and a contribution stemming from the EW (hypercharge) D-term quartic interaction with two Higgs fields taking their VEV's, with coefficients given respectively by

$$D_{q,L} = I_{3,q} - Q_q \sin^2\theta_W , \quad D_{q,R} = Q_q \sin^2\theta_W , \tag{2.35}$$

ϕ	g_u^ϕ	g_d^ϕ
h	$\cos\alpha/\sin\beta$	$-\sin\alpha/\cos\beta$
H	$\sin\alpha/\sin\beta$	$\cos\alpha/\cos\beta$
A	$\cot\beta$	$\tan\beta$

Table 2.1: The couplings of CP-even and CP-odd Higgs mass eigenstates to up-type (u) and down-type (d) quarks.

where $I_{3,q} = \pm 1/2$ for up-type and down-type squark and Q_q is the corresponding electric charge ($\sin\theta_W$ is the weak angle). The LR and RL entries are entirely due to the soft trilinear coupling in (2.14) and the μ-term in the superpotential (2.9). The eigenvalues of such a matrix are easily found to be

$$m^2_{\tilde{q}_{1,2}} = \frac{1}{2}\left(m^2_{\tilde{q}_L} + m^2_{\tilde{q}_R} + \frac{D_{q,L}+D_{q,R}}{2}\, m_Z^2 \cos 2\beta\right) + m_q^2 \\ \pm \sqrt{\frac{1}{2}\left(m^2_{\tilde{q}_L} - m^2_{\tilde{q}_R} + \frac{D_{q,L}-D_{q,R}}{2}\, m_Z^2 \cos 2\beta\right)^2 + m_q^2\left(A_q + \mu \begin{Bmatrix}\cot\beta \\ \tan\beta\end{Bmatrix}\right)^2}, \tag{2.36}$$

where we adopt the convention that $m^2_{\tilde{q}_1} > m^2_{\tilde{q}_2}$. The mass eigenstates basis can be obtained by a rotation of the chiral fermions superpartners:

$$\begin{pmatrix}\tilde{q}_1 \\ \tilde{q}_2\end{pmatrix} = \begin{pmatrix} c_{\theta_q} & s_{\theta_q} \\ -s_{\theta_q} & c_{\theta_q}\end{pmatrix}\begin{pmatrix}\tilde{q}_L \\ \tilde{q}_R\end{pmatrix}, \tag{2.37}$$

where $\theta_{\tilde{q}}$ is the squark mixing angle, given by

$$s_{2\theta_q} = \frac{2\, m_q \left(A_q + \mu \begin{Bmatrix}\cot\beta \\ \tan\beta\end{Bmatrix}\right)}{m^2_{\tilde{q}_1} - m^2_{\tilde{q}_2}}. \tag{2.38}$$

Thus in general one expects that mixing can be large for third generation sfermions, stops in particular, while in many scenarios the eigenstates $\tilde{q}_{1,2}$ of the first two generation squarks will roughly correspond to the interaction eigenstates $\tilde{q}_{L,R}$.

Higgs-quark-quark vertices

The interaction of the neutral CP-even H_1^0 (H_2^0) Higgs boson with the quarks is analogous to that in the SM, the only difference being a rescaling of the SM couplings by a factor $1/s_\beta$ ($1/c_\beta$). The CP-odd Higgs couples to the CP-odd quarks bilinears $\bar{q}\gamma_5 q$. Up to a rescaling factor, the CP-even Higgs-quark-quark interaction terms take the standard form

(we consider only a generic up-down doublet and use the definition of the Higgs-quark-quark Yukawa coupling h_q given in (A.3))

$$\begin{aligned}\mathcal{L}_{\text{MSSM}} \ni & -\frac{gm_u}{2m_W} g_u^h \, h\bar{u}u - \frac{gm_d}{2m_W} g_d^h \, h\bar{d}d \\ & -\frac{gm_u}{2m_W} g_u^H \, H\bar{u}u - \frac{gm_d}{2m_W} g_d^H \, H\bar{d}d \,, \end{aligned} \tag{2.39}$$

The couplings of the mass eigenstates h, H are obtained from those of $H_1^0 \,, H_2^0$ with the help of (2.30). The interaction with the CP-odd Higgs is given instead by

$$\mathcal{L}_{\text{MSSM}} \ni + i\frac{gm_u}{2m_W} g_u^A \, A\bar{u}\gamma_5 u + i\frac{gm_d}{2m_W} g_d^A \, A\bar{d}\gamma_5 d \,, \tag{2.40}$$

Explicit expressions for the couplings in (2.39)-(2.40) can be found in tab. 2.1.

Higgs-squark-squark vertices

The trilinear interactions of the CP-even and CP-odd Higgses with the squarks, analogously to the case of the squark mass matrix, are more involved. They result from the many D-term and F-term contributions to the scalar potential (2.2) and from the soft SUSY-breaking trilinear vertices. We qualitatively describe their origin and refer the reader to app. A for the explicit couplings.

F-term contributions consist in the sum of (the modulus squared of) derivatives of the superpotential (2.9) with respect to one superfield. The relevant terms will thus contain quartic interactions between two Higgses and two sfermions. When one of the two Higgses is replaced by its VEV, a trilinear interaction is generated. In particular, the structure of the superpotential is such that those terms will always couple L and R sfermions together. Note that such interactions are proportional to the Yukawa couplings in the superpotential, so that they will basically be important only for third generation sfermions. A-terms are introduced in the Lagrangian in order to generate (soft) SUSY-breaking trilinear couplings between the sfermions and the Higgses, with the same structure as the ones described above but with couplings which in principle are arbitrary (see (2.14)). In our simplified framework the $\underline{\mathrm{A}}^X$ are basically zero for the first two generations.

D-term contributions are instead generation-independent. The structure of the sfermion bilinears which enter the D-term part of the scalar potential forces the resulting interaction to couple either LL or RR sfermions together with two Higgses. Again, when one of the two Higgses gets its VEV, a trilinear interaction is generated.

Quark-squark-gluino vertices

Let us now comment on the last ingredient needed for our computation. Quark-squark-gluino vertices arise from the $SU(3)_c$ contribution to the first term in the last line of the SUSY Lagrangian (2.1) and, as already noted, are genuinely supersymmetric interactions whose coupling strength is fixed by SUSY and gauge invariance. Note that in the mass

eigenstates basis the couplings will involve the entries of the sfermion mixing matrix appearing in (2.37). What we want to highlight here is that these vertices generate diagrams in which many different mass scales appear (quark, squark and gluino mass), which represents a complication if one pursues the exact evaluation of Feynman amplitudes. The computational effort grows strongly when loop diagrams are considered, so that the evaluation of two-loop contributions to gluon fusion represents a challenging task. The strategies for tackling such a challenge will be the subject of part II of this thesis. In the next chapter we will give some details about the process being studied.

Chapter 3

Neutral MSSM Higgs production at hadron colliders: gluon fusion at NLO

The total cross section for neutral Higgs boson(s) production at hadron colliders is predicted to be extremely large both in the SM and the MSSM, e.g. $\mathcal{O}(100\,\text{pb})$ for a SM Higgs at the LHC with $\sqrt{s} = 14\,\text{TeV}$. An important task for Higgs phenomenology on the theory side is the accurate determination of the cross sections, taking into account higher order effects and aiming at having all the uncertainties well under control.

In sec. 3.1 we will give a brief overview on the mechanisms of SM and MSSM Higgs production are hadron colliders. Then in sec. 3.2 we will concentrate on the gluon fusion process, introducing the hadronic cross section for (pseudo)scalar production through gluon fusion and then specializing to the cases of SM, scalar MSSM and pseudoscalar MSSM Higgs production. In each case we will recall the leading order (LO) cross section and discuss the structure of the form factors which encode the one- and two-loop contributions to the process. Explicit, original results for the two-loop virtual form factors for scalar and pseudoscalar MSSM Higgs production, will be presented in chaps. 7 and 8.

3.1 Main production mechanisms at hadron colliders

Neutral Higgs bosons phenomenology in the MSSM can in principle differ considerably from the SM case. In particular, the large number of couplings in the model and the richer spectrum of the Higgs sector (e.g. no pseudoscalar Higgs is present in the SM) have as a consequence that the couplings involved in the production/decay of a MSSM Higgs boson may be much different from those in the SM. Another complication may arise in CP violating extensions of the MSSM, where h, H, A mixing must be taken into account. The presence of the additional SUSY particle spectrum can significantly influence production and decay processes. Several production mechanisms, like the production in association with SUSY particles or in the decay of SUSY particles (or even of heavier Higgs particles),

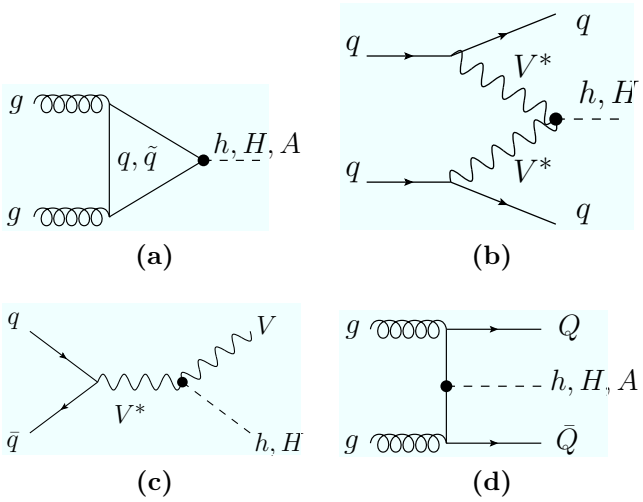

Figure 3.1: Parton level processes for MSSM Higgs production at hadron colliders: gluon fusion $gg \to h, H, A$ 3.1a, vector-boson fusion $qq \to qqV^*V^* \to qqh, qqH$ 3.1b, Higgs-strahlung $q\bar{q} \to V^* \to hV, HV$ 3.1c and the associated production $gg \to Q\bar{Q}h, Q\bar{Q}H$ 3.1d. Diagrams drawn with Jaxodraw [109]

can contribute in some regions of the MSSM parameter space. Nevertheless, if the SUSY particles are heavy enough that these processes are kinematically forbidden, the main production and decay mechanisms of Higgs bosons at hadron colliders are basically the same as in the SM. Moreover, as already illustrated in chap. 2, there is also the possibility ("decoupling limit", roughly for $m_A \gtrsim 2m_Z$) that the light neutral CP-even MSSM Higgs boson mimics the SM Higgs boson.

A complete survey of the production mechanisms relevant for hadron colliders searches is beyond the scope of this thesis. Below we will only summarize the main features of the most important production channels and highlight some differences between the SM and the MSSM case.

The main SM Higgs production mechanisms at hadron colliders are those involving the Higgs couplings to the heavy particles, namely the massive vector bosons, the top quark and, to a lesser extent, the bottom quark. The gluon fusion channel, although the Higgs-gluon-gluon coupling originates at one-loop, is strongly enhanced by the high gluon luminosity at hadron colliders and by the high sensitivity of the Higgs coupling to the mass of the particle running in the loop. The parton level processes contributing to the above mechanisms are shown in fig. 3.1. Figure 3.2 shows the SM cross section for the main channels at the LHC for the two values of the center of mass (c.o.m.) energy, $\sqrt{s} = 7\,\text{TeV}$ (the current LHC c.o.m. energy) and $\sqrt{s} = 14\,\text{TeV}$ (LHC design c.o.m. energy). Figures 3.3 and 3.4 show the same cross sections in the MSSM case ($\sqrt{s} = 14\,\text{TeV}$ only), respectively for scalar and pseudoscalar Higgs production, considering only the QCD corrections and focusing on two representative scenarios, $\tan\beta = 3$ and $\tan\beta = 30$. For a comprehensive and rather recent review of Higgs phenomenology, respectively in the SM and in the MSSM,

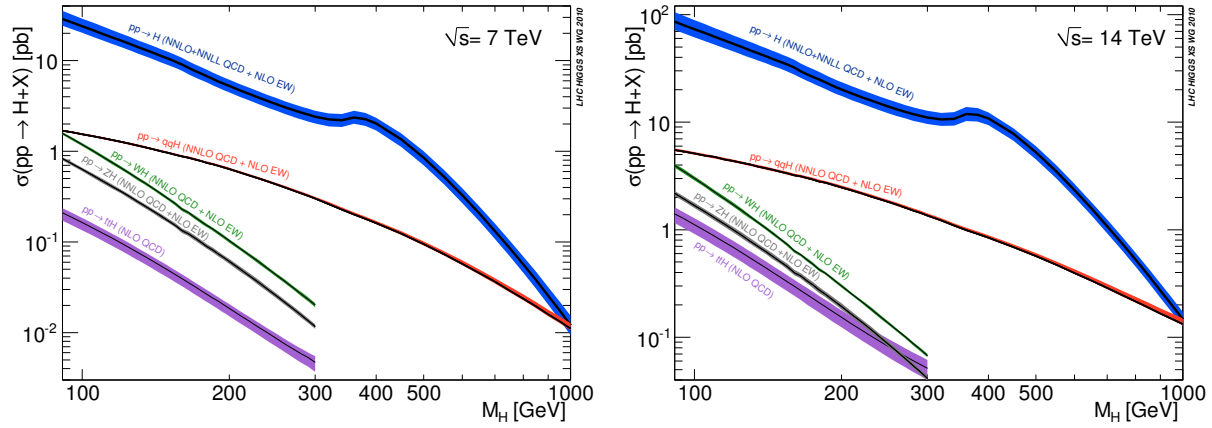

(a) **(b)**

Figure 3.2: SM Higgs boson production cross section at the LHC as a function of $m_{H_{\rm SM}}$ for (a) $\sqrt{s} = 7\,\text{TeV}$ and (b) $\sqrt{s} = 14\,\text{TeV}$. Each curve represents the contribution of the different channels. The most important channel is gluon fusion. The curves below (in order of importance), show the cross section for vector boson fusion, associated production with W and Z, associated production with heavy quarks ($t\bar{t}$ pairs, in particular). Figure from ref. [110].

see e.g. refs. [111] and [112].

Gluon fusion

The name gluon fusion refers to the partonic process $gg \to \phi$. As already noted, despite the fact that the Higgs-gluon-gluon coupling is absent at tree level and therefore only arises as a loop suppressed effect, the large mass of the heavy particles the Higgs couples to and the high gluon luminosity at hadron colliders renders the gluon fusion channel the prominent production mechanism. Moreover, since the process starts at one-loop, it is in principle sensitive to loops of non SM particles. Actually, in the MSSM, the squarks contribution scales as the ratio $m_q^2/m_{\tilde{q}_1}^2$, so the squarks contribute only if they are not too heavy (masses less than, say, 500 GeV). Another interesting effect arises in the MSSM, in which the relative contribution of top and bottom quarks is weighted by $\tan\beta$ as we will see in sec. 3.2.3. In particular, the bottom contribution is enhanced for large values of $\tan\beta$ despite $m_b \ll m_t$. This channel will be the object of our study in this work in the following chapters, both in the case of scalar and pseudoscalar Higgs. For more details on the hadronic cross section and a discussion of the NLO contributions see sec. 3.2 below.

Vector boson fusion

Vector boson fusion (VBF) is the partonic process $qq \to VV^* \to qq + \phi$. The A boson cannot be produced in VBF at tree level if we assume a CP conserving MSSM. It is the second important channel in the SM, which becomes competitive with gluon fusion for

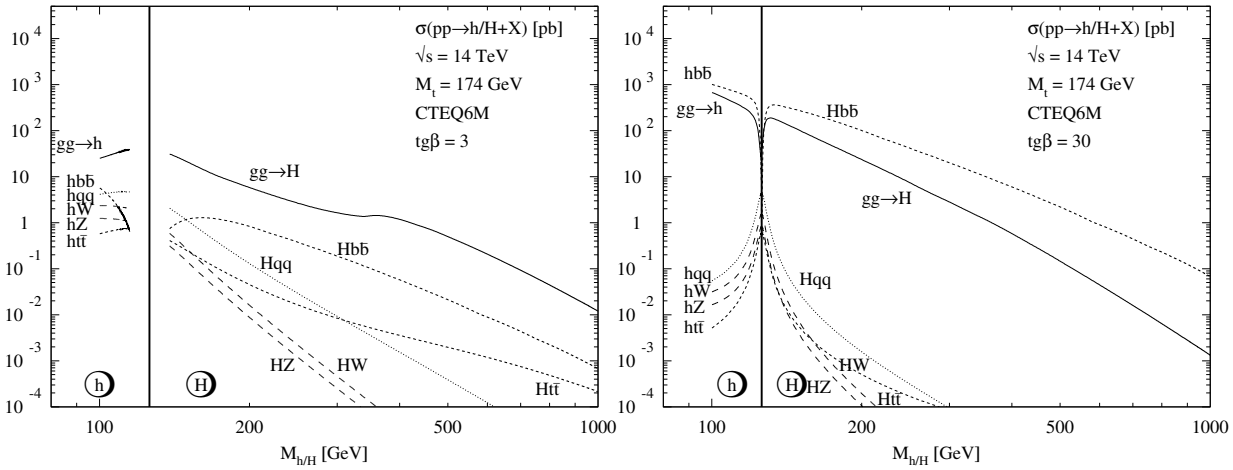

(a) $\tan\beta = 3$ **(b)** $\tan\beta = 30$

Figure 3.3: Neutral ($\phi = h, H$) MSSM Higgs production cross sections at the LHC ($\sqrt{s} = 14\,\text{TeV}$) for gluon fusion $gg \to \phi$, vector-boson fusion $qq \to qqVV \to qq\phi$, Higgs-strahlung $q\bar{q} \to V^* \to \phi V$ and the associated production $gg, q\bar{q} \to b\bar{b}\phi/t\bar{t}\phi$, including all known QCD corrections. Figure from ref.[113]

large Higgs mass. In the MSSM it is an important channel in the decoupling (antidecoupling) limit, $m_A \gtrsim 2m_Z$ ($m_A \lesssim 2m_Z$), where the h (H) boson becomes SM-like. In other regions of the parameter space, the cross section is typically suppressed by the structure of SUSY couplings. Still, it may provide essential information of the Higgs coupling to the electroweak vector bosons.

Associated production with $V = W, Z$

Associated production together with the massive vector bosons, or *Higgsstrahlung*, $q\bar{q} \to V^* \to \phi + V$ ($V = W, Z$) is another process which can be important in the (anti)decoupling limit. Againt, the A boson cannot be produced in association with W, Z bosons at tree level if we assume a CP conserving MSSM. The cross section is considereably smaller than that for the gluon fusion channel, but the advantage is that one can use the clean signature of the leptonic decays of the vector bosons in order to discriminate Higgs events, which come with a huge QCD background. We note that this process ($V = Z$) is important also at e^+e^- colliders.

Associated production with heavy quarks

The process $gg, q\bar{q} \to \phi + Q\bar{Q}$, where Q is a heavy quark, is important for low values of the Higgs mass. Top quarks decay almost exclusively in W and b quarks, which produce b-jets. It is clear that a perfect understanding of the QCD background and of the b-tagging procedures is essential if one wants to disentangle the signal for this process from the background. On the other hand, it is worth noting that this process would allow to

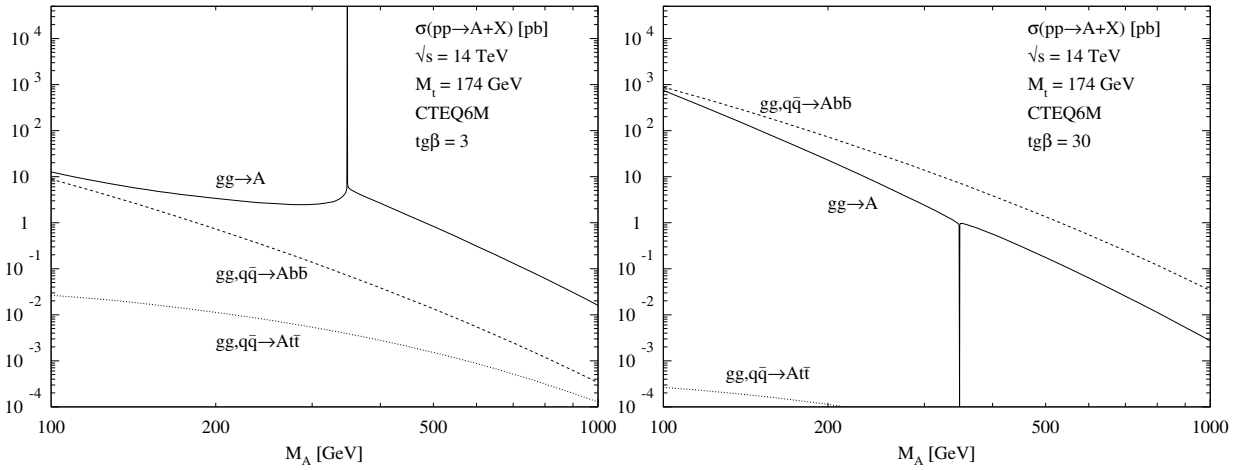

(a) $\tan\beta = 3$ **(b)** $\tan\beta = 30$

Figure 3.4: Neutral ($\phi = A$) MSSM Higgs production cross sections at the LHC ($\sqrt{s} = 14\,\text{TeV}$) for gluon fusion $gg \to A$ and the associated production $gg, q\bar{q} \to b\bar{b}A/t\bar{t}A$, including all known QCD corrections. Figure from ref.[113]

measure the Higgs-Q-Q coupling properties. Concerning the MSSM, a last comment is in order: as shown in figs. 3.3b and 3.4b, for large values of $\tan\beta$ the case $Q = b$ becomes dominant, despite the smallness of m_b.

3.2 Hadronic cross section for $gg \to \phi$ ($\phi = h, H, A$)

In this section we recall for completeness some general results on scalar and pseudoscalar Higgs boson production via gluon fusion. The hadronic cross section at c.o.m. energy $\sqrt{s}$ can be written as ($\phi = h, H, A$)

$$\sigma(h_1{+}h_2 \to \phi{+}X) = \sum_{a,b} \int_0^1 dx_1 dx_2 \; f_{a,h_1}(x_1,\mu_F)\, f_{b,h_2}(x_2,\mu_F) \int_0^1 dz\, \delta\left(z - \frac{\tau_\phi}{x_1 x_2}\right) \hat{\sigma}_{ab}(z)\,, \tag{3.1}$$

where $\tau_\phi = m_\phi^2/s$, μ_F is the factorization scale, $f_{a,h_i}(x,\mu_F)$ the parton density of the colliding hadron h_i for the parton of type a (for $a = g, q, \bar{q}$), and $\hat{\sigma}_{ab}$ the cross section for the partonic subprocess $ab \to \phi + X$ at the center-of-mass energy $\hat{s} = x_1\, x_2\, s = m_\phi^2/z$. The partonic cross section can be written in terms of the LO contribution $\sigma^{(0)}$ and a coefficient function $G_{ab}(z)$:

$$\hat{\sigma}_{ab}(z) = \sigma^{(0)}\, z\, G_{ab}(z)\,. \tag{3.2}$$

The LO cross section can always be written as

$$\sigma^{(0)} = \frac{G_\mu\, \alpha_s^2(\mu_R)}{128\sqrt{2}\,\pi} \left|\mathcal{H}_\phi^{1\ell}\right|^2\,, \tag{3.3}$$

where G_μ is the muon decay constant, $\alpha_s(\mu_R)$ is the strong gauge coupling expressed in the $\overline{\rm MS}$ renormalization scheme at the scale μ_R and $\mathcal{H}_\phi^{1\ell}$ is the one-loop contribution to the ϕ-gluon-gluon form factor $\mathcal{H}_\phi$, which up to and including NLO terms can be decomposed as

$$\mathcal{H}_\phi = \mathcal{H}_\phi^{1\ell} + \frac{\alpha_s}{\pi}\,\mathcal{H}_\phi^{2\ell} + \mathcal{O}(\alpha_s^2)\,. \tag{3.4}$$

In the same spirit, the coefficient function $G_{ab}(z)$ in eq. (3.2) can be decomposed as

$$G_{ab}(z) = G_{ab}^{(0)}(z) + \frac{\alpha_s}{\pi}\,G_{ab}^{(1)}(z) + \mathcal{O}(\alpha_s^2)\,, \tag{3.5}$$

with the LO contribution given only by the gluon-fusion channel:

$$G_{ab}^{(0)}(z) = \delta(1-z)\,\delta_{ag}\,\delta_{bg}\,. \tag{3.6}$$

The NLO terms include, besides the gg channel, also the one-loop induced processes $gq \to q\phi$ and $q\bar{q} \to g\phi$:

$$\begin{aligned} G_{gg}^{(1)}(z) = \delta(1-z)\left[C_A\,\frac{\pi^2}{3} + \beta_0\,\ln\left(\frac{\mu_R^2}{\mu_F^2}\right) + 2\,\mathrm{Re}\left(\frac{\mathcal{H}_\phi^{2\ell}}{\mathcal{H}_\phi^{1\ell}}\right)\right] \\ + P_{gg}(z)\,\ln\left(\frac{\hat{s}}{\mu_F^2}\right) + C_A\,\frac{4}{z}\,(1-z+z^2)^2\,\mathcal{D}_1(z) + C_A\,\mathcal{R}_{gg}^\phi\,, \end{aligned} \tag{3.7}$$

$$G_{q\bar{q}}^{(1)}(z) = \mathcal{R}_{q\bar{q}}^\phi\,, \qquad G_{qg}^{(1)}(z) = P_{gq}(z)\left[\ln(1-z) + \frac{1}{2}\ln\left(\frac{\hat{s}}{\mu_F^2}\right)\right] + \mathcal{R}_{qg}^\phi\,, \tag{3.8}$$

where the LO Altarelli-Parisi splitting functions are

$$P_{gg}(z) = 2\,C_A\left[\mathcal{D}_0(z) + \frac{1}{z} - 2 + z(1-z)\right]\,, \tag{3.9}$$

$$P_{gq}(z) = C_F\,\frac{1+(1-z)^2}{z}\,. \tag{3.10}$$

In the equations above, $C_A = N_c$ and $C_F = (N_c^2-1)/(2\,N_c)$ (N_c being the number of colors), $\beta_0 = (11\,C_A - 2\,N_f)/6$ (N_f being the number of active flavors) is the one-loop β-function of the strong coupling in the SM, and

$$\mathcal{D}_i(z) = \left[\frac{\ln^i(1-z)}{1-z}\right]_+\,, \tag{3.11}$$

where the plus prescription is defined by

$$\int_0^1 \mathrm{d}x f(x) g(x)_+ = \int_0^1 \mathrm{d}x\,[f(x) - f(1)]\,g(x)\,. \tag{3.12}$$

The gg-channel contribution, eq. (3.7), involves two-loop virtual corrections to $gg \to \phi$ and one-loop real corrections from $gg \to \phi g$. The former, regularized by the infrared-singular part of the real emission cross section, are displayed in the first line of eq. (3.7).

The second line contains the non-singular contribution from the real gluon emission in the gluon fusion process. The latter contribution as well as the ones due to the $q\bar{q} \to \phi g$ annihilation channel and the quark-gluon scattering channel, eq. (3.8), are obtained from one-loop diagrams where only quarks (or squarks, in the MSSM) circulate in the loop.

In the following sections we will specialize (3.3) to the cases of SM (for completeness), scalar MSSM and pseudoscalar MSSM Higgs production, by giving the explicit expression of the form factor $\mathcal{H}_\phi^{1\ell}$ in $\sigma^{(0)}$ and discussing the origin of the NLO contributions.

3.2.1 SM Higgs production ($gg \to H_{\rm SM}$)

We will specialize here to the SM Higgs boson $\phi = H_{\rm SM}$. We are interested in the QCD corrections to the gluon fusion process, so we will focus on the contribution due to quarks. As well known, the coupling of $H_{\rm SM}$ to fermions $f\bar{f}$ is proportional to m_f/v, where m_f is the fermion mass and v is the vacuum expectation value of the (real part of the down-type component of the) Higgs doublet.

Neglecting the contributions of the first two generations by virtue of the smallness of their Higgs coupling, the SM one-loop contribution to the form factor (3.4) which enters (3.3) can be written as

$$\mathcal{H}_{H_{\rm SM}}^{1\ell} = T_F \left[\mathcal{G}_{1/2}^{1\ell}(\tau_t) + \mathcal{G}_{1/2}^{1\ell}(\tau_b)\right] , \tag{3.13}$$

where $T_F = 1/2$ is a color factor and $\tau_q = 4\, m_q^2/m_{H_{\rm SM}}^2$. The function $\mathcal{G}_{1/2}^{1\ell}(\tau)$ originates from the quark-loop diagram, which represents the sole contribution at LO, and is defined as:

$$\mathcal{G}_{1/2}^{1\ell}(\tau) = -2\,\tau \left[1 - \frac{1-\tau}{4}\, \ln^2\left(\frac{\sqrt{1-\tau}-1}{\sqrt{1-\tau}+1}\right)\right] . \tag{3.14}$$

The analytic continuation is obtained with the replacement $m_{H_{\rm SM}}^2 \to m_{H_{\rm SM}}^2 + i\varepsilon$. It is interesting to consider the function $\mathcal{G}_{1/2}^{1\ell}$ in the limit in which the Higgs boson mass is much smaller or much larger than the mass of the particle running in the loop. In the first case ($\tau \gg 1$), which applies to the top contributions if the Higgs is light as suggested by the EW global fits (as discussed in sec. 1.1),

$$\mathcal{G}_{1/2}^{1\ell}(\tau) \to -\frac{4}{3} - \frac{14}{45\,\tau} \;+\; \mathcal{O}(\tau^{-2}) , \tag{3.15}$$

while in the opposite case ($\tau \ll 1$), which is relevant for the bottom quark,

$$\mathcal{G}_{1/2}^{1\ell}(\tau) \to -2\,\tau + \frac{\tau}{2} \ln^2\left(\frac{-4}{\tau}\right) \;+\; \mathcal{O}(\tau^2) . \tag{3.16}$$

The crucial remark is that if the quark running in the loop is much heavier than the Higgs boson, its contribution goes to a constant, while if the quark running in the loop is much lighter than the Higgs boson, its contribution is suppressed by one power of τ. For the actual hierarchy between m_b and $m_{H_{\rm SM}}$ (given the known SM Higgs bounds, see sec. 1.1), in the SM the bottom contribution can be safely neglected.

In this approximation, two-loop contributions to the form factor arise in the SM only from diagrams with virtual top quarks and gluons. If the Higgs is below the top-pair production thresold, it has been shown in ref. [39] that the approximation of keeping only the zeroth-order in τ in the two-loop top contributions to the cross section allows to reproduce the full result with an accuracy of a few percent. The important advantage of such an approximation is that it allows for compact analytic results that can be implemented in computer codes for a fast and efficient evaluation of the Higgs production cross section.

The NLO real corrections have been first evaluated in ref. [114] in the $\tau \gg 1$ limit and then in ref. [115] also in the $\tau \ll 1$ limit. General, exact expressions for the functions $\mathcal{R}^{\phi}_{gg}$, $\mathcal{R}^{\phi}_{q\bar{q}}$, $\mathcal{R}^{\phi}_{qg}$ entering (3.7) and (3.8) for $\phi = H_{\rm SM}$ can be found in ref. [37] where, together with an independent evaluation of the fermion loop contributions, also new results for the contributions due to a colored massive scalar loop were presented.

3.2.2 Scalar MSSM Higgs production ($gg \to h, H$)

Concerning the MSSM Higgs bosons, we consider now the production of the CP-even Higgs bosons, $\phi = h, H$, via gluon fusion. In this case the one-loop term of (3.4), which enters the LO cross section (3.3), can be written as

$$\mathcal{H}^{1\ell}_h = T_F \left(-\sin\alpha\, \mathcal{H}^{1\ell}_1 + \cos\alpha\, \mathcal{H}^{1\ell}_2 \right) , \tag{3.17}$$

$$\mathcal{H}^{1\ell}_H = T_F \left(\cos\alpha\, \mathcal{H}^{1\ell}_1 + \sin\alpha\, \mathcal{H}^{1\ell}_2 \right) , \tag{3.18}$$

where α is the mixing angle in the CP-even Higgs sector of the MSSM. $\mathcal{H}_i$ $(i = 1, 2)$ are the form factors for the coupling of the neutral, CP-even component of the Higgs doublet H_i with two gluons, which we decompose in one- and two-loop parts as

$$\mathcal{H}_i = \mathcal{H}^{1\ell}_i + \frac{\alpha_s}{\pi}\, \mathcal{H}^{2\ell}_i + \mathcal{O}(\alpha_s^2) . \tag{3.19}$$

The one-loop form factors $\mathcal{H}^{1\ell}_1$ and $\mathcal{H}^{1\ell}_2$ contain contributions from diagrams involving quarks or squarks. The two-loop form factors $\mathcal{H}^{2\ell}_1$ and $\mathcal{H}^{2\ell}_2$ contain contributions from diagrams involving quarks, squarks, gluons and gluinos. Focusing on the contributions involving the third-generation quarks and squarks, and exploiting the structure of the Higgs-quark-quark and Higgs-squark-squark couplings, the form factors $\mathcal{H}_i$ can be written to all orders in the strong interactions as [34]

$$\mathcal{H}_1 = \lambda_t \left[m_t\, \mu\, s_{2\theta_t}\, F_t + m_Z^2\, s_{2\beta}\, D_t \right] + \lambda_b \left[m_b\, A_b\, s_{2\theta_b}\, F_b + 2\, m_b^2\, G_b + 2\, m_Z^2\, c_\beta^2\, D_b \right] , \tag{3.20}$$

$$\mathcal{H}_2 = \lambda_b \left[m_b\, \mu\, s_{2\theta_b}\, F_b - m_Z^2\, s_{2\beta}\, D_b \right] + \lambda_t \left[m_t\, A_t\, s_{2\theta_t}\, F_t + 2\, m_t^2\, G_t - 2\, m_Z^2\, s_\beta^2\, D_t \right] . \tag{3.21}$$

In the equations above $\lambda_t = 1/\sin\beta$ and $\lambda_b = 1/\cos\beta$ and the parameters entering the equations above have been defined in chap. 2. Note that A_q (for $q = t, b$) are the soft SUSY-breaking Higgs-squark-squark couplings in the simplified framework described at the end of sec. 2.2). The functions F_q and G_q appearing in eqs. (3.20) and (3.21) denote the contributions controlled by the third-generation Yukawa and A-term couplings, while

D_q denotes the contribution controlled by the electroweak, D-term-induced Higgs-squark-squark couplings. The latter can be decomposed as

$$D_q = \frac{I_{3q}}{2}\,\widetilde{G}_q + c_{2\theta_{\tilde{q}}}\left(\frac{I_{3q}}{2} - Q_q\, s^2_{\theta_W}\right)\widetilde{F}_q\,, \tag{3.22}$$

where I_{3q} and Q_q denote respectively the third component of the electroweak isospin and the electric charge of the quark q, while θ_W is the weak angle.
The one-loop functions entering $\mathcal{H}_1^{1\ell}$ and $\mathcal{H}_2^{1\ell}$ are:

$$F_q^{1\ell} = \widetilde{F}_q^{1\ell} = \frac{1}{2}\left[\frac{1}{m^2_{\tilde{q}_1}}\mathcal{G}_0^{1\ell}(\tau_{\tilde{q}_1}) - \frac{1}{m^2_{\tilde{q}_2}}\mathcal{G}_0^{1\ell}(\tau_{\tilde{q}_2})\right], \tag{3.23}$$

$$G_q^{1\ell} = \frac{1}{2}\left[\frac{1}{m^2_{\tilde{q}_1}}\mathcal{G}_0^{1\ell}(\tau_{\tilde{q}_1}) + \frac{1}{m^2_{\tilde{q}_2}}\mathcal{G}_0^{1\ell}(\tau_{\tilde{q}_2}) + \frac{1}{m_q^2}\mathcal{G}_{1/2}^{1\ell}(\tau_q)\right], \tag{3.24}$$

$$\widetilde{G}_q^{1\ell} = \frac{1}{2}\left[\frac{1}{m^2_{\tilde{q}_1}}\mathcal{G}_0^{1\ell}(\tau_{\tilde{q}_1}) + \frac{1}{m^2_{\tilde{q}_2}}\mathcal{G}_0^{1\ell}(\tau_{\tilde{q}_2})\right], \tag{3.25}$$

where $\tau_k \equiv 4\,m_k^2/m_\phi^2$, the function $\mathcal{G}_0^{1\ell}$ reads

$$\mathcal{G}_0^{1\ell}(\tau) = \tau\left[1 + \frac{\tau}{4}\,\ln^2\left(\frac{\sqrt{1-\tau}-1}{\sqrt{1-\tau}+1}\right)\right], \tag{3.26}$$

and $\mathcal{G}_{1/2}^{1\ell}$ has been defined in (3.14). As usual, the analytic continuation is obtained with the replacement $m_\phi^2 \to m_\phi^2 + i\varepsilon$. We recall the behavior of $\mathcal{G}_0^{1\ell}$ in the limit in which m_ϕ is much smaller or much larger than the mass of the particle running in the loop. In the first case, i.e. $\tau \gg 1$,

$$\mathcal{G}_0^{1\ell} \to -\frac{1}{3} - \frac{8}{45\,\tau} \;+\; \mathcal{O}(\tau^{-2})\,, \tag{3.27}$$

while in the opposite case, i.e. $\tau \ll 1$,

$$\mathcal{G}_0^{1\ell} \to \tau \;+\; \mathcal{O}(\tau^2)\,, \tag{3.28}$$

The two-loop top/stop contributions to the form factors $\mathcal{H}_{1,2}^{2\ell}$ entering eq. (3.7) are fully under control when the mass ratios between the ϕ boson and the particles running in the loops allow for the evaluation of the relevant diagrams via a Taylor expansion in m_ϕ. In most of the MSSM parameter space the lightest Higgs h is sufficiently light. On the other hand, the H boson is light enough only in specific regions of the parameter space. This scenario has been extensively studied in the literature (see e.g. [34] and the references therein) and it was also shown that the zero-order term in the series is already a very good approximation of the full result, as in the SM. Even if the H boson is moderately heavy (but still below the top-pair production threshold), neglecting the first-order contributions proves to be a still acceptable, although worse, approximation.

The case in which the Higgs mass is close to or above the first physical threshold is completely different. In general, Taylor-expanded evaluations of the relevant diagrams are

no longer viable, due to the presence of the light particles in the loops. Thus, the diagrams must be evaluated either exactly or via an asymptotic expansion in the large masses. An exact evaluation of the two-loop quark-squark-gluino diagrams is well beyond our current possibilities due to the presence of a large number of different mass scales (up to four different particles running in the loops and the center of mass energy $s = m_\phi$). The two-loop bottom-sbottom-gluino contributions have been considered (for in ref. [42] (and then confirmed in ref. [43]), where compact analytic formulae were computed via an asymptotic expansion in the large supersymmetric particle masses valid up to and including terms of $\mathcal{O}(m_b^2/m_\phi^2)$, $\mathcal{O}(m_b/M)$ and $\mathcal{O}(m_Z^2/M^2)$ (assuming that the Higgs is below the top-pair production threshold).

In the case of top/stop contributions to the production of a Higgs which is not too far from the top-pair threshold, an asymptotic expansion in the large M should give a more accurate determination of the NLO cross section than a Taylor expansion in the small momentum. No such results have been made available so far. In chap. 7 we present our result for the top/stop contribution, obtained by combining earlier results in the literature with a new calculation of the top-stop-gluino diagrams obtained via an asymptotic expansion valid up to and including $\mathcal{O}(m_\phi^2/M^2)$, $\mathcal{O}(m_t^2/M^2)$ and $\mathcal{O}(m_Z^2/M^2)$, where M is a superparticle mass and no specific hierarchy between m_ϕ^2 and m_t^2 is assumed.

Concerning the NLO one-loop real corrections, these arise from diagrams involving either a fermion or a squark loop. General expressions for the functions $\mathcal{R}_{gg}^{\phi}$, $\mathcal{R}_{q\bar{q}}^{\phi}$, $\mathcal{R}_{qg}^{\phi}$, describing both contributions for general Higgs-fermion-fermion and Higgs-scalar-scalar couplings and valid for arbitrary values of the Higgs mass, can be found in ref. [37]. Such formulae have been specialized to the case of relatively light CP-even MSSM Higgs production in ref. [42], where they are provided in a compact form suitable for an efficient numerical evaluation. There the contributions due to top, stop and sbottom loops is evaluated in the approximation of neglecting the Higgs mass, while the contribution due to the bottom loop is kept exact. Analogous formulae can be derived in our approximation by suitably combining and expanding the general results of ref. [37].

3.2.3 Pseudoscalar MSSM Higgs production ($gg \to A$)

Here we will discuss the case of pseudoscalar Higgs boson production through gluon fusion ($\phi = A$). The form factor for the coupling of the pseudoscalar A with two gluons decomposes as usual in one- and two-loop parts as

$$\mathcal{H}_A = \mathcal{H}_A^{1\ell} + \frac{\alpha_s}{\pi}\mathcal{H}_A^{2\ell} + \mathcal{O}(\alpha_s^2)\,. \tag{3.29}$$

Due to the structure of the pseudoscalar coupling to squarks (see sec. 8.3), only diagrams involving top or bottom quarks contribute to the one-loop form factor $\mathcal{H}_A^{1\ell}$. The latter can be decomposed into top and bottom contributions as

$$\mathcal{H}_A^{1\ell} = T_F\left[\cot\beta\,\mathcal{K}^{1\ell}(\tau_t) + \tan\beta\,\mathcal{K}^{1\ell}(\tau_b)\right], \tag{3.30}$$

where $\tau_q = 4\,m_q^2/m_{_A}^2$ and

$$\mathcal{K}^{1\ell}(\tau) = \frac{\tau}{2}\,\ln^2\left(\frac{\sqrt{1-\tau}-1}{\sqrt{1-\tau}+1}\right)\,. \tag{3.31}$$

We recall the behavior of $\mathcal{K}^{1\ell}$ in the limit in which the pseudoscalar mass is much smaller or much larger than twice the mass of the particle running in the loop. In the first case, i.e. $\tau \gg 1$, which may apply to the top contribution if $m_{_A}$ is relatively small,

$$\mathcal{K}^{1\ell}(\tau) \;\longrightarrow\; -2 - \frac{2}{3\tau} \;+\; \mathcal{O}(\tau^{-2})\,, \tag{3.32}$$

while in the opposite case, i.e. $\tau \ll 1$, which is relevant for the bottom contribution,

$$\mathcal{K}^{1\ell}(\tau) \;\longrightarrow\; \frac{\tau}{2}\,\ln^2\left(\frac{-4}{\tau}\right) \;+\; \mathcal{O}(\tau^2)\,. \tag{3.33}$$

The analytic continuation of $\mathcal{K}^{1\ell}(\tau)$ corresponds to the replacement $m_{_A}^2 \to m_{_A}^2 + i\varepsilon$, thus the imaginary part of eq. (3.33) can be recovered via the replacement $\ln(-4/\tau) \to \ln(4/\tau) - i\pi$.

The two-loop form factor $\mathcal{H}_{_A}^{2\ell}$ entering the one-loop/two-loop interference term in the first line of (3.7) receives contributions from diagrams involving quarks and gluons, as well as from diagrams involving quarks, squarks and gluinos. The contributions from two-loop diagrams with quarks and gluons valid for any Higgs mass were first computed in ref. [4], and later confirmed in ref. [36]. As a consequence of the A-squark-squark coupling structure, no two-loop contributions with squarks and gluons are allowed. The contribution to $\mathcal{H}_{_A}^{2\ell}$ arising from top-stop-gluino diagrams was computed in ref. [51] in the limit of vanishing $m_{_A}$ but the analytic result for generic values of the stop and gluino masses was deemed too voluminous to be explicitly displayed and was instead made available in the Fortran code `evalcsusy.f` [32, 33]. No genuine two-loop calculation has been made available so far for the contribution arising from quark-squark-gluino diagrams when such approximation cannot be done, that is when $m_{_A}$ is above or not too far from the threshold for quark-pair production. Also, no compact analtytic formulae for the case of vanishing $m_{_A}$ have ever been made available. Concerning the real NLO contributions, general expressions for the functions $\mathcal{R}_{gg}^{_A}$, $\mathcal{R}_{q\bar{q}}^{_A}$, $\mathcal{R}_{qg}^{_A}$ entering the coefficient functions (3.7)-(3.8) were first computed in ref. [4] (see also ref. [116]). In app. C.1 we present our independent results. We compared our formulae with the corresponding results in ref. [4] and found full agreement.

In chap. 8 we present our original results for the two-loop virtual contributions. First, we have computed the two-loop diagrams via a Taylor expansion in the small external momenta, up to and including terms of $\mathcal{O}(m_{_A}^2/m_t^2)$ and $\mathcal{O}(m_{_A}^2/M^2)$. We provide compact analytic formulae for the terms of order zero in $m_{_A}$ and investigate the effect of the first-order terms. Then, we have also evaluated the same two-loop virtual contributions via an asymptotic espansion in the large supersymmetric masses valid up to and including terms of $\mathcal{O}(m_{_A}^2/M^2)$ and $\mathcal{O}(m_t^2/M^2)$, without assuming any particular hierarchy between $m_{_A}^2$ and m_t^2. These results are expected to be a better approximation of the full result when $m_{_A}$

is near threshold. As a byproduct, we obtained formulae for the bottom-sbottom-gluino contributions through the obvious replacements of masses and couplings and a further expansion in the small ratio m_b^2/m_A^2. In particular, we provide results valid up to and including $\mathcal{O}(m_b^2/m_A^2)$, $\mathcal{O}(m_b/M)$, that is at the same expansion order as the ones for the scalar Higgs production computed in ref. [34] (where of course m_A is replaced by m_ϕ, $\phi = h, H$).

Part II

Tools

Chapter 4

Regularization and Renormalization of loop integrals

In this chapter we will discuss two equivalent strategies for overcoming the ultraviolet (UV) and infrared (IR) divergences of loop integrals.

In Dimensional Regularization (DREG) the integrals are computed in d-dimensional spacetime, where $d < 4$ in such a way that the integral converges in the UV and can be evaluated. The 4-dimensional result is then recovered by analytic continuation. It is interesting to note that also IR divergences can be regularized in DREG.

Pauli-Villars regularization (PVREG) is instead based on a systematic subtraction procedure which renders each UV divergent integral finite, while keeping $d = 4$. In this case a suitable treatment of IR divergences is needed.

The chapter is structured as follows. In sec. 4.1 and sec. 4.2 we will present respectively DREG and PVREG, discussing the issue of γ_5 and the violation of SUSY Ward identities in DREG and the regularization of IR divergences. In sec. 4.3 we will briefly comment on the renormalization procedure we followed in our computation.

4.1 Dimensional Regularization (DREG)

The Dimensional Regularization (DREG) scheme introduced in refs. [55, 117–119] (see [120] for a systematic and formal development) represents an extremely convenient means to regulate the UV divergences of perturbation theory, two important features being its manifest Lorentz invariance and the fact the it does respect all the symmetries (hence the Ward identies) in non-abelian gauge theories. As we will see below, IR divergences can be regularized with basically the same strategy. DREG represents thus a very efficient regularization scheme and has actually become the *de facto* standard in loop computations. Below we will discuss the two main drawbacks of DREG, namely the treatment of γ_5 in chiral theories, which can be cumbersome, and the fact that it breaks SUSY Ward identities. Let us now recall some basic facts about DREG.

In DREG the loop integrals are computed in d-dimensional spacetime, where $d = 4 - 2\epsilon$

and is chosen sufficiently smaller than 4 in such a way that the integral converges in the UV and can be evaluated. The 4-dimensional result is recovered by analytic continuation and the UV divergences show up as poles in the variable ϵ, irrespectively of them being quadratic, linear or logarithmic. Consider for instance the integral

$$\int \frac{\mathrm{d}^4 p}{(2\pi^4)} \frac{1}{[p^2 - \Delta + i\varepsilon]^\alpha} \longrightarrow \mu^{4-d} \int \frac{\mathrm{d}^d p}{(2\pi^d)} \frac{1}{[p^2 - \Delta + i\varepsilon]^\alpha} \equiv I_\alpha^{(d)}(\Delta)\,. \tag{4.1}$$

In $d = 4$ the above integral is quadratically (logarithmically) divergent for $\alpha = 1$ ($\alpha = 2$). We note that in d-dimensions we must introduce an arbitrary mass scale μ in order to preserve the original mass dimension of the integral. Dimensional regularization is most easily performed on Wick-rotated integrals: consider the p^0 integral as a contour integral in the complex p^0 plane. The location of the poles, crucially determined by the Feynman prescription $+i\varepsilon$, and the fact that the integrand falls off sufficiently rapidly at large p^0 for a convenient choice of d (for a given α), allow us to effectively rotate the contour counterclockwise by $\pi/2$ without hitting any pole. With the replacements

$$p^0 = i p_E^0\,, \quad \vec{p} = \vec{p}_E\,, \tag{4.2}$$

since now $-p^2 = +p_E^2 = (p^0)^2 + |\vec{p}|^2$, we obtain the Euclidean version of our original Minkowskian integral which can be evaluated in spherical coordinates with standard techniques:

$$I_\alpha^{(d)}(\Delta) = \mu^{4-d} \int_{\mathbb{R}^d} \frac{\mathrm{d}^d p_E}{[-p_E^2 - \Delta + i\varepsilon]^\alpha} \tag{4.3}$$

$$= \mu^{4-d}\,(-1)^\alpha \int_{\Omega_d} \mathrm{d}\Omega_d \int_0^\infty \frac{\mathrm{d}|p|\,|p|^{d-1}}{[|p|^2 + \Delta - i\varepsilon]^\alpha} \tag{4.4}$$

$$= \mu^{4-d}\,\frac{i(-1)^\alpha}{(4\pi)^{d/2}}\,\frac{\Gamma(\alpha - d/2)}{\Gamma(\alpha)}\,\left(\frac{1}{\Delta - i\varepsilon}\right)^{\alpha - d/2}\,, \tag{4.5}$$

where Ω_d is the d-dimensional solid angle and $\Gamma(z)$ is the Euler Gamma function

$$\Gamma(z) = \int_0^\infty \mathrm{d}t\, t^{z-1}\, \mathrm{e}^{-t}\,, \tag{4.6}$$

which has the property $\Gamma(n) = (n-1)!$ for $n = 1, 2, \ldots$. The function $\Gamma(z)$ is analytic everywhere in the complex plane except for non-positive integer values of its argument, $z = 0, -1, -2, \ldots$, where it develops simple poles. Its Laurent expansion around $z = 0$ reads

$$\Gamma(z) = \frac{1}{z} - \gamma + \mathcal{O}(z)\,, \tag{4.7}$$

where $\gamma_E \simeq 0.5772$ is the Euler-Mascheroni constant. The expansion around all the other poles can be obtained by using the above equation and exploiting the property

$$(z-1)\Gamma(z-1) = \Gamma(z)\,. \tag{4.8}$$

The $+i\varepsilon$ prescription in (4.3) is crucial for the determination of the branch of the exponential function involving Δ in case $\Delta < 0$. In that case the integral acquires a non vanishing imaginary part, which implies a discontinuty of the related S-matrix elements across the cut, as well known from the optical theorem. As a concrete example, loop integrals often contain logarithms which can have negative arguments such as $\ln(-s - i\varepsilon) = \ln(s) - i\pi$, where the sign of the $i\varepsilon$ part determines that of the imaginary part.

Once the integral has been performed (for some suitable value of d), all the ingredients are available for a straightforward analytic continuation of the result to arbitrary values of d. In particular we are interested to the limit $d \to 4$, which we perform by writing $d = 4 - 2\epsilon$ and expanding in the small quantity ϵ. The UV divergences thus stem from the analytic behaviour of the Γ function and appear as poles in ϵ. For instance, in the case $\alpha = 1$, one obtains

$$I_1^{4-2\epsilon}(\Delta) = \Delta \left(\frac{1}{\epsilon} - \gamma_E + \ln 4\pi - \ln \left(\frac{\Delta - i\varepsilon}{\mu^2} \right) + 1 \right) + \mathcal{O}(\epsilon) \,. \tag{4.9}$$

4.1.1 DREG and γ_5

Up to now we have discussed just scalar integrals, but in a theory of particle interactions involving fermions and vector bosons other objects need special care when considered in dimension different than four. In particular one has to define what is meant by d-dimensional space when d is not integer, and what the vector space of d-vectors looks like. As discussed in [120], it actually turns out that in order to guarantee the existence and the uniqueness, besides the desired properties, of the integration operation, such space must be an infinite dimensional vector space. We will not dwell on these technical details, but let us just note that a consistent definition of the metric tensor such that $g^\mu_\mu = d$ can be devised.

We would rather discuss a subtle point related to the definition of the Dirac γ_5 matrix in this infinite dimensional space, since this matrix is crucial the calculation of the cross section for the pseudoscalar Higgs production. It is tempting to assume the direct generalization to d dimensions of the equations defining the Dirac algebra

$$\left.\begin{array}{rl} \{\gamma^\mu, \gamma^\nu\} & = 2g^{\mu\nu} \\ \{\gamma^\mu, \gamma^5\} & = 0 \\ \gamma_5^2 & = 1 \end{array}\right\} \quad \text{for } \mu = 0, 1, \ldots, d \,, \tag{4.10}$$

which is commonly referred to as *Naive Dimensional Regularization* (NDR). As observed already by 't Hooft and Veltman [55], this prescription is legitimate only in the case of theories with vector-like gauge symmetries like QCD. In particular an inconsistency arises when the theory under consideration has chiral gauge symmetries like the SM or the MSSM.

Following [120], let us consider the trace of a single γ_5:

$$\begin{aligned} d\,\mathrm{Tr}\,(\gamma_5) &= \mathrm{Tr}\,(\gamma_5\gamma_\alpha\gamma^\alpha) && (\gamma_\alpha\gamma^\alpha = 1/2\{\gamma^\alpha,\gamma_\alpha\} = g^\alpha_\alpha = d) \\ &= \mathrm{Tr}\,(\gamma^\alpha\gamma_5\gamma_\alpha) && (\text{ciclycity}) \\ &= -\mathrm{Tr}\,(\gamma_5\gamma_\alpha\gamma^\alpha) && (\text{anticommutation}) \\ &= -d\,\mathrm{Tr}\,(\gamma_5)\,, \end{aligned} \tag{4.11}$$

from which we deduce that, as in 4 dimensions, it must hold $\mathrm{Tr}\,(\gamma_5) = 0$ since our result is required to be a meromorphic function of the spacetime dimension d. Now let us perform analogous manipulations on the following trace:

$$\begin{aligned} d\,\mathrm{Tr}\,(\gamma_5\gamma^\mu\gamma^\nu) &= \mathrm{Tr}\,(\gamma_5\gamma^\mu\gamma^\nu\gamma_\alpha\gamma^\alpha) \\ &= \mathrm{Tr}\,(\gamma^\alpha\gamma_5\gamma^\mu\gamma^\nu\gamma_\alpha) \\ &= -\mathrm{Tr}\,(\gamma_5\gamma_\alpha\gamma^\mu\gamma^\nu\gamma^\alpha) \\ &= -2g^\mu_\alpha\,\mathrm{Tr}\,(\gamma_5\gamma^\nu\gamma^\alpha) + 2g^\mu_\nu\,\mathrm{Tr}\,(\gamma_5\gamma^\nu\gamma^\nu) - d\,\mathrm{Tr}\,(\gamma_5\gamma^\mu\gamma^\nu) \\ &= -2\,\mathrm{Tr}\,(\gamma_5)\,\{\gamma^\mu,\gamma^\nu\} + (4-d)\,\mathrm{Tr}\,(\gamma_5\gamma^\mu\gamma^\nu) \\ &= (4-d)\,\mathrm{Tr}\,(\gamma_5\gamma^\mu\gamma^\nu)\,, \end{aligned} \tag{4.12}$$

where in the last step we used the identity $\mathrm{Tr}\,(\gamma_5) = 0$ derived above. Thus we see that also $\mathrm{Tr}\,\left(\gamma_5\gamma^\alpha\gamma^\beta\right)$ must vanish and again we recover the 4 dimensonal result. We can now check what happens to the trace of a γ_5 together with four other Dirac matrices, which in 4-dimensions obeys the identity

$$\mathrm{Tr}\,(\gamma_5\gamma^\mu\gamma^\nu\gamma^\rho\gamma^\sigma) = 4i\epsilon^{\mu\nu\rho\sigma}\,, \tag{4.13}$$

involving the (intrinsincally 4-dimensional) totally antisymmetric Levi-Civita tensor, defined as

$$\epsilon^{\mu\nu\rho\sigma} = \begin{cases} +1 & \text{if } (\mu\nu\rho\sigma) \text{ is an } \textit{even} \text{ permutations of } (0123)\,, \\ -1 & \text{if } (\mu\nu\rho\sigma) \text{ is an } \textit{odd} \text{ permutations of } (0123)\,, \\ 0 & \text{otherwise}\,. \end{cases} \tag{4.14}$$

In d-dimensions let us consider, as in [121],

$$\mathrm{Tr}\left(\prod_{j=0}^{4}\gamma^{\mu_j}\gamma_5\gamma^\alpha\right) = \mathrm{Tr}\left(\prod_{j=0}^{4}\gamma^{\mu_j}\{\gamma_5,\gamma^\alpha\}\right) - 2\sum_{i=0}^{4}(-1)^i g^{\alpha\mu_i}\,\mathrm{Tr}\left(\prod_{j=0,\,j\neq i}^{4}\gamma^{\mu_j}\gamma_5\right)\,. \tag{4.15}$$

Contracting with $g_{\alpha\mu_0}$ one obtains

$$2\,(d-4)\,\mathrm{Tr}\left(\prod_{j=1}^{4}\gamma^{\mu_j}\gamma_5\right) + \mathrm{Tr}\left(\prod_{j=1}^{4}\gamma^{\mu_j}\gamma_\alpha\,\{\gamma_5,\gamma^\alpha\}\right) = 0\,. \tag{4.16}$$

Therefore it is clear that, if the left hand side must vanish for any d *and* we insist that γ_5 anticommutes with γ^μ for any μ (so that chiral fields remain well defined in chiral gauge theories and no Ward identity is violated), the trace of γ_5 together with four Dirac matrices must vanish as well. This is in sharp contrast with the well known 4-dimensional result. Moreover, it poses a serious problem in the computation of amplitudes involving genuinely chiral couplings, just as in the case of the triangle anomaly and the process $gg \to A$ studied in this thesis.

Therefore, if one wishes to employ DREG as a regulator, a choice has to be made: either the anticommutativity of γ_5 with γ^μ for any μ is abandoned, or one must separately treat the integrals involving traces of Dirac matrices with an odd number of γ_5. In particular, one has to restore the correct value of the axial-vector current anomaly.

The former solution, proposed by 't Hooft and Veltman [55] and Breitenlohner and Maison [122] (HVBM scheme), consists in separately treating the first four components $\mu = 0, 1, 2, 3$ of the d-dimensional vectors. In the four dimensional subspace both the anticommutativity of γ_5 *and* the non vanishing of γ_5-odd traces can be retained. In particular, the definition of $\epsilon^{\mu\nu\rho\sigma}$ (4.14), which is intrinsically 4-dimensional, still makes sense in this subspace. One can then use it to write a concrete expression for γ_5, namely

$$\gamma_5 = i\gamma^1\gamma^2\gamma^3\gamma^4 = \frac{i}{4!}\epsilon_{\mu\nu\rho\sigma}\gamma^\mu\gamma^\nu\gamma^\rho\gamma^\sigma \,. \tag{4.17}$$

In the complementary space, one trades the *anti*-commutativity of γ_5 with commutativity. This separation is explicitly not Lorentz invariant on the full d-dimensional space, since the first four components are picked out as special. In particular, since γ_5 does not commute with all the γ^μ, chirality is broken and so are the Ward-Takahashi identities of chiral gauge theories. These spurious anomalies would spoil renormalizability, which is indeed guaranteed by the Ward-Takahashi identities. It is thus necessary to restore them "by hand", order by order in perturbation theory, by the introduction of extra finite counterterms. On the other hand, physics is actually confined to the first four dimensions, so one would expect that when the regularator is removed (and the WT identities have been fixed), the correct result is recovered. As an example, the correct result for the axial-vector current anomaly is obtained. A main practical drawback of this approach is that one has actually to split every γ^μ in the sum of two orthogonal Dirac matrices, living in the two complementary subspaces. The same has to be done with the loop momenta. It is not hard to imagine the algebraic complications which are therefore introduced in multiloop computations.We will thus not adopt this procedure.

The more efficient approach that we will follow in the computation of the NLO corrections to the $gg \to A$ cross section is the one advocated by Larin [56]. The idea is to write γ_5 as in (4.17), where the Levi-Civita tensor is a 4-dimensional object kept out of the renormalization operation. The crucial difference with the strategy outlined above is that the indices $(\mu\nu\rho\sigma)$ are treated as d-dimensional. Anticommutativity of γ_5 with the d-dimensional γ^μ is clearly lost when γ_5 is written in this form. When the singlet axial current (just like in the case of $gg \to A$) is involved, it can be restored by introducing an extra finite counterterm, fixed by the requirement that the one-loop character of the axial

anomaly (Adler-Bardeen theorem [123]) is preserved. Explicitly, if $Z^{\overline{\rm MS}}_{Aq\overline{q}}$ is the renormalization constant of the vertex $Aq\overline{q}$ in the $\overline{\rm MS}$ scheme, the full renormalization constant of such vertex reads

$$Z_{Aq\overline{q}} = Z^{\overline{\rm MS}}_{Aq\overline{q}}\, Z^{\rm fin}_{Aq\overline{q}}\,, \tag{4.18}$$

where

$$Z^{\rm fin}_{Aq\overline{q}} = 1 + 2C_F\frac{\alpha_S}{\pi}\,. \tag{4.19}$$

One further simplification can be made: products of Levi-Civita tensors can be represented in a standard way in terms of the determinant of the 4-dimensional metric tensor:

$$\epsilon^{\mu\nu\rho\sigma}\epsilon_{\mu'\nu'\rho'\sigma'} = g^{[\mu}_{[\mu'}\, g^{\ \nu}_{\nu'}\, g^{\ \rho}_{\rho'}\, g^{\ \sigma]}_{\ \sigma']}\,, \tag{4.20}$$

where the square bracket denotes antisymmetrization. Nevertheless, since the renormalized Agg vertex is finite, we can effectively consider the above metric tensors as d-dimensional (which will add only irrelevant $\mathcal{O}(d-4)$ terms to the renormalized vertex) and contract them with the remaining vectors. In such a way one obtains a scalar expression exclusively made of d-dimensional quantities.

As a last comment, when a fermion trace contains more than one γ_5, before using (4.17), we naively anticommute them past the Dirac matrices until either they are all eliminated by the use of $\gamma_5^2 = 1$ or only one is left.

4.1.2 DREG and IR divergences

It is remarkable that DREG can be actually employed as a means for regularizing both the UV and the IR divergences. An important consequence is that also the IR regularization is again both Lorentz and gauge invariant. This implies that all the Ward-Takahashi identities are respected even in non-abelian gauge theories with massless particles and renormalizability is not spoiled.

Let us first consider an integral which has no UV divergences but is singular in the IR, e.g. (from here on the $+i\varepsilon$ prescription will be understood)

$$\int \frac{{\rm d}^d p}{(2\pi)^d}\frac{1}{(p^2)^2(p^2-m^2)}\,. \tag{4.21}$$

In 4 dimensions this integral is manifestly UV convergent by power counting, but we see that it is singular in the IR. In the integration region $p\sim 0$ it behaves like

$$\int_{p\sim 0}\frac{{\rm d}^d p}{(2\pi)^d}\frac{1}{(p^2)^2} \propto \int_{p\sim 0}\frac{{\rm d}|p|}{(2\pi)^d}\frac{|p|^{d-4}}{|p|}\,, \tag{4.22}$$

which is indeed logarithmically divergent if $d=4$. On the other hand, it is also clear that if d is chosen sufficiently greater than 4 (in this case $d>4$ is enough), the integral is IR convergent. Thus, as in the case of UV divergences, it can be unambiguously computed and the result can be continued back to $d=4$. IR divergences will again show up as poles

in ϵ. In particular, each loop integration can give rise to a double IR pole (corresponding to soft and collinear singularities) or to a single pole (corresponding to subleading collinear singularities).

We are now in the condition to state that UV and IR divergences can be regularized *at the same time*, with great calculational simplifications. One would object that that the UV and the IR divergences are regularized by non-overlapping choices of d in the complex plane (respectively $d < 4$ and $d > 4$). Nevertheless, for integrals that are singular in both the UV and the IR, it sufficient to carefully split the integration region by introducing an arbitrary separation scale. One can then regularize the UV and the IR singularities with suitable, independent choices of d. The analytic continuation of the separate results to arbitrary d guarantees that we can consistently combine them and we end up with the desired result. As an example, let us consider the diagram

$$\int \frac{\mathrm{d}^d p}{(2\pi)^d} \frac{1}{(p^2)^2}\,, \tag{4.23}$$

which, being a scaleless integral, is known to vanish in DREG. By power counting we also see that it is both UV and IR divergent (logarithmically, for $d = 4$). Let us see how these different behaviours combine and produce the correct result. By applying our above strategy, we separately regulate the two kinds of singularities. The UV region gives ($d < 4$)

$$\int_\lambda^\infty \frac{\mathrm{d}^d p}{(2\pi)^d} \frac{1}{(p^2)^2} = \Omega_d \int_\lambda^\infty \mathrm{d}|p||p|^{d-5} = -\Omega_d \frac{\lambda^{d-4}}{d-4}\,, \tag{4.24}$$

while the IR region gives ($d > 4$)

$$\int_0^\lambda \frac{\mathrm{d}^d p}{(2\pi)^d} \frac{1}{(p^2)^2} = \Omega_d \int_0^\lambda \mathrm{d}|p||p|^{d-5} = +\Omega_d \frac{\lambda^{d-4}}{d-4}\,. \tag{4.25}$$

After continuation to arbitrary d we can sum the two pieces and obtain the expected vanishing result.

4.1.3 DREG and SUSY

Despite being fully invariant and consistent in the cases discussed above, it is known that DREG explicitly breaks SUSY (see ref. [124] for a review on the topic of SUSY regularization). In particular the SUSY Ward-Takhashi identities and relations in SUSY gauge theories do not hold and would have to be restored by adding suitable counterterms (much in the spirit of the what said about γ_5 in DREG), whose existence is always guaranteed by the renormalizability of SUSY gauge theories. It is not hard to imagine why DREG should break SUSY: a necessary condition for supersymmetry to hold is the equality of bosonic and fermionic degrees of freedom. When non-gauge theories are considered, only scalars and fermions are involved and DREG is still a supersymmetry invariant regulator. Gauge theories require a special attention, due to the fact that the number of components of a

vector field is determined by the spacetime dimension d. If $d \neq 4$, the number of bosonic (gauge bosons) and fermionic (gauginos) degrees of freedom do not match.

Dimensional Reduction (DRED) is an elegant modification of DREG in which the analytic continuation from 4 to d dimensions is made by *compatctification* [125–127]. Basically, one splits the ordinary 4-dimensional spacetime in the sum of a d-dimensional and a 2ϵ-dimensional spaces. The crucial assumption is that the fields, whose number of field components remains unchanged, do not depend on the coordinates in the 2ϵ space *. In this way, the loop momenta are effectively d-dimensional, just as in DREG, but supersymmetry is preserved. It is worth to mention the fact that, concerning the issues with γ_5, DRED is completely equivalent to DREG, and ambiguities still arise [127, 128].

For the computation of the $gg \to h$ NLO corrections presented in this thesis, we have employed DREG and used the $\overline{\text{MS}}$ scheme for simplicity. The conversion of the parameters from the $\overline{\text{MS}}$ scheme to the $\overline{\text{DR}}$ scheme (the equivalent of $\overline{\text{MS}}$ in DRED) was discussed in ref. [129]. In particular, the $\overline{\text{DR}}$ and the $\overline{\text{MS}}$ Higgs-quark-quark Yukawa couplings differ by a finite one-loop shift. When inserted in the one-loop diagrams, this shift generates an additional two-loop contribution. Concerning the Higgs-squark-squark couplings, since we are only considering the corrections due to strong interactions, they are the same in both schemes and they are related by supersymmetry to the corresponding $\overline{\text{DR}}$ Yukawa couplings.

4.2 Pauli-Villars Regularization (PVREG)

Pauli-Villars Regularization (PVREG) [130] is conceptually based on the introduction of auxiliary massive auxiliary fields with the "wrong" statistics. Such fields essentially contribute with an opposite sign w.r.t the standard fields and the UV behaviour of divergent integrals is improved. These extra massive fields formally correspond to indefinite metric sectors of the Hilbert space of the theory. Nevertheless this does not pose problems with unitarity since the original theory is recovered (after renormalization) in the limit in which the auxiliary fields are infinitely heavy, so that it corresponds to the effective theory in which those auxiliary states decouple.

We recall that in PVREG, given an UV divergent integral $I(q, m^2)$ where q and m^2 denote collectively the external momenta and masses, its regularized version is constructed as

$$I^R(q, m^2, c_i, m_i^2) \;=\; I(q, m^2) \;+\; \sum_{i=1}^{n} c_i \, I(q, m_i^2) \; . \tag{4.26}$$

In the equation above the original integral $I(q, m^2)$ is combined with a number n of replicas, weighted by coefficients c_i, in which some of the masses of the original integral are replaced by the PV mass regulators (m_i), in such a way that the regularized integral is finite if

*Still, a vector field has to be split in d-dimensional and 2ϵ-dimensional parts. The former behaves like a standard vector boson, while the latter effectively is an extra Lorentz scalar in the adjoint representation, usually referred to as ϵ-scalar, with its corresponding Feynman rules.

m_i are kept finite, but tends to infinity as $m_i \to \infty$. The number of added terms, as well as the relation that the coefficients c_i should satisfy in order to make I^R convergent, depend on the divergent nature of the original integral. If the latter is only logarithmically divergent, a single subtraction is sufficient to construct I^R, i.e., $n = 1$, $c_1 = -1$, $m_1 = M_{PV}$. We will not discuss here the other cases since all the diagrams contributing to the virtual NLO contributions to pseudoscalar Higgs production are at most logarithmically UV-divergent (and we stick to DREG for the case of scalar Higgs production). Therefore a single subtraction is sufficient to make them convergent. In this case, PVREG reduces to subtracting from the original diagrams the same diagrams with some of the masses replaced by M_{PV}, and then taking the limit $M_{PV} \to \infty$.

PVREG, just as DREG, is a fully Lorentz invariant regulation which, at the cost of increasing the computational effort needed to compute one integral due to introduction of additional terms (the number of which essentially depending on how much severe is the UV divergence), has been used for fully consistent computations in *abelian*, *non-chiral* theories. The limitation of this formulation of PVREG to non-chiral theories stems from the fact that fermions cannot be regularized by introducing massive, opposite statistics spinor fields, since a mass term explicitly breaks chiral invariance. More sophisticated strategies have been devised, see e.g. [131], but as we will see in sec. 8.2 for the case $gg \to A$ it will be enough to introduce heavy replicas of the squark (scalar) fields. In the next subsection, we will comment on the use of PVREG in *non-abelian* gauge theories, which is intimately related to the presence of massless particles (the gluons).

4.2.1 PVREG and IR divergences

For what concerns the IR divergences associated to massless particles, in PVREG they are regularized by giving a fictitious mass λ to the massless particle, and later considering the limit $\lambda \to 0$.

In the case of abelian gauge theories like QED, although a photon mass term is forbidden by gauge invariance, one can actually consistently prove that the Ward-Takahashi identities still hold (the Lagrangian is still BRST invariant) and so renormalizability is not spoiled even if a photon mass term is introduced (see [120] for a thorough discussion). The case of non-abelian gauge theories as QCD is more subtle. There a gluon mass term badly violates the Slavnov-Taylor identities and severe problems follow such as the fact that Faddeev-Popov ghosts no more cancel in the sum over intermediate states.

As discussed in sec. 8.2, the choice of quantizing with the Background Field Method (BFM) [60–64] seems to provide a way out: in the BFM the external background gluons satisfy QED-like Ward identities, so one would expect that a formal renormalizability proof can be done for QCD with a gluon mass as in the case of abelian gauge theories. What we actually find is that, provided the PVREG IR-divergent term $1/2 \log^2(-m_A^2/\lambda^2)$ (m_A is the pseudoscalar Higgs boson mass) is identified in DREG with $1/\epsilon^2$, our PVREG result for the NLO pure QCD (thus top-gluon only) corrections to the $gg \to A$ cross section exactly matches the known DREG result [4, 36].

4.2.2 PVREG and SUSY

Concerning PVREG as a regulator for supersymmetric theories, its use has been advocated in the literature by West in combination with higher derivative regularization [132] and by Gaillard at one loop [133, 134] (see also [135] for a recent paper). A formal investigation of the issues related to the usage of PVREG in (spontaneously broken) SUSY is beyond the scope of this thesis. Here we adopt a more pragmatical point of view. DREG and PVREG computations of the NLO QCD corrections to $gg \to A$ in the MSSM give the same result in a common On-Shell (OS) scheme (see chap. 8 for the details on the computation and on the OS scheme). The shifts of the input parameters needed to bring the DREG OS result to the $\overline{\text{MS}}$ scheme are known and, as we have noted in sec. 4.1.3, it is known how to convert from $\overline{\text{MS}}$ to $\overline{\text{DR}}$, which is based on DRED and preserves SUSY.

4.3 Renormalization in the Background Field Gauge

We have mentioned in the previous section that in the computation presented in this thesis we made use of the so-called Background Field Method (BFM) [60–64]. Here we wish to illustrate a few generalities about the method and discuss how the renormalization has been concretely performed in the case at hand.

It is well known that the quantization of non-abelian gauge theories, due to the d.o.f.'s redundancy intrinsic to the concept of gauge invariance, is a subtle procedure. In particular, the standard approach to covariant quantization is the one proposed by Faddeev-Popov [136], where a parametric gauge fixing term

$$\mathcal{L}_{\text{gf}} = -\frac{1}{2\xi} G^a G^a \,, \tag{4.27}$$

$$G^a = \partial^\mu A^a_\mu \,, \tag{4.28}$$

is added to the classical Yang-Mills Lagrangian

$$\mathcal{L}_{\text{YM}} = -\frac{1}{4} F^{a\mu\nu} F^a_{\mu\nu} \,, \tag{4.29}$$

$$F^{a\mu\nu} = \partial_\mu A^a_\nu - \partial_\nu A^a_\mu + g f^{abc} A^b_\mu A^c_\nu \,, \tag{4.30}$$

(A^a_μ is the non-abelian vector gauge field). Moreover, one has to add a suitable Lagrangian term for unphysical, complex scalar fields obeying fermionic statistics (the ghost fields c^a and $\bar{c}^a$)

$$\mathcal{L}_{\text{gf}} = \bar{c}^a \frac{\partial G^a}{\partial A^b_\mu} D^{bc}_\mu c^c \,. \tag{4.31}$$

These fields basically serve as negative degrees of freedom and compensate the redundancy due to the fact that we are treating as independent all the four components of A^a_μ, despite only two of them being independent. The generating functional is then obtained by integrating over the gauge field and the ghosts (here and in the following we compactly

indicate as A and J the $SU(N)$ gauge field matrix $T^a A^a_\mu$ and the sources $T^a J^a_\mu$, while the notation $A \cdot J$ stands for the integral over the 4-dimensional space of the contraction $A_\mu J^\mu$)

$$Z[J] = \mathcal{N} \int \mathcal{D}A \mathcal{D}c \mathcal{D}\bar{c} \, \exp i \left\{ S[A, c, \bar{c}] + J \cdot A \right\}, \tag{4.32}$$

with

$$S[A, c, \bar{c}] = \int \mathrm{d}^4 x (\mathcal{L}_{\mathrm{YM}} + \mathcal{L}_{\mathrm{gf}} + \mathcal{L}_{\mathrm{gh}}) \,. \tag{4.33}$$

The effective action is derived, as usual, by Legendre transforming $(-i)$ times the logarithm of the generating functional (which generates the connected Green's functions)

$$\Gamma[\bar{A}] = -i \ln Z[J] - J \cdot \bar{A} \,, \tag{4.34}$$

where J is the solution of $\delta(i \ln Z[J])/\delta J(x) = -\bar{A}$. All the 1PI diagrams can be obtained by functional differentiation of the effective action.

The introduction of a gauge fixing term, by definition, breaks the gauge invariance of the original Lagrangian. Still, we know that the full quantum Lagrangian exhibits a residual BRST symmetry, which is enough in order to prove renormalizability. Moreover, physical quantities still have to be gauge invariant and so independent of the particular gauge chosen. Nevertheless, quantities like off-shell Green's functions or divergent counterterms, which do not have a direct physical interpretation, will not be gauge invariant. Most importantly, in a perturbative approach, the individual Feynman diagrams for a particular process will be gauge dependent as well.

The BFM represents a clever strategy of writing the effective action of the theory with a choice of the gauge fixing term that allows one to retain explicit gauge invariance. In practice [137], one first introduces a classical *background field* $\tilde{A}^a_\mu$ and the corresponding covariant derivative $\tilde{D}_\mu \equiv \partial_\mu - igT^a \tilde{A}^a_\mu$. The gauge fixing functional is now chosen to be

$$\tilde{G}^a = (\tilde{D}^\mu)^{ab} (A - \tilde{A})^b_\mu \,, \tag{4.35}$$

so that the corresponding ghost (c^a and $\bar{c}^a$ fields) Lagrangian can be written as

$$\mathcal{L}_{\mathrm{gh}} = -(\tilde{D}^\mu \bar{c})^a (D_\mu c)^a \,. \tag{4.36}$$

The interesting feature of such a Lagrangian is that it is invariant under a combined inifinitesimal local transformation $(\mathcal{G} \times \tilde{\mathcal{G}})(\theta)$, where

$$\mathcal{G}(\theta) := \begin{cases} \delta A^a_\mu(x) = -D^{ac}_\mu \theta^c(x) \,, \\ \delta c^b_\mu(x) = -ig\theta^a(x)(T^a)^{bc} c^c(x) \,, \\ \delta \bar{c}^b_\mu(x) = -ig\theta^a(x)(T^a)^{bc} \bar{c}^c(x) \,, \\ \delta \tilde{A}^a_\mu(x) = 0 \,, \end{cases} \qquad \tilde{\mathcal{G}}(\theta) := \begin{cases} \tilde{\delta} A^a_\mu(x) = 0 \,, \\ \tilde{\delta} c^b_\mu(x) = 0 \,, \\ \tilde{\delta} \bar{c}^b_\mu(x) = 0 \,, \\ \tilde{\delta} \tilde{A}^a_\mu(x) = -\tilde{D}^{ac}_\mu \theta^c(x) \,. \end{cases} \tag{4.37}$$

In the equations above, $\mathcal{G}(\theta)$ is an infinitesimal gauge transformation, under which the full Lagrangian is not invariant for the reasons discussed above (but $\mathcal{L}_{\mathrm{YM}}$, by definition, is).

The transformation $\tilde{\mathcal{G}}(\theta)$ is a *background gauge transformation* and it can be shown that $\mathcal{L}_{\rm gf} + \mathcal{L}_{\rm ghost}$ is invariant under the combined $(\mathcal{G} \times \tilde{\mathcal{G}})(\theta)$ (while of course $\mathcal{L}_{\rm YM}$ is invariant under $\tilde{\mathcal{G}}(\theta)$ because it does not depend on the background field).

The next step is to remember that the (quantum) effective action $\Gamma[\bar{A}, c, \bar{c}|\tilde{A}]$ (which parametrically depends on $\tilde{A}$ through the gauge fixing functional $\tilde{G}^a$) inherits all the (non-anomalous) symmetries of the classical Lagrangian, so it is invariant under the same transformation. If we choose the external field $\bar{A}$ to be equal to $\tilde{A}$, we see that $\Gamma[\tilde{A}, c, \bar{c}|\tilde{A}]$ is invariant under a gauge trasformation with gauge field $\tilde{A}$, since $(\mathcal{G} \times \tilde{\mathcal{G}})(\theta)$ reduces to

$$(\mathcal{G} \times \tilde{\mathcal{G}})(\theta) = \begin{cases} \tilde{\delta}\tilde{A}^a_\mu(x) = -\tilde{D}^{ac}_\mu \theta^c(x)\,, \\ \delta c^b_\mu(x) = -ig\theta^a(x)(T^a)^{bc} c^c(x)\,, \\ \delta \bar{c}^b_\mu(x) = -ig\theta^a(x)(T^a)^{bc} \bar{c}^c(x)\,. \end{cases} \tag{4.38}$$

In order to compute a 1PI function at loop level, the trick is start from a modified generating functional $\tilde{Z}[J]$, in which we replace $S[A, c, \bar{c}]$ by $S[\tilde{A} + \mathcal{A}, c, \bar{c}]$, where $\mathcal{A}$ represents the quantum fluctuations over which we integrate and $\tilde{A}$ is just the fixed background (with no associated sources):

$$\tilde{Z}[J|\tilde{A}] = \mathcal{N} \int \mathcal{D}\mathcal{A}\mathcal{D}c\mathcal{D}\bar{c}\, \exp i \left\{ S[\tilde{A} + \mathcal{A}, c, \bar{c}] + J \cdot \mathcal{A} \right\}. \tag{4.39}$$

Incidentally, now the gauge fixing term (4.35) does not depend anymore on the background field. Then one defines the modified effective action

$$\tilde{\Gamma}[\bar{\bar{A}}|\tilde{A}] = -i \ln \tilde{Z}[J|\tilde{A}] - J \cdot \bar{\bar{A}}\,, \tag{4.40}$$

where J is now the solution of $\delta(i \ln \tilde{Z}[J])/\delta J(x) = -\bar{\bar{A}}$. The modified effective action is just a conventional effective action computed in the presence of a background field $\tilde{A}$, thus it generates all the 1PI Green's functions when functional derivatives with respect to $\bar{\bar{A}}$ are taken. At this point, it is easy to derive the crucial identity

$$\tilde{\Gamma}[\bar{\bar{A}}|\tilde{A}] = \Gamma[\bar{\bar{A}} + \tilde{A}]\,, \tag{4.41}$$

which means that by computing $\tilde{\Gamma}[0|\tilde{A}]$ one actually gets the gauge invariant effective action $\Gamma[\tilde{A}]$. Functional derivatives of $\tilde{\Gamma}[0|\tilde{A}]$ with respect to $\tilde{A}$ result in 1PI diagrams which do not have $\bar{\bar{A}}$ field external lines (since we set $\bar{\bar{A}} = 0$) and do not have $\tilde{A}$ internal lines in loop diagrams (since we are not integrating over $\tilde{\mathcal{A}}$). The Feynman rules can be read off the shifted action $S[\tilde{A} + \mathcal{A}, c, \bar{c}]$. Interactions involving $\mathcal{A}$ only are used in the vertices *inside* the diagrams and the corresponding Feynman rules are exactly identical to those obtained in the standard Faddeev-Popov approach. Interactions involving both $\mathcal{A}$ and $\tilde{A}$ are used to generate the external lines and their Feynman rules may be different.

The advantage of such procedure is that $\tilde{\Gamma}[0|\tilde{A}]$ is invariant under gauge transformations with $\tilde{A}$ as a gauge field. All the Z factors one introduces for renormalizing the theory must respect the gauge invariance of the effective action. In general, all the 1PI functions one computes in the BFM will obey the "naive" QED-like Ward-Identities.

In the BFM treatment of Yang-Mills theories, the only renormalization constants one has to introduce are those of the background field $\tilde{A}$ ($Z_{\tilde{A}}$), the gauge coupling (Z_g) and the gauge fixing parameter (Z_ξ). Due to gauge invariance of the effective action, the counterterms must be gauge invariant as well and it must hold, as in QED,

$$Z_g = Z_{\tilde{A}}^{-1/2}\,. \tag{4.42}$$

Thus the renormalization of the gauge coupling can be performed by computing the corrections to the $\tilde{A}$ propagator without considering any vertex correction. The renormalization of the gauge fixing parameter can in principle be avoided by considering physical, ξ independent quantities or by fixing the Landau gauge $\xi = 0$. No Z factors will be needed instead for ghosts and $\mathcal{A}$ since they do only appear in internal lines: the Z coming from each propagator would cancel with the two $\sqrt{Z}$ factors coming from each vertex connected to the propagator.

When fermions and other fields that do not enter $\mathcal{L}_{\rm gf}$ are introduced, the BFM is completely transparent to them and the Feynman rules are identical to the standard formalism. For a systematic BFM treatment of the SM, see [138].

In our calculation, we have generated all the relevant two-loop diagrams with the aid of the `Mathematica` [57] package `FeynArts` [58], using a modified version of the MSSM model file [59] which implements the BFM.

4.3.1 $\mathcal{O}(\alpha_s)$ renormalization of the parameters in the LO $gg \to h, H$ and $gg \to A$ cross sections

Below we present the the counterterms for the $\mathcal{O}(\alpha_s)$ renormalization of the parameters entering the LO cross sections for the processes $gg \to h, H$ and $gg \to A$ discussed in sec. 3.2. The only parameters that at one-loop receive corrections due to the strong interactions are α_s, the quark mass m_q, the squark masses $m_{\tilde{t}_1}, m_{\tilde{t}_2}$, the squark mixing angle θ_q and the coupling A_q. Actually, only 4 of the last 5 parameters are independent.

The computation of $gg \to h, H$ was performed in DREG, while the computation of $gg \to A$ was performed both in DREG and in PVREG. At one loop, only the fermion loop contributes to the latter process, implying that only m_q renormalization has to be considered. For completeness, we will quote the OS counterterms for both DREG and DRED (by dropping the finite part one immediately gets the $\overline{\rm MS}$ and $\overline{\rm DR}$ counterterms). Note that in the equations below we have suppressed all the constants (γ_E and $\ln 4\pi$) that always show up together with the pole: by writing ϵ^{-1} we actually mean $\epsilon^{-1} - \gamma_E + \ln 4\pi$.

Renormalization of α_s

The $gg \to h, H$ and $gg \to A$ production at LO is proportional to α_s. Thus the two-loop result must include the one-loop renormalization of α_s. As discussed above, the renormalization of α_s is easily determined in the BFM by computing the background gluon one-loop propagator and no vertex correction must be computed. In particular, α_s

renormalization completely decouples from the computation of the two-loop corrections to the $gg \to h, H$ and $gg \to A$ vertices. We choose to stick to the standard $\overline{\rm MS}$ running $\alpha_s(\mu)$, even when PVREG is employed for regularizing the two-loop vertex, which at one-loop is given by the well known formula

$$\alpha_s(\mu) = \frac{\alpha_s(\mu_0)}{1 + \frac{\alpha_s(\mu_0)}{\pi}\beta_0 \ln\left(\frac{\mu}{\mu_0}\right)}\,, \tag{4.43}$$

where the one-loop coefficient of the QCD beta function β_0 is

$$\beta_0 = \frac{11 C_A - 4 n_f T_R}{12}\,, \tag{4.44}$$

in which $C_A = N_c = 3$ and $T_R = 1/2$ are color factors.

Renormalization of quark and squark masses

For completeness, we collect below the OS counterterms for the squarks and quark masses. The OS masses are defined as the poles of the corresponding propagators (DREx stands for both DREG and DRED). The squark mass counterterms read

$$\begin{aligned}\left.\frac{\delta m^2_{\tilde{q}_1}}{m^2_{\tilde{q}_1}}\right|_{\rm DREx} = C_F \frac{\alpha_S}{4\pi}\Bigg\{ & \frac{1}{\epsilon}\left(\frac{4 s_{2\theta_q} m_{\tilde{g}} m_q - 4 m^2_{\tilde{g}} - s^2_{2\theta_q}(m^2_{\tilde{q}_1} - m^2_{\tilde{q}_2}) - 4 m^2_q}{m^2_{\tilde{q}_1}}\right) \\ & + 3 \ln\frac{m^2_{\tilde{q}_1}}{Q^2} - 7 - c^2_{2\theta_q}\left(\ln\frac{m^2_{\tilde{q}_1}}{Q^2} - 1\right) - s^2_{2\theta_q}\frac{m^2_{\tilde{q}_2}}{m^2_{\tilde{q}_1}}\left(\ln\frac{m^2_{\tilde{q}_2}}{Q^2} - 1\right) \\ & + 2\Bigg[\frac{2 m_{\tilde{g}} s_{2\theta_q} m_q - m^2_{\tilde{g}} - m^2_q + m^2_{\tilde{q}_1}}{m^2_{\tilde{q}_1}}\mathcal{B}(m^2_{\tilde{q}_1}, m^2_{\tilde{g}}, m^2_q) \\ & + \frac{m^2_{\tilde{g}}}{m^2_{\tilde{q}_1}}\left(\ln\frac{m^2_{\tilde{g}}}{Q^2} - 1\right) + \frac{m^2_q}{m^2_{\tilde{q}_1}}\left(\ln\frac{m^2_q}{Q^2} - 1\right)\Bigg]\Bigg\} + \mathcal{O}(\epsilon)\,,\end{aligned} \tag{4.45}$$

$$\left.\frac{\delta m^2_{\tilde{q}_2}}{m^2_{\tilde{q}_2}}\right|_{\rm DREx} = \left.\frac{\delta m^2_{\tilde{q}_1}}{m^2_{\tilde{q}_1}}\right|_{\rm DREx} \left[(\tilde{q}_1, s_{2\theta_q}) \leftrightarrow (\tilde{q}_2, -s_{2\theta_q})\right]\,, \tag{4.46}$$

while the fermion mass counterterms read (DREx)

$$\begin{aligned}\left.\frac{\delta m_q}{m_q}\right|_{\rm DREx} = C_F \frac{\alpha_S}{4\pi}\Bigg\{ & -\frac{2}{\epsilon} + d + 3\ln\frac{m^2_q}{Q^2} + \frac{m^2_{\tilde{g}}}{m^2_q}\left(\ln\frac{m^2_{\tilde{g}}}{Q^2} - 1\right) + \\ & - \frac{1}{2}\Bigg[\mathcal{B}(m^2_q, m^2_{\tilde{q}_1}, m^2_{\tilde{g}})\left(\frac{2 m_q m_{\tilde{g}} s_{2\theta_q} - m^2_{\tilde{g}} + m^2_{\tilde{q}_1} - m^2_q}{m^2_q}\right) \\ & + \frac{m^2_{\tilde{q}_1}}{m^2_q}\left(\ln\frac{m^2_{\tilde{q}_1}}{Q^2} - 1\right) + (\tilde{q}_1, s_{2\theta_q}) \leftrightarrow (\tilde{q}_2, -s_{2\theta_q})\Bigg]\Bigg\} + \mathcal{O}(\epsilon)\,.\end{aligned} \tag{4.47}$$

In the above expressions $\mathcal{B}(m^2_{\tilde{q}_1}, m^2_{\tilde{g}}, m^2_q)$ is the finite part of the one-loop Passarino-Veltman two-point function $B_0(m^2_{\tilde{q}_1}, m^2_{\tilde{g}}, m^2_q)$, which is defined in eq. (B.2). The quark counterterm is different in DREG ($d = -4$) and DRED ($d = -5$). With the corresponding choice of d, one can get the $\overline{\text{MS}}$ and $\overline{\text{DR}}$ counterterms by keeping only the divergent parts of the above expressions.

Renormalization of the squark mixing angle

The $gg \to h, H$ processs arises at one-loop through two classes of diagrams, respectively due to quark and squark loop. Therefore, in the case of scalar production we have to consider also the one-loop renormalization of the Higgs-squark-squark form factors due strong interactions (see eqs. (3.20) and (3.21) for a definition of the form factors valid to all orders in the strong interactions). Besides the quark mass, the squark mixing angle and the trilinear coupling A_q are the only parameters entering the Higgs-squark-squark coupling that are renormalized at $\mathcal{O}(\alpha_s)$ by the strong interactions.

While the OS prescription for the renormalization of the quark/squark masses is given by defining the physical masses as the poles of the corresponding propagators, there is no obvious definition for the stop mixing angle. Following the discussion of refs. [34, 139], we adopt the following "symmetrical" definition [140–143]

$$\delta\theta_q := \frac{1}{2}\frac{\hat{\Pi}_{12}(m^2_{\tilde{q}_1}) + \hat{\Pi}_{12}(m^2_{\tilde{q}_2})}{m^2_{\tilde{q}_1} - m^2_{\tilde{q}_2}}\,, \tag{4.48}$$

where $\hat{\Pi}_{12}(q^2)$ denotes the finite part of the off-diagonal self-energy of the squarks. The squark mixing angle takes then the form

$$\begin{aligned}\delta\theta_q|_{\text{DREx}} = C_F\frac{\alpha_S}{4\pi}\frac{c_{2\theta_q}}{m^2_{\tilde{q}_1} - m^2_{\tilde{q}_2}}\Bigg\{&\frac{1}{\epsilon}\big(4m_{\tilde{g}}m_q - s_{2\theta_q}(m^2_{\tilde{q}_1} - m^2_{\tilde{q}_2})\big) + 2m_{\tilde{g}}m_q\Big[\mathcal{B}(m^2_{\tilde{q}_1}, m^2_{\tilde{g}}, m^2_q)\\ &+ \mathcal{B}(m^2_{\tilde{q}_2}, m^2_{\tilde{g}}, m^2_q)\Big]\\ &+ s_{2\theta_q}\left[m^2_{\tilde{q}_1}\left(\ln\frac{m^2_{\tilde{q}_1}}{Q^2} - 1\right) - m^2_{\tilde{q}_2}\left(\ln\frac{m^2_{\tilde{q}_2}}{Q^2} - 1\right)\right]\Bigg\}\\ &+ \mathcal{O}(\epsilon)\,.\end{aligned} \tag{4.49}$$

No dependence on the choice of DREG or DRED arises so, by taking the pole of the above expression, one can get both the $\overline{\text{MS}}$ and $\overline{\text{DR}}$ counterterm.

Renormalization of trilinear coupling A_t

As already stated, only four among $m_q, m^2_{\tilde{q}_1}, m^2_{\tilde{q}_2}, s_{2\theta_q}, A_q$ are independent and the constraint is given by the tree-level relation (2.38). In the present work we are considering only the top sector contribution to $gg \to h, H$, therefore we specialize to A_t. In fact the

case of A_b is more subtle since loop corrections are $\tan\beta$ enhanced and it is convenient to adopt a different renormalization prescription [42]. Using (2.38) and the fact that $\tan\beta$ and μ do not receive any $\mathcal{O}(\alpha_s)$ correction, the counterterm δA_t can be expressed as a combination of the other counterterms

$$\delta A_t = \left(\frac{\delta m^2_{\tilde{t}_1} - \delta m^2_{\tilde{t}_2}}{m^2_{\tilde{t}_1} - m^2_{\tilde{t}_2}} + \frac{\delta s_{2\theta_t}}{s_{2\theta_t}} - \frac{\delta m_t}{m_t} \right) (A_t + \mu \cot\beta) \,, \tag{4.50}$$

where $\delta s_{2\theta_t} = 2 c_{2\theta_t} \delta\theta_t$.

Chapter 5

Asymptotic Expansions of Loop Integrals

5.1 The need for an approximate evaluation

In order to compute the NLO QCD corrections to the $gg \to h, H, A$ cross sections, two-loop vertex diagrams must be evaluated.

Due to the structure of the MSSM interactions, the NLO QCD corrections to the gluon fusion process in the MSSM involve up to 5 different mass scales. Those scales are the center of mass energy $(q_1 + q_2)^2 = s$ (where q_i is the four momentum of the i-th gluon, which is massless and is considered on-shell, while s will be equal the Higgs mass, which is assumed to be produced on-shell) and the masses of the particles running in the loops, namely the quark mass m_q, the squark masses $m_{\tilde{q}_1}, m_{\tilde{q}_2}$ and the gluino mass $m_{\tilde{g}}$.

Contrarily to the evaluation of general one-loop integrals, in the two-loop case no universal algorithm has been devised yet. The analyitic structure of two-loop diagrams can be very rich, due to the fact that many propagators appear and in general a large number of different masses and scales can be present. In particular, these mass scales determine the (pseudo)thresholds of the diagrams and influence its IR structure.

There are essentially two approaches to the calculation of two-loop amplitudes, based respectively on the numerical and analytical evaluation of the integrals. While numerical methods have in principle no problems with the presence of many mass scales, it is actually quite complicated to cope with the several thresholds, pseudothresholds and IR singularities for reasons of numerical stability. Sometimes a way out in these cases is represented by a semi-analytic approach. On the other hand, the analytical evaluation is basically a complementary approach. The integrals that can be exactly evaluated (e.g. through the method of Differential Equations, see for instance [144–146]) are those depending on at most three different mass scales. The advantage of the analytic approach is that no problems arise when manipulating objects with thresholds etc.

Since we aim at providing compact analytic formulae for the NLO QCD corrections in such a way that they can be easily implemented in computer codes (a straightforward, fast

numerical evaluation is essential for phenomenological studies), we will pursue the analytic way. Nevertheless, given the number of mass scales in the processes under study, an *exact* analytic evaluation of the two-loop integrals is not feasible with the techniques developed so far. We will therefore seek for approximate results, valid when some hierarchy is realized between the various scales, aiming to an accuracy of the percent level. In the following section we discuss the general features of the method employed.

5.2 Asymptotic expansions in large masses

In particular, for the process $gg \to h, H$ we will consider the case in which $s = m_{h,H}$ and m_q are much smaller than the SUSY masses $m_{\tilde{q}_1}, m_{\tilde{q}_2}, m_{\tilde{g}}$, but we will not assume no specific hiearchy among the s and m_q. Infact, results for the case in which $m_{h,H} \ll 2m_q$ have been already discussed in the literature [32–34]. This hierarchy holds almost certainly in the case of the lightest scalar Higgs h, but its validity is questionalble when the H boson is considered. The opposite regime $m_{h,H} \gg 2m_q$ has been investigated in the bottom sector [42], where it is realized for both h and H. It is thus interesting to compute the NLO corrections in the regime $m_{h,H} \sim m_q$, which may be the case for the top contribution to heavy Higgs(es) production. For the process $gg \to A$, results have been made available in the literature only in the form of a Fortran code, valid only in the case $m_A \ll 2m_q$ [51], but no compact analytic results have ever been published. Since the corrections for $m_A \sim 2m_q$ and $m_A \gg 2m_q$ have never been computed (and can be relevant in the top sector for heavy A and in the bottom sector for large $\tan\beta$), we investigate all the three above mentioned regimes.

The general method for obtaining approximate results valid when *all* the internal masses are much heavier than the external momenta is well known and relies on the Taylor expansion *under* the integral sign in the small ratio q^2/M^2 (where q is a small momentum and M is a heavy mass). The simplification consists in the fact that the approximate amplitude to be computed will consist of vacuum integrals (i.e. integrals where no momenta appear in the propagators) that can be evaluated with the techniques developed in ref. [147].

A naive Taylor expansion in q^2/m^2 (where now m is a *light* mass) obviously fails when an external momentum reaches the real particle production threshold, since it cannot fully reproduce the non-analytic structure (e.g. the logarithms which develop an imaginary part above threshold, according to the optical theorem). A characteristic feature of a wrong, naive Taylor expansion in q^2/m^2 is that in the limit $m \to 0$ the result exhibits an (IR) divergent behaviour.

The correct approach for obtaining approximate results is that of *asymptotic expansions*. A comprehensive review of several methods and different cases in which asymptotic expansions can be applied is given in [148], (see also [149] for a brief review). The case of our interest requires an asymptotic expansion in the *large masses* of the supersymmetric particles, of which we describe a practical implementation in the next section.

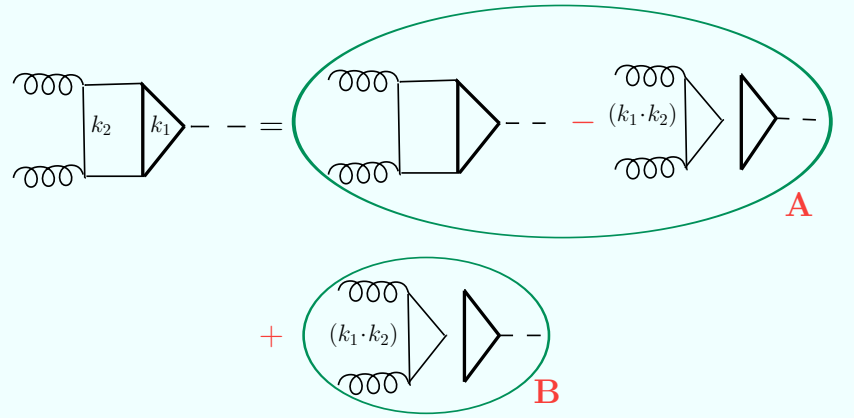

Figure 5.1: Pictorial example (from ref. [42]) of the asymptotic expansion of a two-loop diagram containing one subintegration (k_1) with only heavy particles (bold lines) and the other (k_2) with light particles. The IR-divergent part of original diagram, represented by the disconnected diagram, is subtracted and added. The three terms are grouped in such a way that (A) is the contribution that can be evaluated via a Taylor expansion and (B) is the one that must be evaluated exactly. See sec. 5.3 for a detailed explanation.

5.3 Practical implementation

We now illustrate the practical implementation of the asymptotic expansion in the computation of the two-loop integrals for Higgs production. The technique we use is the one introduced in ref. [42].

The diagrams that contribute to the process $g(q_1) + g(q_2) \to \phi(q)$ (where $\phi = h, H, A$ and $q_1^2 = q_2^2 = 0$ for on-shell gluons) fall in in two classes:

1. those that have no physical thresholds and can be evaluated via an ordinary Taylor expansion in powers of q^2/M^2, for which the general methods of ref. [147] can be applied;

2. the diagrams that require an asymptotic expansion because of the presence of physical thresholds.

In the previous subsection we have explained why a Taylor expansion of a two-loop diagram in an external momentum q^2 is viable for values of q^2 up to the first physical threshold. Diagrams with a physical threshold at $q^2 = 4\,m_q^2$ are those which, e.g. according to the Cutkosky rules, can contribute to the imaginary part when a cut is applied. As already noted, if those diagrams are Taylor-expanded in q^2, they exhibit an infrared (IR) divergent behavior as $m_q \to 0$. This will be the criterion for assigning the integrals to class-1 or class-2.

In practice, we generate the asymptotic expansion of a diagram of class-2 by adding and subtracting to it the part of the diagram itself that becomes IR-divergent when m_q

and q^2 are sent to zero. In fig. 5.1*, we show how this construction allows us to concretely compute the asymptotic expansion. We see that the diagram is separated in two parts: part A in fig. 5.1 which, being by construction IR-convergent, can be evaluated via a Taylor expansion in the same way as class-1 diagrams; part B in fig. 5.1, containing the IR-divergent contribution, which must be evaluated exactly.

The IR-divergent part of a diagram is constructed with the following strategy. One condition must hold, namely that one can choose a routing of the loop momenta such that the propagators containing both loop momenta k_1 and k_2, are always accompanied by a heavy mass M. This is the case in all the diagrams entering our calculation. Then, one can rewrite such connecting propagators applying the identity [42]

$$\frac{1}{(k_1+k_2)^2-M^2} = \frac{1}{k_1^2-M^2} - \frac{k_2^2+2\,k_1\cdot k_2}{[(k_1+k_2)^2-M^2](k_1^2-M^2)}\ . \tag{5.1}$$

The first term on the r.h.s. of eq. (5.1) generates a disconnected integral (product of two one-loop integrals) that contains *all* the IR-divergent contributions present in the original diagram. This term must be evaluated exactly, i.e. for arbitrary q^2 and will bring the correct $\ln(q^2/m_q^2)$ terms characteristic of the physical threshold (which in general a naive Taylor expansion fails to reproduce). The strategy for the exact evaluation of these integrals will be discussed in chap. 6.

The second term, instead, gives rise to a two-loop integral with improved IR convergence in the k_2 integration and improved UV convergence in the k_1 integration. Therefore if, for example, the original integral is logarithmically IR divergent in the k_2 integration when $q \to 0$ and $m_q \to 0$, the corresponding two-loop integral associated with the second term in eq. (5.1) evaluated at $q^2 = m_q^2 = 0$ is no longer IR divergent, but it actually gives a finite result that differs from the result valid for $q^2 \neq 0$ and $m_q \neq 0$ by terms of $\mathcal{O}(m^2/M^2\ln(m^2/M^2))$, where m^2 denotes either q^2 or m_q^2.

In general, by iteratively applying the identity of eq. (5.1) while keeping track term by term of the degree of IR divergence, one can build the IR-divergent part of any diagram (satisfying our hypotheses) in terms of products of one-loop integrals with numerators that contain terms of the form $(k_i\cdot q_j)^m$, $(k_i\cdot k_j)^n\,(i,j=1,2)$ where m, n are generic natural powers.

Two checks of the validity of procedure of ref. [42] for generating the asymptotic expansion can be devised:

- One can verify that the algorithm correctly produces the IR-divergent part of a diagram. Indeed, by evaluating its part A with a Taylor expansion, one can check explicitly whether the IR-divergent contributions of the original diagram are canceled by the disconnected terms constructed via eq. (5.1). This means that the final result for part A should be free of any $\ln(q^2/m_q^2)$ or q^2/m_q^2 term, as it must if a Taylor expansion is viable. We verify that this is always the case.

* The diagrams have been drawn using JaxoDraw [109].

- One can also verify that the asymptotic expansion of a diagram which does not exhibit any physical threshold produce a result identical to that obtained by a Taylor expansion. In practice, we evaluate the diagrams of class-1 with the same procedure we employ for class-2 diagrams. What we expect for class-1 diagrams is that the Taylor expansion and the exact evaluation of the disconnected contribution give the same result. In fact this implies that their contributions to the asymptotic expansion sum to zero and effectively only the Taylor expansion of the original two-loop diagram survives. We verify that this is always the case.

In the next chapter we will discuss the strategy we followed for the exact evaluation of the two-loop disconnected diagrams.

Chapter 6

Evaluation of disconnected two-loop integrals through Integration By Parts (IBP) identities

In this chapter we will discuss the exact evaluation of the disconnected two-loop integrals entering the asymptotic expansion of the original diagram. In general, a very large number of different Feynman integrals will be generated by the expansion. Algebraic algorithms can be devised for expressing most of those integrals as combinations of few independent Master Integrals (MI's). The evaluation of Feynman integrals separates thus in two distinct problems. One is algebraic and, despite it can be very challenging in multiloop/multiscale calculations, can be fully automatized through the use of symbolic manipulation software. The other is related to the analytic properties of the MI's, which in the case of two-loop disconnected diagrams is completely solved since only one-loop MI's are involved. In 6.1 we will set the notation for the disconnected integrals under study and define the MI's that will result from the reduction to MI's. In particular, in sec. 6.2 we will focus on the reduction to MI's through Integration By Parts identities, which hold in DREG. An alternative approach, the standard Passarino-Veltman reduction, has been used when regularizing with PVREG (where we stick to $d = 4$ in order to evade the problems with γ_5) and a brief comment is made in sec. 6.3.

6.1 Disconnected two-loop integrals

We recall that by "disconnected" we mean that no propagators involving both the loop momenta (say p and k) appear in the diagram, while it is still possible to have scalar products of the form $p \cdot k$ at the numerator. We assume that a tensor decomposition of the original amplitude has been performed and that the scalar form factors have been singled out with suitable projectors. When considering a two-loop vertex diagram, the asymptotic expansion will at most produce products of one-loop vertex diagrams, so we will limit our

discussion to that case. The most general integral will be

$$J(r_1,\ldots,r_6;s_1\ldots,s_7) = \iint \mathrm{d}^4p\,\mathrm{d}^4k\,\frac{S_1^{s_1}\cdots S_7^{s_7}}{D_1^{r_1}\cdots D_6^{r_6}}\,, \tag{6.1}$$

where the factors in the denominator are the propagators

$$\begin{aligned} D_1 &= p^2 - m_1^2\,, & D_4 &= k^2 - m_4^2\,,\\ D_2 &= (p-q_1)^2 - m_2^2\,, & D_5 &= (k-q_1)^2 - m_5^2\,,\\ D_3 &= (p+q_2)^2 - m_3^2\,, & D_6 &= (k+q_2)^2 - m_6^2\,, \end{aligned} \tag{6.2}$$

and the scalar products in the numerator are all the possible combinations of an internal loop momentum with the available internal and external four-vectors

$$\begin{aligned} S_1 &= p^2\,, & S_4 &= k^2\,,\\ S_2 &= p\cdot q_1\,, & S_5 &= k\cdot q_1\,,\\ S_3 &= p\cdot q_2\,, & S_6 &= k\cdot q_2\,, \end{aligned} \tag{6.3}$$

and

$$S_7 = p\cdot k\,. \tag{6.4}$$

We can apply some standard techniques for the evaluation of (multiloop) integrals [144–146]. Since, in general, denominators form a basis for the scalar products in one-loop diagrams, one can express S_1, S_2 and S_3 as linear combinations of D_1, D_2 and D_3 (we use $q_1^2 = q_2^2 = 0$ since we consider massless on-shell gluons):

$$\begin{aligned} S_1 &= D_1 + m_1^2\,,\\ S_2 &= -\frac{1}{2}[D_2 + m_2^2 - (D_1 + m_1^2)]\,,\\ S_3 &= +\frac{1}{2}[D_3 + m_3^2 - (D_1 + m_1^2)]\,, \end{aligned} \tag{6.5}$$

and the same can be done for the three scalar products involving k only. The scalar product S_7 is a remnant of the two-loop nature of the diagram we expanded. A trick is to introduce a seventh (auxiliary) denominator, which is not really present in the diagram but serves in order to complete the denominator basis:

$$D_7 = (p-k)^2 \quad\Rightarrow\quad S_7 = -\frac{1}{2}\left[D_7 - (D_1 + m_1^2) - (D_4 + m_4^2)\right]\,. \tag{6.6}$$

Having expressed the scalar products in terms of denominators, we have effectively written our original integral (6.1) as a linear combination of independent (with respect to the D_i's) integrals of the type

$$I(n_1,\ldots,n_7) = \iint \mathrm{d}^4p\,\mathrm{d}^4k\,\frac{1}{D_1^{n_1}\cdots D_7^{n_7}}\,, \tag{6.7}$$

where the indices n_i can be positive (for $i \neq 7$, corresponding to a propagator in the corresponding diagram), negative (corresponding to scalar products in the numerator) or zero (in the case some D_i cancel between the numerator and the denominator).

To set the notation, we call *auxiliary topology* the set of denominators $A_7 = \{D_1, \ldots, D_7\}$ such that each of the scalar products $\{S_1 \ldots S_7\}$ can be expressed as a linear combination of denominators belonging to it. We call *topology* the set of denominators involved in one integral $I(n_1, \ldots, n_7)$ for which $n_i > 0$. For instance, $I(1,1,1,1,-1,-1,0)$ and $I(2,1,1,2,-2,-1,0)$ belong to the same topology $T = \{D_1, D_2, D_3, D_4\}$, while the integral $I(1,0,1,1,-1,-1,0)$ belongs to a different topology $T' = \{D_1, D_3, D_4\}$. T' is a *sub-topology* of a topology T since it can be obtained by removing one or more denominators from T. Topologies made of t propagators $\{D_{i_1} \ldots D_{i_t}\}$ can be uniquely identified by an identification number N defined as

$$N := \sum_{k=1}^{t} 2^{i_k - 1} \,, \tag{6.8}$$

so that $N \in [1, 2^n - 1]$, where n is the number of denominators in the auxiliary topology.

When an integral of the form (6.1) is brought to a combination of integrals of the form (6.7), in every term it can happen that a number of D_i's in the denominator cancel with other D_i's coming from the application of (6.5) and (6.6). Thus, if one starts with an integral belonging to some topology, all its possible sub-topologies must in principle be considered.

If the divergences of such integrals are regularized through DREG, actually a large number of these integrals can be reduced to a linear combination of a smaller set of Master Integrals (MI's) with coefficients that are rational functions of polynomials in the kinematic invariants and the dimension d. In particular, in the case at hand of disconnected two-loop integrals, those MI's will be the well known three scalar functions [150]

$$\frac{i}{16\pi^2} A_0(m_1^2) := \frac{\mu^{4-d}}{(2\pi)^d} \int \frac{\mathrm{d}^d p}{D_1} \,, \tag{6.9}$$

$$\frac{i}{16\pi^2} B_0(s, m_2^2, m_3^2) := \frac{\mu^{4-d}}{(2\pi)^d} \int \frac{\mathrm{d}^d p}{D_2 D_3} \,, \tag{6.10}$$

$$\frac{i}{16\pi^2} C_0(0, 0, s, m_2^2, m_1^2, m_3^2) := \frac{\mu^{4-d}}{(2\pi)^d} \int \frac{\mathrm{d}^d p}{D_1 D_2 D_3} \,, \tag{6.11}$$

where, besides $q_i^2 = 0$ for on-shell gluons, $s = (q_1 + q_2)^2$ is the center of mass energy. Some results concerning the three MI's are collected in app. B.1. In the following section we will describe the method that allows such reduction.

6.2 Integration By Parts (IBP) identities

The extension of Gauss' theorem to d-dimensional space states that the integral over a total derivative is zero. On the basis of this fact, the so called Integration By Parts (IBP)

identities have been introduced [151, 152], relating combinations of scalar integrals of the same topology with different indices $\{n_1, \ldots, n_7\}$ among themselves *and* to scalar integrals of subtopologies. The idea is to exploit such relations when computing a given (large) number of integrals, hoping to recursively express most of the integrals of each topology in terms of *few* integrals belonging to that topology and to its sub-topologies.

IBP identities for a generic two-loop integral of the form (6.7) (where the S_i have already been expressed in terms of the D_i) are generated starting from

$$\iint \mathrm{d}^d p \, \mathrm{d}^d k \, \frac{\partial}{\partial l^\mu} \left[v^\mu \frac{1}{D_1^{n_1} \cdots D_7^{n_7}} \right] = 0 \,, \tag{6.12}$$

which holds in DREG because the integrand is a total derivative. In the above equation $l = p, k$ and $v = q_1, q_2, p, k$. We can thus establish 8 IBP identities, though in general not all of them will be independent. When explicitly evaluating the derivatives one obtains a combination of terms where the exponents n_i are shifted by ± 1, so integrals belonging to subtopologies of the original topology may be involved. In general it will thus be necessary to consider IBP identities for those integrals as well if one wants to completely reduce to MI's the integral to be computed. We will illustrate below the strategy and the tools employed in the IBP reduction of the actual disconnected integrals involved in our computation. Before that, let us first see a couple of simple examples of IBP identity in the case of one-loop vertex integrals.

6.2.1 One-loop examples of IBP reduction

The auxiliary topology for one-loop vertex integrals is simply given by the three denominators D_1, D_2, D_3. Let us consider a general vertex, relaxing the hypotesis that $q_1^2 = q_2^2 = 0$. Let us consider massive tadpole diagrams (subtopology $N = 1$) with the denominator raised to an arbitrary integer power n_1 and the remaining indices equal to zero:

$$I(n_1, 0, 0) = \int \mathrm{d}^d p \, \frac{1}{D_1^{n_1}} \,. \tag{6.13}$$

It is immediate to obtain the (only) IBP identity

$$(d - 2n_1) I(n_1, 0, 0) - 2m_1^2 n_1 I(n_1 + 1, 0, 0) = 0 \,, \tag{6.14}$$

which can be written as

$$[(d - 2n_1)\mathbf{Id} - 2m_1^2 n_1 \mathbf{1}^+] I(n_1, 0, 0) = 0 \,, \tag{6.15}$$

where we have introduced the identity operator $\mathbf{Id}$ and the plus and minus operators $\mathbf{i}^\pm$ defined as

$$\begin{aligned} \mathbf{Id} I(n_1, n_2, n_3) &= I(n_1, n_2, n_3) \,, \\ \mathbf{i}^\pm I(\ldots, n_i, \ldots) &= I(\ldots, n_i \pm 1, \ldots) \,. \end{aligned} \tag{6.16}$$

We can symbolically solve (6.15) for $\mathbf{1}^+$,

$$\mathbf{1}^+ = \frac{d-2n_1}{2m_1^2 n_1}\mathbf{Id} \equiv C_{n_1}\mathbf{Id}\,. \tag{6.17}$$

By the repeated application of the above equation, we see that a generic integral $I(n_1,0,0)$ with $n_1 > 0$ is completely determined in terms of one scalar integral, which we may choose to be $I(1,0,0)$:

$$I(n_1,0,0) = \left(\prod_{k=1}^{n_1} C_k\right) I(1,0,0)\,, \tag{6.18}$$

which is proportional to an $A_0(m_1)$ function as defined in (6.9). It is easy to see that integrals with $n_1 < 1$ vanish by solving the IBP for $\mathbf{Id}$ instead of $\mathbf{1}^+$. One gets

$$I(n_1,0,0) = \frac{2m_1^2 n_1}{d-2n_1} I(n_1+1,0,0)\,, \tag{6.19}$$

which tells us that $I(0,0,0) = 0$ (after all, it is a scaleless integral, which is known to be vanishing in DREG) and so, $I(n_1,0,0)$ will be zero for any $n_1 < 1$. By a simple shift in the integration variable, it is easy to see that analogous identities hold for the sub-topologies $I(0,n_2,0)$ and $I(0,0,n_3)$, which then result proportional to $A_0(m_2)$ and $A_0(m_3)$.

An analogous procedure can be applied to the bubble

$$I(n_1,n_2,0) = \int \mathrm{d}^d p\, \frac{1}{D_1^{n_1} D_2^{n_2}}\,, \tag{6.20}$$

where two IBP identities are obtained:

$$\begin{aligned} 0 =& \left(d-2n_1-n_2\right) I\left(n_1,n_2,0\right) - 2m_1^2 n_1 I\left(n_1+1,n_2,0\right) \\ &+ \left(-m_1^2-m_2^2+q_1^2\right) n_2 I\left(n_1,n_2+1,0\right) - n_2 I\left(n_1-1,n_2+1,0\right)\,, \end{aligned} \tag{6.21}$$

$$\begin{aligned} 0 =& \left(m_2^2-m_1^2-q_1^2\right) n_1 I\left(n_1+1,n_2,0\right) + \left(m_2^2-m_1^2+q_1^2\right) n_2 I\left(n_1,n_2+1,0\right) \\ &+ n_1 I\left(n_1+1,n_2-1,0\right) - n_2 I\left(n_1-1,n_2+1,0\right) + \left(n_2-n_1\right) I\left(n_1,n_2,0\right)\,, \end{aligned} \tag{6.22}$$

These two equations can again be symbolically solved in terms of identity, plus and minus operators

$$\mathbf{2}^+ = \frac{\mathbf{Id}\left(-d+2n_1+n_2\right)}{n_2\left(-m_1^2-m_2^2+q_1^2\right)} + \frac{\mathbf{1}^-\mathbf{2}^+}{-m_1^2-m_2^2+q_1^2} + \frac{2m_1^2 n_1 \mathbf{1}^+}{n_2\left(-m_1^2-m_2^2+q_1^2\right)} \qquad (\text{with } n_2 \neq 0)\,, \tag{6.23}$$

$$\begin{aligned} \mathbf{1}^+ =& \frac{\mathbf{Id}\left(n_2-n_1\right)}{n_1\left(m_1^2-m_2^2+q_1^2\right)} + \mathbf{2}^+\left(\frac{n_2\left(-m_1^2+m_2^2+q_1^2\right)}{n_1\left(m_1^2-m_2^2+q_1^2\right)} - \frac{\mathbf{1}^- n_2}{n_1\left(m_1^2-m_2^2+q_1^2\right)}\right) \\ &+ \frac{\mathbf{2}^-\mathbf{1}^+}{m_1^2-m_2^2+q_1^2} \qquad (\text{with } n_1 \neq 0)\,. \end{aligned} \tag{6.24}$$

We have already shown that if one of the two indices is negative and the other is zero the integral (6.20) vanishes in DREG. Also the case $n_1\,, n_2 < 0$ is zero in DREG: by solving e.g. $(n > 0)$

$$\begin{aligned} 0 &= I(-n+1,0,0) \\ &= \mathbf{1}^+ I(-n,0,0) \\ &= \frac{1}{m_1 - m_2 + q_1^2}\left(I(1-n,-1,0) - I(-n,0,0)\right)\,, \end{aligned} \tag{6.25}$$

and using $I(-n,0,0) = 0$, it follows that $I(1-n,-1,0) = 0$. One can easily verify that analogous relations hold for all the integrals without positive powers for the denominators, as actually expected in DREG.

Let us now consider the case in which one index is positive and the other one is negative, e.g. $n_1 > 0\,, n_2 < 0$, corresponding to a tadpole integral with scalar products at the numerator. In fact, we are forced to introduce the auxiliary (bubble) topology $N = 3$ in order to treat integrals belonging to the sub-topology $N = 1$ with numerators S_2 (see (6.5)). It is immediate to see that the system $(n > 1)$

$$\begin{cases} I(n,0,0) = \mathbf{1}^+ I(n-1,0,0) \\ I(n-1,0,0) = \mathbf{2}^+ I(n-1,-1,0) \end{cases} \tag{6.26}$$

allows to express $I(n,-1,0)$ and $I(n-1,-1,0)$ in terms of integrals of the type $I(k,0,0)$ $(k > 0)$, which as already seen can be written in terms of one MI, $I(1,0,0)$. Then one can proceed further and consider the system

$$\begin{cases} I(n,-1,0) = \mathbf{1}^+ I(n-1,-1,0) \\ I(n-1,-1,0) = \mathbf{2}^+ I(n-1,-2,0) \end{cases} \tag{6.27}$$

which can be solved for $I(n,-2,0)$ and $I(n-1,-2,0)$. By the structure of (6.23)-(6.24), we see that the solution will involve again integrals of the type $I(k,0,0)$ $(k > 0)$, together with integrals of the type $I(k,-1,0)$ $(k > 0)$, for which a reduction was found in the previous step. The proof that all the integrals $I(n_1,n_2,0)$ with $n_1 > 0$ and $n_2 < 0$ are reducible in terms of $I(1,0,0)$ can be completed by induction and an analogous reasonings hold for the other cases $\{n_1 > 0, n_2 < 0, n_3 = 0\}$, $\{n_1 = 0, n_2 > 0, n_3 < 0\}$ etc.

As a last example we may now consider the bubble sub-topology $\{n_1, n_2 > 0, n_3 = 0\}$. The idea is again to use the plus operators in order to write all the integrals $I(n_1,n_2,0)$ in terms of known integrals. Let us define $\mathcal{D} = n_1 + n_2$. The integral $I(1,1,0)$ cannot be written in terms of the plus operators since the solutions (6.23)-(6.24) for $\mathbf{1}^+$ and $\mathbf{2}^+$ are defined only for $n_1 \neq 0$ and $n_2 \neq 0$. Therefore we assume it is a MI for the bubble topology (note that it is the only one with $\mathcal{D} = 2$). Let us now consider integrals with $\mathcal{D} = \delta > 2$. If we substitute (6.23) in $I(n_1,n_2,0) = \mathbf{1}^+ I(n_1 - 1, n_2, 0)$, several terms will be generated in the r.h.s, all proportional to integrals different from that in the l.h.s. The operator **Id** produces a term proportional to $I(n_1 - 1, n_2, 0)$, which has

$\mathcal{D} = \delta - 1$. The action of $\mathbf{2}^-\mathbf{1}^+$ and $\mathbf{2}^+\mathbf{1}^-$ brings into the expression other integrals with $\mathcal{D} = \delta - 1$. The operator $\mathbf{2}^+$ generates an integral with $\mathcal{D} = \delta$. Minus operators can make denominators disappear, thus bringing into the expressions integrals belonging to the tadpole sub-topologies $N = 1, 2$, which we have already solved. Analogous observations hold for $I(n_1, n_2, 0) = \mathbf{2}^+ I(n_1, n_2 - 1, 0)$.

Therefore, since the number $\mathcal{N}_\delta$ of integrals with a given $\mathcal{D} = \delta$ is finite, $N_\delta = \delta - 1$, we can generate $\mathcal{N}_\delta$ independent equations and solve them for such integrals. The solution will be given in terms of integrals with $\mathcal{D} = \delta - 1$. We have already seen that we can by no means eliminate $I(1, 1, 0)$ in favour of integrals with $\mathcal{D} = 1$. We can then start from $\mathcal{D} = 3$, writing a system for $I(1, 2, 0)$ and $I(2, 1, 0)$. The solution will involve $I(1, 1, 0)$ and the tadpole integrals. Then we may proceed with $\mathcal{D} = 4$, considering the integrals $I(3, 1, 0)$, $I(2, 2, 0)$, $I(1, 3, 0)$. By iterating the procedure, we see that in general we can express all the $\mathcal{D} = \delta$ integrals in terms of the $\mathcal{D} = \delta - 1$ integrals. So, by recursively applying this procedure to the l.h.s. down to $\mathcal{D} = 2$, we can reduce a general bubble diagram of the type (6.20) to the following form:

$$I(n_1, n_2, 0) = A(n_1, n_2) I(1, 1, 0) + B(n_1, n_2) I(1, 0, 0) + C(n_1, n_2) I(0, 1, 0)\,, \tag{6.28}$$

where the coefficients A, B and C are algebraically determined as discussed above. We have thus seen that the evaluation of a generic bubble diagram reduces to the *algebraic* task of computing the coefficients A, B and C and the integrals that must be actually evaluated are only two (since $I(1, 0, 0)$ and $I(0, 1, 0)$ have the same functional form). The MI $I(1, 1, 0)$ is proportional to the $B_0(q_1^2, m_1, m_2)$ function defined in (6.10). It is clear that as $\mathcal{D}$ grows, the needed algebrical effort increases considerably. Apart from the solution of the linear system, the number of nested substitutions for the reduction of the r.h.s. to MI's becomes high. A systematic approach is thus needed if one aims at employing the IBP reduction strategy in the evaluation of actual Feynman diagrams.

We can conclude by noting that, if one applies the same procedure to all the subtopologies of the vertex topology ($N = 1, 2, 3, 4, 5, 6$) and to the vertex topology itself $N = 7$, this will result in the full reduction of any general one-loop vertex diagrams to a combination of MI's. We will not show it here, but all the subtopologies can be reduced in terms of the MI's A_0 and B_0 (with all the possible arguments). The vertex topology needs one more MI belonging to that topology, namely $I(1, 1, 1)$, which is proportional to the C_0 function (6.11). The number of MI's actually decreases if some of the masses vanish. For instance, if one has $q_1^2 = q_2^2 = 0$ and all the masses vanish, only one MI is needed: $A_0(0)$ vanishes in DREG and each vertex integral is seen to be fully reducible to the MI of its subtopology $N = 6$, $B_0(s, 0, 0)$.

6.2.2 Automatized IBP reduction

For general l-loop, n-point diagrams the procedure is exactly the same, except that it becomes more and more algebraically complicated. Again, $\mathbf{i}^\pm$ operators for each exponent n_i will enter the IBP identities, which gives rise to a rather complex system of linear

equations in the integrals. The full reduction of a given integral can be achieved by performing the IBP reduction of that integral and all its subtopologies.

A systematic procedure for automatizing this algebraic task is indispensable since it can be rather heavy for big topologies and when the number of scales is high. A strategy has been devised by Laporta [153]. We will not enter the details of the algorithm, but rather explain the idea behind it. The algorithm is based on writing several particular cases of the IBP identities by replacing the indices n_i in the IBP identities with (negative, zero and positive) explicit values. If a sufficient number of equations is generated, one ends up with a (typically huge) system of linear equations, where the unknowns are the particular integrals (with explicit n_i's) themselves. The system is then solved by means of the Gauss-Jordan elimination method. Actually not all the equations need to be independent. If the system for a given topology is overconstrained, then all the integrals of that topology can be reduced to a linear combination of the MI's of the corresponding subtopologies (upon substitution of the full tree of IBP equations for the topology and its subtopologies). In case the system is not overconstrained, there will be also some MI's belonging to the topology one has started from (as we have seen in the case of the two-mass bubble diagram). In any case, the result will be that a large number of scalar integrals, $\mathcal{O}(100 \div 1000)$, can be typically reduced to $\mathcal{O}(1 \div 10)$ independent scalar integrals. We have already stated that for one-loop diagrams, there can be at most 3 MI's.

The important point relative to the Laporta algorithm is that it can be automated in a rather general way. Several private and public codes have in fact been written, such as `AIR` [154], `FIRE` [155] and `REDUZE` [66]. The number of equations to be generated is related to the maximum and minimun value that can be taken by the sum r of the positive n_i's and the sum s of the negative n_i's. The resulting list of particular IBP reduction identities for a given mass pattern can easily exceed the size of $\mathcal{O}(100)$ megabytes on a computer. It is thus necessary implement their application in some symbolic manipulation software like `FORM` [65] (which is the one employed in the present work) or `MATHEMATICA` [57].

6.2.3 Application to disconnected integrals

The Laporta algorigthm "blindly" generates the system of equations for all the possible combinations of powers of the D_i with exponents such that $r \in [r_{min}, r_{max}]$ and $s \in [s_{min}, s_{max}]$. We have said that the calculational effort needed for the solution of the system grows strongly with the number of loops and with the number of different mass scales available. It is inefficient to consider the two-loop disconnected diagram as a single two-loop diagram, since many generated identities will actually never be used. We exploited the disconnected nature of the two-loop integrals we need to (exactly) evaluate in order to improve the computational efficience of the IBP reduction for the case at hand. In particular, we reduce separately the two one-loop integrals by assigning the scalar product $p \cdot k$ to the easiest integral. Suppose we assign it to the k integration. Then p is effectively an extra external momentum in the k integration, and we need the auxiliary denominator D_7 in order to express it in terms of denominators. So we first perform the reduction of the one-loop integrals $I_k(n_1, n_2, n_3, n_7)$, where as already noted n_7 is never positive. This

observation about the auxiliary denominator is crucial, because it allows us to avoid the IBP reduction of the full topology $\{D_1, D_2, D_3, D_7\}$, which would be rather heavy. The reduction of the vertex subtopology $\{D_1, D_2, D_3\}$ and its subtopologies is what we need. The resulting expression will depend on the spacetime dimension d, the kinematic invariants *and* on the scalar products p^2, $p \cdot q_1$ and $p \cdot q_2$, which are functions of the remaining loop momentum. But now we are left with the standard one-loop integration of a vertex topology. The scalar products resulting from the k integration are again expressed in terms of the denominators and the IBP reduction of $I_p(n_4, n_5, n_6)$ is performed (note that the topology is now simpler since it does not involve D_7).

We remark that the typical structure we encouter in our computation is the product of a one-loop integral with to three different masses times a one-loop integral where each of the three masses entering the denominators can be either 0 or a common mass m. So, by always assigning $p \cdot k$ to the easiest of the two (say k), we will optimize the complexity of the IBP formulae we obtain. In general the IBP identities for that integral where the coefficients will be rational functions of polynomials in the available kinematical invariants ($(q_1 + q_2)^2 = s$) and the spacetime dimension d

$$C_k(d, m, s, p^2, p \cdot q_1, p \cdot q_2)\,, \tag{6.29}$$

while the IBP identities for the p integral will involve coefficient of the kind

$$C_p(d, m_1, m_2, m_3, s)\,. \tag{6.30}$$

The IBP identities have been generated (in `FORM` syntax) with the open source program `REDUZE` [66], which implements the Laporta algorithm. The advantage of IBP reduction is that one can generate the IBP identities for generic masses once and for all (for a given problem) and store them in a suitable way. Moreover, the reduction to MI's is the most computationally heavy step. Note anyway that it is necessary to generate several sets of identities corresponding to the cases in which some of the masses m_i are equal or vanish, since it is in general hard and inefficient to analytically compute the corresponding limits from the general formulae. It is much more efficient to have the IBP identities at our disposal for all the cases and focus on the algebraic problem of reading and applying the stored identities and manipulating the rather complex coefficients entering the expressions.

The problem of reducing the actual integrals entering our computation was solved by writing a `FORM` code that processes generic and possibly very long expressions made of arbitrary coefficients times arbitrary disconnected integrals of the form

$$\begin{aligned}\mathcal{A} = {} & C \times J(r_1, \ldots, r_6; s_1 \ldots, s_7) \times M(m_1, \ldots, m_6) \\ & + C' \times J(r'_1, \ldots, r'_6; s'_1 \ldots, s'_7) \times M(m'_1, \ldots, m'_6) \\ & + \ldots\,,\end{aligned} \tag{6.31}$$

where $C, C', \ldots$ are the coefficients and the functions $J \times M$ are nothing else than the integral (6.1) where we have explicited the masses m_i entering the denominators D_i:

$$J(r_1, \ldots, r_6; s_1, \ldots, s_7) \times M(m_1, \ldots, m_6) = \int \mathrm{d}^d p\, \mathrm{d}^d k\, \frac{S_1^{s_1} \cdots S_7^{s_7}}{D_1^{n_1}(m_1) \cdots D_6^{n_6}(m_6)}\,. \tag{6.32}$$

Our FORM code performs a series of manipulations to bring expressions like $\mathcal{A}$ in (6.31) to a suitable and efficient form in order to allow a fast application of the previously generated IBP identities. First of all, scaleless integrals and integrals that are known to vanish by symmetry arguments are set to zero. Scalar products in the numerators are expressed in terms of denominators as described in sec. 6.1. Then integrals that are equivalent upon a rerouting of the loop momenta are brought to a common form. We also collect the coefficients of the same integrals into compact objects, considerably reducing the number of terms to be processed. We end up with an expression of the type

$$C \times I(n_1, \ldots, n_7) \times M(m_1, \ldots, m_6, 0) + C' \times I(n'_1, \ldots, n'_7) \times M(m'_1, \ldots, m'_6, 0) + \ldots , \tag{6.33}$$

where again $I \times M$ is just the integral (6.7) where we explicitly keep track of the mass pattern (for the reasons discussed above, the auxiliary denominator D_7 is always massless) and each of the $I \times M$ occurs only once.

A further, crucial simplifications stems from the fact that many of the integrals generated by the asymptotic expansions are equal except for a different labelling of the masses involved. One would end up reading and applying the same identity several times (which can be extremely complex, depending on the number of mass scales involved) while processing a long expression. It is much more efficient to collect all the occurrences of equivalent integrals, read and apply the IBP identities just once for generic masses and substitute back the masses term by term only as a last step. To this end, we have implemented an algorithm which efficiently identifies integrals with the same *abstract* mass pattern, in the sense that e.g.

$$I(n_1, n_2, n_3) \times M(a, b, b) \sim I(n_1, n_2, n_3) \times M(c, d, d) \tag{6.34}$$

where $\sim$ is an equivalence relation. Having identified those integrals, we write them as, e.g.

$$I(n_1, n_2, n_3) \times M(m_1, m_2, m_2) \left[P(a, b, b) + P(c, d, d)\right] , \tag{6.35}$$

where the function M will enter the IBP reduction (which in this case is therefore performed *once* and not twice), while the funtions P are merely coefficients in this step and keep track of the actual particular pattern of masses, which is replaced term by term at the end.

We remark that no approximation needs to be done in order to perform each of these steps, so the result of the IBP reduction will be the exact evaluation of the the disconnected two-loop contributions in d-dimensions. It will consist of a combination of products of two of the one-loop MI's ($A_0(m_1) \times A_0(m_2)$, $B_0(p^2, m_1, m_2) \times C_0(0, 0, s, m_3, m_4, m_5)$ etc.) times coefficients that depend on the masses, s and d.

At this stage, it is possible to set $d = 4 - 2\epsilon$ and evaluate the limit $\epsilon \to 0$. One has to carefully expand each function of d to a sufficiently high order in ϵ since each one-loop integration can contain at most a double pole ϵ^{-2} (in the fully massless case) and can generate a finite result (pole) when hitting the $\mathcal{O}(\epsilon^2)$ ($\mathcal{O}(\epsilon)$) part of the result of other integration.

6.3 An alternative strategy

Another way of solving the one-loop problem is the traditional Passarino-Veltman (PV) procedure [156] (see also [157] for a systematic review of one-loop calculations techniques). We recall that the PV procedure is an algebraic algorithm based on the Lorentz decomposition of a generic one-loop tensor integral as combinations of tensors constructed from the external momenta q_i and the metric tensor with totally symmetric coefficients. By contracting the tensor integral in all possible ways with the external momenta and the metric tensor one obtains a set of linear equations for the coefficient functions. The solution of such linear system yelds the latter in terms of the coefficients of the tensor decomposition of integrals with fewer tensor indices. In principle one can interate this procedure until the coefficient functions of the original tensor integral are expressed in terms of the three MI's A_0, B_0 and C_0.

In the case of three- or higher-point functions, if the matrix $(G)_{ij} = \{q_i \cdot q_j\}$ has vanishing (Gram) determinant, the algorithm breaks down and more sophisticated approaches or workarounds must be devised. This essentially happens when some of the kinematic invariants vanish or in some particular regions of the phase space. Reduction via IBP identities represents in these cases a much more efficient strategy. Nevertheless, since PV reduction is vaild for any value of the spacetime dimension d, including $d = 4$, we have employed it when PVREG is used. The problem of vanishing Gram determinants is circumvented a priori since we give a small mass λ to the gluons because we need to regularize the IR divergences (see sec. 4.2.1).

Part III

Results

Chapter 7

Two-loop NLO QCD corrections to $gg \to h, H$ cross-section

In this chapter we present the result for the two-loop NLO QCD top/stop contributions to the $gg \to \phi$ cross section for the CP-even case $\phi = h, H$. We combine earlier results available in the literature with our new calculation of the top-stop-gluino contribution. The latter is based on an asymptotic expansion in the large supersymmetric masses and is valid up to and including terms of $\mathcal{O}(m_\phi^2/M^2)$, $\mathcal{O}(m_t^2/M^2)$ and $\mathcal{O}(m_Z^2/M^2)$, where M denotes a generic superparticle mass. Our results are obtained by extending the method of ref. [42] for the bottom-sbottom-gluino contributions, valid for m_ϕ^2 below all the heavy particle thresholds, where only terms of $\mathcal{O}(m_b^2/m_\phi^2)$, $\mathcal{O}(m_b/M)$ and $\mathcal{O}(m_Z^2/M^2)$ were retained. The explicit top-stop-gluino results available in the literature are either based on an effective theory where the heavy particles have been integrated out [33] or on a Taylor expansion in the small momenta in the full theory [34]. Such results give a good approximation of the full result when the ϕ mass is below the top-pair production threshold, $m_\phi^2 \ll m_t^2$. In our calculation no specific hiearchy between the Higgs and the top quark mass is assumed, therefore our formulae are expected to provide a better approximation of the full result in the threshold region $m_\phi \simeq 2m_t$.

The chapter is organized as follows. In sec. 7.1 we give a detailed overview of the calculation workflow, which will basically apply also to the CP-odd case. In sec. 7.2 we describe the structure of the two-loop contributions to the form factors, which are due to top-gluon, stop-gluon, four-stop and top-stop-gluino diagrams. Then we report our NLO top result. For completeness we recall and adapt to our approximation the earlier results available in the literature for the first three classes of contributions. Our $\overline{\text{DR}}$ results for the top-stop-gluino contributions are provided in compact form, by writing them in terms of a few functions. We gather the explicit expressions in app. D. In sec. 7.3 we provide the shifts for converting our $\overline{\text{DR}}$ results to a suitable On-Shell (OS) scheme.

A numerical study of our result and a quantitative comparison with the Taylor expansion based result is underway.

7.1 Details on the computation

Concerning the actual computational details, a few remarks are in order. We generated the relevant two-loop diagrams with the help of the `Mathematica` [57] package `FeynArts` [58], using a modified version of the MSSM model file [59] which implements the Background Field Method [60–64] (see sec. 4.3 for an overview and some remarks). The ϕ-g-g amplitude can always be written as ($\phi = h, H$)

$$\mathcal{M}_\phi = \mathcal{M}_\phi^{\mu\nu} \varepsilon_\mu(q_1) \varepsilon_\nu(q_2) \,, \tag{7.1}$$

where $\varepsilon(q_i)$ is the polarization four-vector of the i-th gluon (with momentum q_i, which we consider on-shell). By Lorentz invariance considerations, we can write the most general tensor structure for $\mathcal{M}_\phi^{\mu\nu}$:

$$\mathcal{M}_\phi^{\mu\nu} = \mathcal{T}_1 \, q_1^\mu q_1^\nu + \mathcal{T}_2 \, q_2^\mu q_2^\nu + \mathcal{T}_3 \, q_1^\mu q_2^\nu + \mathcal{T}_4 \, q_2^\mu q_1^\nu + \mathcal{T}_5 \, (q_1 \cdot q_2) \, g^{\mu\nu} + \mathcal{T}_6 \, \epsilon^{\mu\nu\rho\sigma} q_{1\rho} q_{2\sigma} \,, \tag{7.2}$$

where $\mathcal{T}_i$ are the scalar form factors. Bose symmetry requires that $\mathcal{T}_1 = \mathcal{T}_2$, gauge invariance requires that $q_{1\mu} \mathcal{M}_\phi^{\mu\nu} = 0$, which for on-shell gluons ($q_i^2 = 0$ for $i = 1, 2$) is satisfied if $\mathcal{T}_4 = -\mathcal{T}_5$. Applying the other gauge invariance constraint $q_{2\nu} \mathcal{M}_\phi^{\mu\nu} = 0$ is equivalent to imposing Bose symmetry. For on-shell gluons it also holds that $q_i^\mu \varepsilon_\mu(q_i) = 0$, which implies that the form factors $\mathcal{T}_1$, $\mathcal{T}_2$ and $\mathcal{T}_3$ are irrelevant for the computation of $\mathcal{M}_\phi$. Concerning $\mathcal{T}_6$, such form factor is related to parity violation and vanishes exactly in our case. Thus we can effectively write

$$\mathcal{M}_\phi^{\mu\nu} = \mathcal{T}_5 \, [(q_1 \cdot q_2) \, g^{\mu\nu} - q_2^\mu q_1^\nu] \,. \tag{7.3}$$

We regularize the loop integrals in DREG as described in sec. 4.1. Since it is convenient to work with scalar quantities, we introduce the projector

$$P_\phi^{\mu\nu} = \frac{1}{(d-2)} \left[\frac{g^{\mu\nu}}{(q_1 \cdot q_2)} - \frac{q_1^\mu q_2^\nu + q_2^\mu q_1^\nu}{(q_1 \cdot q_2)^2} \right] \,, \tag{7.4}$$

such that

$$P_\phi^{\mu\alpha} \, P_{\phi\,\alpha}{}^{\nu} = P_\phi^{\mu\nu} \tag{7.5}$$

$$P_{\phi\,\mu\nu} \, \mathcal{M}_\phi^{\mu\nu} = \mathcal{T}_5 \,. \tag{7.6}$$

The calculation is fully automatized. The scalar amplitudes are processed with a chain of `Mathematica` [57] and `FORM` [65] programs that implement the several needed steps. First color and Dirac algebra (in $d = 4 - 2\epsilon$ dimensions) are carried on, then we identify the diagrams that are equivalent upon a redefinition of the loop momenta or by symmetry arguments and group them in order to improve the computational efficiency. At this stage the asymptotic expansion is performed, according to the strategy outlined in chap. 5. For each diagram (including those without physical thresholds) we:

1. Generate its IR contribution, which has the form of a sum of (possibly a large number of) two-loop disconnected integrals.

2. Taylor expand in the small external momentum the IR finite part (obtained by subtracting the disconnected part from the original diagram). Then we process the output with a code that implements the vertex diagram tensor reduction algorithm of ref. [158], follwed by the application of the methods of ref. [147] for the integration of the resulting scalar massive vacuum tadpoles. These steps are implemented in a `Mathematica` code.

3. Carry on the exact evaluation of the disconnected part as described in chap. 6 through a `FORM` code which performs the IBP reduction to one-loop Master Integrals (MI's), computes the limit $\epsilon \to 0$ and expands the MI's assuming $m_\phi^2, m_t^2 \ll m_{\tilde{t}_1}^2, m_{\tilde{t}_2}^2, m_{\tilde{g}}^2$.

4. Check that the result for the IR finite part obtained through the Taylor expansion is actually free of terms that exhibit an IR divergent behaviour in the limit $m_t^2 \to 0$, as we expect by construction.

5. Check that the result of the asymptotic expansion coincides with that of a naive Taylor expansion of the original two-loop diagram in case the latter does not exhibit any physical threshold.

6. Also perform the following validation test of our programs through a check on the disconnected diagrams: we *i*) Taylor expand the diagrams and integrate the resulting massless tadpoles with the methods of [147] and *ii*) process the diagrams with our IBP reduction code and then we further expand the exact results for $m_\phi^2 \ll m_t^2$. Since the two operations of Taylor expansion and integration must commute, we verify that *i*) and *ii*) actually produce the same result.

Renormalization is carried on according to the discussion in sec. 4.3.1 (note that, by construction, counterterm diagrams are disconnected contributions). We perform the calculation in the $\overline{\text{MS}}$ scheme and then we apply the known $\overline{\text{MS}} \to \overline{\text{DR}}$ shifts. We also compute the shifts for the transition to an OS scheme as defined in [34] and discussed in sec. 4.3.1. We explicitly verify that the dependence on the renormalization scale Q^2 cancels in the OS scheme.

As a last check we verify that, with the correct replacements $t \to b$ (see (A.6)) and after a further Taylor expansion for $m_b^2 \ll m_\phi^2, M^2$ in such a way that only terms of $\mathcal{O}(m_b^2/m_\phi^2)$, $\mathcal{O}(m_b/M)$ and $\mathcal{O}(m_Z^2/M^2)$ are retained, our result for the bottom contributions agrees with that in ref. [42].

7.2 Two-loop top/stop contributions

In the following we present the result for the two-loop top/stop contributions to the form factor for CP-even Higgs boson production via gluon fusion. For clarity, let us recall the

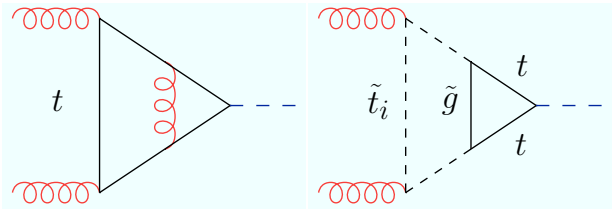

(a) top-gluon **(b)** top-stop-gluino

Figure 7.1: Examples of two-loop diagrams involving the Higgs-top coupling.

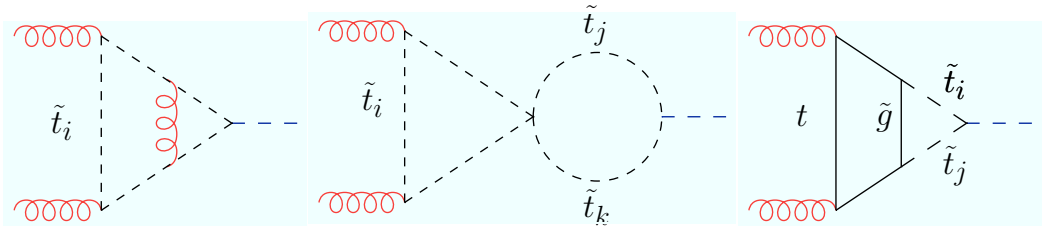

(a) stop-gluon **(b)** 4-stop **(c)** top-stop-gluino

Figure 7.2: Examples of two-loop diagrams involving the Higgs-stop coupling.

structure (to all orders in the strong interactions) of the form factor entering the LO cross section (3.3) for the CP-even case in the MSSM (see sec. 3.2.2)

$$\mathcal{H}_h = T_F \, (-\sin\alpha \, \mathcal{H}_1 + \cos\alpha \, \mathcal{H}_2) \, , \tag{7.7}$$

$$\mathcal{H}_H = T_F \, (\cos\alpha \, \mathcal{H}_1 + \sin\alpha \, \mathcal{H}_2) \, , \tag{7.8}$$

where

$$\mathcal{H}_1 = \lambda_t \left[m_t \, \mu \, s_{2\theta_t} \, F_t \, + m_Z^2 \, s_{2\beta} \, D_t \right] \, + \lambda_b \left[m_b \, A_b \, s_{2\theta_b} \, F_b \, + 2 \, m_b^2 \, G_b \, + 2 \, m_Z^2 \, c_\beta^2 \, D_b \right] \, , \tag{7.9}$$

$$\mathcal{H}_2 = \lambda_b \left[m_b \, \mu \, s_{2\theta_b} \, F_b \, - m_Z^2 \, s_{2\beta} \, D_b \right] + \lambda_t \left[m_t \, A_t \, s_{2\theta_t} \, F_t \, + 2 \, m_t^2 \, G_t \, - 2 \, m_Z^2 \, s_\beta^2 \, D_t \right] \, , \tag{7.10}$$

(see below (3.20)-(3.21) for a description of the quantities entering the above expressions). For later convenience we also recall that the D-term-induced Higgs-squark-squark contribution can be decomposed as (see (3.22))

$$D_q = \frac{I_{3q}}{2} \, \widetilde{G}_q + c_{2\theta_{\tilde{q}}} \left(\frac{I_{3q}}{2} - Q_q \, s_{\theta_W}^2 \right) \, \widetilde{F}_q \, . \tag{7.11}$$

There are several classes of two-loop diagrams which contribute to the form factors. The diagrams involving the Higgs-top coupling generate two kinds of two-loop contributions, namely diagrams with top quarks and gluons (e.g. fig. 7.1a) and diagrams with top-stop-gluino vertices (e.g. fig. 7.1b). The diagrams involving the Higgs-stop coupling generate three kinds of two-loop contributions, namely diagrams with stops and gluons (e.g.

fig. 7.2a), diagrams with four-stop vertices (e.g. fig. 7.2b) and diagrams with top-stop-gluino vertices (e.g. fig. 7.2c).

We can express our results for the functions G_t, F_t, $\widetilde{F}_t$, $\widetilde{G}_t$ in a rather compact way by writing them as linear combinations of four functions Y_t, $Y_{\tilde{t}_1}$, $Y_{\tilde{t}_2}$, $Y_{c^2_{2\theta_t}}$. Each of these functions receives two-loop contributions due to gluon exchange in diagrams with top or stop loops (g), diagrams involving the four stop vertices ($4\tilde{t}$) and diagrams involving the top-stop-gluino vertices ($\tilde{g}$):

$$Y_x = Y_x^g + Y_x^{4\tilde{t}} + Y_x^{\tilde{g}} \qquad (x = t,\, \tilde{t}_1,\, \tilde{t}_2,\, c^2_{2\theta_t})\ . \tag{7.12}$$

The contributions due to gluon exchange and to diagrams involving the quartic coupling are already known, respectively retaining the full dependence on the masses* [34, 36] and in the limit of vanishing Higgs mass [34]. For completeness we recall their expressions, which we decompose as

$$Y_x^g = C_F Y_x^{(g,C_F)} + C_A Y_x^{(g,C_A)}\,, \tag{7.13}$$

$$Y_x^{4\tilde{t}} = C_F Y_x^{(4\tilde{t},C_F)}\,, \tag{7.14}$$

(due to the MSSM coupling structure the diagrams with four stop vertices have no C_A part). Assuming that the the one-loop form factor $\mathcal{H}_2^{1\ell}$ is expressed in terms of $\overline{\rm DR}$-renormalized parameters evaluated at the scale Q^2, the gluon contributions read

$$Y_t^{(g,C_F)} = \frac{1}{2m_t^2}\left[\mathcal{F}_{1/2}^{(2\ell,a)}\left(x(\tau_t)\right) + \mathcal{F}_{1/2}^{(2\ell,b)}\left(x(\tau_t)\right)\left(\ln\frac{m_t^2}{Q^2} - \frac{1}{3}\right)\right]\,, \tag{7.15}$$

$$Y_t^{(g,C_A)} = \frac{1}{2m_t^2}\left[\mathcal{G}_{1/2}^{(2\ell,C_A)}\left(x(\tau_t)\right)\right]\,, \tag{7.16}$$

$$Y_{\tilde{t}_1}^{(g,C_F)} = \frac{1}{2m_{\tilde{g}}^2}\left(-\frac{3}{4\,x_1}\right)\,, \tag{7.17}$$

$$Y_{\tilde{t}_1}^{(g,C_A)} = \frac{1}{2m_{\tilde{g}}^2}\left(-\frac{1}{6\,x_1}\right)\,, \tag{7.18}$$

$$Y_{c^2_{2\theta_t}}^{(g,C_F)} = Y_{c^2_{2\theta_t}}^{(g,C_A)} = 0\,, \tag{7.19}$$

where $\tau_i \equiv 4m_i/m_\phi$, $x(\tau) \equiv \frac{\sqrt{1-\tau}-1}{\sqrt{1-\tau}+1}$ and the variable x_i is defined as $x_i \equiv m_{\tilde{q}_i}^2/m_{\tilde{g}}^2$. Explicit exact expressions for the functions $\mathcal{F}_{1/2}^{(2\ell,a)}$, $\mathcal{F}_{1/2}^{(2\ell,b)}$ and $\mathcal{G}_{1/2}^{(2\ell,C_A)}$ are given in eqs. (2.12), (2.13) and (3.8) of ref. [36].

*The SM contribution $Y_t^{(g)}$, due to top-gluon diagrams, is given by eq. (4.2) of [42] with the trivial replacent $b \to t$.

The four squark contributions read

$$Y_t^{(4\tilde{t},C_F)} = 0\,, \tag{7.20}$$

$$Y_{\tilde{t}_1}^{(4\tilde{t},C_F)} = -\frac{1}{24\,m_{\tilde{g}}^2}\left[\frac{c_{2\theta_t}^2 x_1 + s_{2\theta_t}^2 x_2}{x_1^2} + \frac{s_{2\theta_t}^2}{x_1^2 x_2}\left(x_1^2 \ln\frac{m_{\tilde{t}_1}}{Q^2} - x_2^2 \ln\frac{m_{\tilde{t}_2}}{Q^2}\right)\right], \tag{7.21}$$

$$Y_{c_{2\theta_t}^2}^{(4\tilde{t},C_F)} = -\frac{1}{24}\left[\frac{(x_1-x_2)^2}{x_1 x_2} + \left(1-\frac{x_1}{x_2}\right)\ln\frac{m_{\tilde{t}_1}^2}{Q^2} + \left(1-\frac{x_2}{x_1}\right)\ln\frac{m_{\tilde{t}_2}^2}{Q^2}\right]. \tag{7.22}$$

The results for $Y_{\tilde{t}_2}^t$ and $Y_{\tilde{t}_2}^{4\tilde{t}}$ can be immediatly obtained from those for $Y_{\tilde{t}_1}^t$ and $Y_{\tilde{t}_1}^{4\tilde{t}}$ with the replacement $(1 \longleftrightarrow 2)$, that is by substituting $(x_1,\, \tilde{t}_1)$ with $(x_2,\, \tilde{t}_2)$ and viceversa.

The quark-squark-gluino contribution to the Higgs-gluon-gluon form factor, for Higgs bosons *not below* the $q\bar{q}$ threshold, is known only in the bottom sector [42]. There the relevant diagrams were evaluated in the further approximation $m_b^2 \ll m_\phi^2$ and neglecting terms of $\mathcal{O}(m_b^2/M^2)$ and $\mathcal{O}(m_\phi^2/M^2)$. In this work, we performed a new computation of the relevant diagrams, valid in the top sector for large supersymmetric particle masses. In particular we do not assume any specific hierarchy between the top mass and the Higgs mass and we retain terms up to $\mathcal{O}(m_t^2/M^2)$, $\mathcal{O}(m_\phi^2/M^2)$ and $\mathcal{O}(m_Z^2/M^2)$.

By putting together all the contributions, we can write the full $\overline{\text{DR}}$ result for the Y_x functions as a power series in the small ratio m/M (where we recall that $m = m_t,\, m_\phi, m_Z$ and $M = m_{\tilde{g}}^2,\, m_{\tilde{t}_1}^2,\, m_{\tilde{t}_2}^2$):

$$Y_x = \frac{1}{\mathcal{N}_x}\sum_{n=-1}^{\infty}\left[\left(\frac{m_t}{m_{\tilde{g}}}\right)^n Y_x^{(n)}\right], \tag{7.23}$$

where

$$\mathcal{N}_x = \begin{cases} 2m_t^2 & \text{if } x = t\,, \\ m_{\tilde{g}}^2 & \text{if } x = \tilde{t}_1,\, \tilde{t}_2\,, \\ 1 & \text{if } x = c_{2\theta_t}^2\,. \end{cases} \tag{7.24}$$

Keeping in mind that we aim at $\mathcal{O}(m^2/M^2)$ accuracy and in the form factors $\mathcal{H}_{1,2}$ (eqs. (7.9) and (7.10)):

- G_t is multiplied by $2m_t^2 \sim \mathcal{O}(m^2)$,
- F_t is multiplied by $m_t\, A_t \sim \mathcal{O}(m)$ and $m_t\, \mu \sim \mathcal{O}(m)$,
- $\widetilde{F}_t$ and $\widetilde{G}_t$ are multiplied by $m_Z^2 \sim \mathcal{O}(m^2)$,

our results for the two-loop functions $G_t^{2\ell}$, $F_t^{2\ell}$, $\widetilde{F}_t^{2\ell}$, $\widetilde{G}_t^{2\ell}$ can be cast in the following form

(see also [34, 42]):

$$G_t^{2\ell} = \frac{1}{2m_t^2}\sum_{n=-1}^{2}\left(\frac{m_t}{m_{\tilde{g}}}\right)^n Y_t^{(n)} + \frac{1}{m_{\tilde{g}}^2}\sum_{n=-1}^{0}\left(\frac{m_t}{m_{\tilde{g}}}\right)^n \left[Y_{\tilde{t}_1}^{(n)} + Y_{\tilde{t}_2}^{(n)}\right], \tag{7.25}$$

$$F_t^{2\ell} = \frac{1}{m_{\tilde{g}}^2}\sum_{n=-1}^{1}\left(\frac{m_t}{m_{\tilde{g}}}\right)^n \left[Y_{\tilde{t}_1}^{(n)} - Y_{\tilde{t}_2}^{(n)} - \frac{4\,c_{2\theta_t}^2}{x_1-x_2}\,Y_{c_{2\theta_t}^2}^{(n)}\right], \tag{7.26}$$

$$\widetilde{F}_t^{2\ell} = \frac{1}{m_{\tilde{g}}^2}\sum_{n=-1}^{0}\left(\frac{m_t}{m_{\tilde{g}}}\right)^n \left[Y_{\tilde{t}_1}^{(n)} - Y_{\tilde{t}_2}^{(n)} + \frac{4\,s_{2\theta_t}^2}{x_1-x_2}\,Y_{c_{2\theta_t}^2}^{(n)}\right], \tag{7.27}$$

$$\widetilde{G}_t^{2\ell} = \frac{1}{m_{\tilde{g}}^2}\sum_{n=-1}^{0}\left(\frac{m_t}{m_{\tilde{g}}}\right)^n \left[Y_{\tilde{t}_1}^{(n)} + Y_{\tilde{t}_2}^{(n)}\right], \tag{7.28}$$

where the expansion coefficients $Y_x^{(n)}$ entering (7.25)-(7.28) can be decomposed as (δ_{ij} is the Kronecker delta)

$$Y_x^{(n)} = \mathcal{N}_x\left(Y_x^g + Y_x^{4\tilde{t}}\right)\delta_{n0} + Y_x^{(n,\tilde{g})}, \tag{7.29}$$

in which Y_x^g and $Y_x^{4\tilde{t}}$, given respectively by eqs. (7.13) and (7.14), contribute only for $n = 0$. We decompose as usual the gluino part as

$$Y_x^{(n,\tilde{g})} = C_F\,Y_x^{(n,\tilde{g},C_F)} + C_A\,Y_x^{(n,\tilde{g},C_A)}, \tag{7.30}$$

where our explicit results for the coefficients $Y_x^{(n,\tilde{g},C_F)}$ and $Y_x^{(n,\tilde{g},C_A)}$ can be found in app. D.

For later convenience let us denote with $\mathcal{B}$ the finite part of the $B_0(m_\phi, m_t, m_t)$ function, renormalized at $Q^2 = m_t^2$, and recall the expressions for the one-loop functions (eq. (2.6) of ref. [54] and eq. (2.10) of ref. [42])

$$\mathcal{K}_{1/2}^{1\ell}(\tau) = \frac{\tau}{2}\ln^2\left(\frac{\sqrt{1-\tau}-1}{\sqrt{1-\tau}+1}\right), \tag{7.31}$$

$$\mathcal{G}_{1/2}^{1\ell}(\tau) = -2\tau\left[1 - \frac{1-\tau}{4}\ln^2\left(\frac{\sqrt{1-\tau}-1}{\sqrt{1-\tau}+1}\right)\right]. \tag{7.32}$$

In the explicit formulae we will also use the function $\mathcal{F}_{1/2}^{(2\ell,b)}$, defined in eq. (2.13) of ref. [36], and the supersymmetric contribution to the finite part of top mass self-energy. The finite part of the full top mass self-energy (in DRED, see (4.47)) involves the finite part of a B_0 function depending on heavy (supersymmetric) and light (top quark) masses, which we expand according to our power counting. The resulting expression can be written as

$$\frac{\delta m_t}{m_t} = C_F\frac{\alpha_s}{\pi}\left[\frac{(\delta m_t)^{(\mathrm{QCD})}}{m_t} + \frac{(\delta m_t)^{(\mathrm{SUSY})}}{m_t}\right], \tag{7.33}$$

where

$$\frac{(\delta m_t)}{m_t}^{(\mathrm{QCD})} = \delta^{(0)}_{m_t,\mathrm{QCD}} \equiv \frac{3}{4}\ln\frac{m_t^2}{Q^2} - \frac{5}{4}\,, \tag{7.34}$$

$$\frac{(\delta m_t)}{m_t}^{(\mathrm{SUSY})} = \sum_{n=-1}^{2}\left(\frac{m_t}{m_{\tilde{g}}}\right)^n \delta^{(n)}_{m_t,\mathrm{SUSY}} + \mathcal{O}\left(\frac{m_t^3}{m_{\tilde{g}}^3}\right)\,, \tag{7.35}$$

and the expansion coefficients of the supersymmetric contribution are

$$\delta^{(-1)}_{m_t} = -\frac{1}{4}s_{2\theta_t}\left(\frac{x_1}{1-x_1}\ln x_1 - \frac{x_2}{1-x_2}\ln x_2\right)\,, \tag{7.36}$$

$$\delta^{(0)}_{m_t} = -\frac{1}{4}\left(\ln\frac{m_{\tilde{g}}^2}{Q^2} + f(x_1) + f(x_2)\right)\,, \tag{7.37}$$

$$\begin{aligned}\delta^{(1)}_{m_t} = &-\frac{1}{4}\frac{s_{2\theta_t}}{(1-x_1)^3}\left(x_1\ln x_1 + \frac{1-x_1^2}{2}\right)\\ &-\Big(x_1 \longrightarrow x_2\Big)\,,\end{aligned} \tag{7.38}$$

$$\begin{aligned}\delta^{(2)}_{m_t} = &-\frac{1}{4}\frac{1}{(1-x_1)^4}\left(\frac{(1-x_1)(x_1^2-5x_1-2)}{6} - x_1\ln x_1\right)\\ &+\Big(x_1 \longrightarrow x_2\Big)\,.\end{aligned} \tag{7.39}$$

The function $f(x)$ entering eq. (7.37) is defined as

$$f(x) = \frac{x-3}{4(1-x)} + \frac{x(x-2)}{2(1-x)^2}\ln x\,. \tag{7.40}$$

Note that the expansion of the supersymmetric contribution to the finite part of the top self-energy up to order zero in $m_t/m_{\tilde{g}}$ matches eq. (4.8) of [42] (with the obvious replacements for converting from the bottom sector to the top sector). Together with the remaining terms of the expansion, such quantity represents the shift needed for converting (at one-loop and in our approximation) the top mass from the $\overline{\mathrm{DR}}$ scheme to the On-Shell (OS) scheme (discussed in sec. 4.3.1), in the sense that $m_t^{\overline{\mathrm{DR}}} = m_t^{\mathrm{OS}} + \delta m_t$.

7.3 Shifts $\overline{\mathrm{DR}} \to \mathrm{OS}$

In the spirit of [34] (eqs. (31)-(35)), we now present the shifts for converting our two-loop results, valid if the parameters appearing in the one-loop part of the form factors are expressed in the $\overline{\mathrm{DR}}$ scheme, to formulae which hold if such parameters are expressed in the OS scheme presented in sec. 4.3.1. As in the case of the shift δm_t, already discussed in the previous section (eq. (7.33) and below), the shifts for $m_{\tilde{t}_1}$, $m_{\tilde{t}_2}$, θ_t and A_t (corresponding to the finite parts of eqs. (4.45), (4.46), (4.49) and (4.50)) involve the finite part of B_0

functions depending on the superparticle masses and on the top mass. Therefore they must be expanded according to our power counting. Below we collect the expansions of such quantities up to and including $\mathcal{O}(m_t/m_{\tilde{g}})$, which in our approximation is enough for converting the $\overline{\rm DR}$ results for the two-loop functions $G_t^{2\ell}$, $F_t^{2\ell}$, $\widetilde{F}_t^{2\ell}$, $\widetilde{G}_t^{2\ell}$ to the OS scheme (see the discussion below eq. (7.24)). The shift for $m^2_{\tilde{t}_1}$ is given by

$$\frac{\delta m_{\tilde{t}_1}}{m_{\tilde{t}_1}} = C_F \frac{\alpha_s}{\pi} \sum_{n=-1}^{1} \left(\frac{m_t}{m_{\tilde{g}}}\right)^n \delta^{(n)}_{m_{\tilde{t}_1}} + \mathcal{O}\left(\frac{m_t^2}{m_{\tilde{g}}^2}\right) , \tag{7.41}$$

where

$$\delta^{(-1)}_{m_{\tilde{t}_1}} = 0 \,, \tag{7.42}$$

$$\begin{aligned} \delta^{(0)}_{m_{\tilde{t}_1}} = \frac{1}{4}\Bigg[& 3 \ln \frac{m^2_{\tilde{t}_1}}{Q^2} - 3 - c^2_{2\theta_t} \left(\ln \frac{m^2_{\tilde{t}_1}}{Q^2} - 1 \right) - s^2_{2\theta_t} \frac{x_2}{x_1} \left(\ln \frac{m^2_{\tilde{t}_2}}{Q^2} - 1 \right) \\ & - \frac{6}{x_1} - 2 \left(1 - \frac{2}{x_1}\right) \ln \frac{m^2_{\tilde{g}}}{Q^2} - 2 \left(1 - \frac{1}{x_1}\right)^2 \ln |1 - x_1| \Bigg] \,, \end{aligned} \tag{7.43}$$

$$\delta^{(1)}_{m_{\tilde{t}_1}} = - \frac{s_{2\theta_t}}{x_1} \left[\ln \frac{m^2_{\tilde{g}}}{Q^2} + \left(1 - \frac{1}{x_1}\right) \ln |1 - x_1| - 2 \right] . \tag{7.44}$$

The shift for $m^2_{\tilde{t}_2}$ is obtained from the above with the replacement $(1,\, s_{2\theta_t}) \leftrightarrow (2,\, -s_{2\theta_t})$, where the first rule means that all the occurrences of x_1 and $m^2_{\tilde{t}_1}$ must be replaced by x_2 and $m^2_{\tilde{t}_2}$ and viceversa. The stop mixing angle shift is given by

$$\delta\theta_t = C_F \frac{\alpha_s}{\pi} \sum_{n=-1}^{1} \left(\frac{m_t}{m_{\tilde{g}}}\right)^n \delta^{(n)}_{\theta_t} + \mathcal{O}\left(\frac{m_t^2}{m_{\tilde{g}}^2}\right) , \tag{7.45}$$

where

$$\delta^{(-1)}_{\theta_t} = 0 \,, \tag{7.46}$$

$$\delta^{(0)}_{\theta_t} = - \frac{1}{4} \frac{c_{2\theta_t} s_{2\theta_t}}{x_1 - x_2} \left[x_1 \left(1 - \ln \frac{m^2_{\tilde{t}_1}}{Q^2} \right) - x_2 \left(1 - \ln \frac{m^2_{\tilde{t}_2}}{Q^2} \right) \right] , \tag{7.47}$$

$$\begin{aligned} \delta^{(1)}_{\theta_t} = & - \frac{1}{2} \frac{c_{2\theta_t}}{x_1 - x_2} \left[\ln \frac{m^2_{\tilde{g}}}{Q^2} + \left(1 - \frac{1}{x_1}\right) \ln |1 - x_1| - 2 \right] \\ & - \Big(x_1 \leftrightarrow x_2 \Big) . \end{aligned} \tag{7.48}$$

As already noted in sec. 4.3.1, the shift δA_t can be expressed in terms of the above considered shifts. Starting from eq. (4.50) we can write

$$\delta A_t = C_F \frac{\alpha_s}{\pi} \sum_{n=-1}^{1} \left(\frac{m_{\tilde{g}}}{m_t}\right)^n \delta^{(n)}_{A_t} + \mathcal{O}\left(\frac{m_t^2}{m_{\tilde{g}}^2}\right) , \tag{7.49}$$

where (δ_{ij} is the Kronecker delta)

$$\delta_{A_t}^{(n)} = \left[\frac{m_{\tilde{t}_1}^2 \delta_{m_{\tilde{t}_1}}^{(n)} - m_{\tilde{t}_2}^2 \delta_{m_{\tilde{t}_2}}^{(n)}}{m_{\tilde{t}_1}^2 - m_{\tilde{t}_2}^2} + 2\frac{c_{2\theta_t}}{s_{2\theta_t}} \delta_{\theta_t}^{(n)} - \left(\delta_{m_t,\mathrm{QCD}}^{(n)} \delta_{n0} + \delta_{m_t,\mathrm{SUSY}}^{(n)} \right) \right] (A_t + \mu \cot\beta) \quad (7.50)$$

The shifts for the two-loop results are then given by

$$\begin{aligned} F_t^{2\ell} \longrightarrow F_t^{2\ell} + \frac{C_F}{6} \Bigg[& \frac{1}{m_{\tilde{t}_1}^2} \left(\delta_{m_{\tilde{t}_1}}^{(0)} + \frac{m_t}{m_{\tilde{g}}} \delta_{m_{\tilde{t}_1}}^{(1)} \right) - \frac{1}{m_{\tilde{t}_2}^2} \left(\delta_{m_{\tilde{t}_2}}^{(0)} + \frac{m_t}{m_{\tilde{g}}} \delta_{m_{\tilde{t}_2}}^{(1)} \right) \\ & - \left(\frac{m_{\tilde{g}}}{m_t} \delta_{m_t,\mathrm{SUSY}}^{(-1)} + \delta_{m_t,\mathrm{QCD}}^{(0)} + \delta_{m_t,\mathrm{SUSY}}^{(0)} + \frac{m_t}{m_{\tilde{g}}} \delta_{m_t,\mathrm{SUSY}}^{(1)} \right) \left(\frac{1}{m_{\tilde{t}_1}^2} - \frac{1}{m_{\tilde{t}_2}^2} \right) \\ & - \frac{8}{15} \frac{m_t m_{\tilde{g}}}{\tau_t} \delta_{m_t,\mathrm{SUSY}}^{(-1)} \left(\frac{1}{m_{\tilde{t}_1}^4} - \frac{1}{m_{\tilde{t}_2}^4} \right) \\ & - 2\frac{c_{2\theta_t}}{s_{2\theta_t}} \left(\delta_{\theta_t}^{(0)} + \frac{m_t}{m_{\tilde{g}}} \delta_{\theta_t}^{(1)} \right) \left(\frac{1}{m_{\tilde{t}_1}^2} - \frac{1}{m_{\tilde{t}_2}^2} \right) \Bigg] , \end{aligned} \quad (7.51)$$

$$\begin{aligned} G_t^{2\ell} \longrightarrow G_t^{2\ell} + \frac{C_F}{6} \Bigg[& \frac{\delta_{m_{\tilde{t}_1}}^{(0)}}{m_{\tilde{t}_1}^2} + \frac{\delta_{m_{\tilde{t}_2}}^{(0)}}{m_{\tilde{t}_2}^2} - 2 \left(\frac{m_{\tilde{g}}}{m_t} \delta_{m_t,\mathrm{SUSY}}^{(-1)} + \delta_{m_t,\mathrm{QCD}}^{(0)} + \delta_{m_t,\mathrm{SUSY}}^{(0)} \right) \left(\frac{1}{m_{\tilde{t}_1}^2} + \frac{1}{m_{\tilde{t}_2}^2} \right) \\ & - 4\frac{(\delta m_t)^{(\mathrm{SUSY})}}{m_t^3} \mathcal{F}_{1/2}^{(2\ell,b)}(x(\tau_t)) \Bigg] , \end{aligned} \quad (7.52)$$

$$\widetilde{F}_t^{2\ell} \longrightarrow \widetilde{F}_t^{2\ell} + \frac{C_F}{6} \left[\frac{\delta_{m_{\tilde{t}_1}}^{(0)}}{m_{\tilde{t}_1}^2} - \frac{\delta_{m_{\tilde{t}_2}}^{(0)}}{m_{\tilde{t}_2}^2} + 2\frac{s_{2\theta_t}}{c_{2\theta_t}} \delta_{\theta_t}^{(0)} \left(\frac{1}{m_{\tilde{t}_1}^2} - \frac{1}{m_{\tilde{t}_2}^2} \right) \right] , \quad (7.53)$$

$$\widetilde{G}_t^{2\ell} \longrightarrow \widetilde{G}_t^{2\ell} + \frac{C_F}{6} \left[\frac{\delta_{m_{\tilde{t}_1}}^{(0)}}{m_{\tilde{t}_1}^2} + \frac{\delta_{m_{\tilde{t}_2}}^{(0)}}{m_{\tilde{t}_2}^2} \right] . \quad (7.54)$$

In addition, the shift in A_t generates a two-loop contribution in $\mathcal{H}_2^{2\ell}$:

$$\begin{aligned} \mathcal{H}_2^{2\ell} \longrightarrow \mathcal{H}_2^{2\ell} - \frac{m_t s_{2\theta_t}}{s_\beta} \frac{C_F}{6} & \left(\frac{1}{m_{\tilde{t}_1}^2} - \frac{1}{m_{\tilde{t}_2}^2} \right) \times \\ & \left[\frac{m_{\tilde{g}}}{m_t} \delta_{A_t}^{(-1)} + \delta_{A_t}^{(0)} + \frac{m_t}{m_{\tilde{g}}} \delta_{A_t}^{(1)} + \frac{8}{15} \frac{m_t m_{\tilde{g}}}{\tau_t} \delta_{A_t}^{(-1)} \left(\frac{1}{m_{\tilde{t}_1}^2} + \frac{1}{m_{\tilde{t}_2}^2} \right) \right] , \end{aligned} \quad (7.55)$$

where δA_t is given in eq. (7.49).

Chapter 8

Two-loop NLO QCD corrections to $gg \to A$ cross-section

In this chapter we present our original two-loop results for the NLO QCD contributions to the $gg \to A$ form factor $\mathcal{H}_A^{2\ell}$, defined in sec. 3.2.3. The calculation has been performed in two ways. The first one is based on a Taylor expansion in the small external momentum, retaining terms up to $\mathcal{O}(m_A^2/m_t^2)$. We provide compact analytic formulae for the terms of order zero in m_A and investigate the effect of the first-order terms. The second one is based on an asymptotic expansion in the large supersymmetric masses and is valid up to and including terms of $\mathcal{O}(m_A^2/M^2)$ and $\mathcal{O}(m_t^2/M^2)$, where M denotes a generic superparticle mass. In the second approach, no specific hieararchy between the Higgs and the top quark mass is assumed, therefore our formulae are expected to provide a better approximation of the full result in the threshold region $m_A \simeq 2m_t$ as compared to the Taylor expansion approach. As a byproduct, we obtained formulae for the bottom-sbottom-gluino contributions through the obvious replacements of masses and couplings and a further expansion in the small ratio m_b^2/m_A^2. In particular, we provide results at the same expansion order as the ones for the scalar Higgs production computed in ref. [34], that is valid up to and including $\mathcal{O}(m_b^2/m_A^2)$, $\mathcal{O}(m_b/M)$. Our results have been published in ref. [54].

The chapter is organized as follows. In sec. 8.1 we give a few details on the DREG computation, while in sec. 8.2 we illustrate some technical aspects of the PVREG computation. In sec. 8.3 we describe the structure of the two-loop contributions to the form factor, which are due to quark-gluon and quark-squark-gluino diagrams. First we show that our PVREG results for the quark-gluon part agree with the results available in the literature, then we present our top-stop-gluino and bottom-sbottom-gluino results (as well as a discussion of suitable renormalization schemes in the case of bottom contributions). Sec. 8.4 contains a comparison with the bottom results obtained in the effective-Lagrangian approximation. Finally in sec. 8.5 we assess the validity of the expansion in powers of m_A^2 in the top contributions, and discuss the numerical relevance of the different NLO contributions. In app. C we also include, for completeness, the explicit NLO contributions from one-loop diagrams with emission of a real parton.

8.1 Details on the computation in DREG

In our computation of the two-loop form factor $\mathcal{H}_A^{2\ell}$, defined in sec. 3.2.3, we regularized the loop integrals using both the DREG and the PVREG method.

With the remarks of sec. 4.1 concerning the treatment of γ_5 and the SUSY Ward identities, the DREG computation follows the usual strategy. The workflow closely follows the one described in sec. 7.1, the only difference being the projector we employ in DREG. Due to the coupling structure, the only one-loop contribution is the one with a quark loop, which always involves a γ_5 in the coupling. Thus the tensor structure of the A-g-g amplitude is forced to be

$$\mathcal{M}_A = \mathcal{M}_A^{\mu\nu}\varepsilon_\mu(q_1)\varepsilon_\nu(q_2) = \mathcal{A}\,\epsilon^{\mu\nu\rho\sigma}q_{1\rho}q_{2\sigma}\,\varepsilon_\mu(q_1)\varepsilon_\nu(q_2)\,, \tag{8.1}$$

where $\mathcal{A}$ is the scalar form factor and $\varepsilon_\nu(q_i)$ is the polarization vector of the i-th gluon (with momentum q_i). The scalar form factor can be extracted if we drop the two polarization vectors and contract with the projector

$$P_{\mu\nu}^A = \frac{\epsilon_{\mu\nu\rho\sigma}\,q_1^\rho q_2^\sigma}{(q_1\cdot q_2)^2(d-2)(d-3)}\,. \tag{8.2}$$

Moreover, since we always have in our expressions the product of exactly two Levi-Civita tensors, one coming from the γ_5-odd traces and one from the projector, we can use (4.20) in order to express those products in terms of the antysimmetric combination of 4-dimensional metric tensors. Then, keeping in mind the comment below such equation, we can actually treat them as d-dimensional metric tensors and use them for contracting all the vectors in the integrand. We thus end up with purely scalar integrals. We dedicate the next section to discussing some details of the PVREG computation.

8.2 Technical aspects of the calculation in PVREG

In the following we provide further details about the PVREG computation.

For the purposes of this computation, the main advantage of PVREG with respect to DREG is the fact that all the Lorentz indices remain strictly 4-dimensional, thus the γ_5 matrices anticommute with the other gamma matrices and the trace on a string of gamma matrices can be taken using the standard 4-dimensional relations.

In the case of the top-gluon contributions also the limit $\lambda \to 0$ must be taken on the fictitious gluon mass. In the present calculation, taking the relevant limits for the mass regulators does not introduce additional complications with respect to the same calculation performed in DRED or DREG. This is due to the fact that we are computing the two-loop diagrams via an asymptotic expansion, so that the final result is expressed in terms of two-loop vacuum integrals with different masses and of one-loop integrals. Both kinds of terms are fully known analytically, including all the relevant limits when one or more masses are sent to infinity or to zero.

In order to test our implementation of PVREG we first considered the two-loop top-gluon contributions. These contributions can be split in two parts, one proportional to C_F and the other proportional to C_A. The latter, which stems from the non-abelian nature of $SU(3)$, is not IR finite but contains a soft and collinear divergence that factorizes on the lowest-order cross-section. In DREG, this IR divergence appears as a $1/\epsilon^2$ pole multiplying the top contribution to $\sigma^{(0)}$. We computed the top-gluon contributions via an asymptotic expansion in the top mass up to and including terms $\mathcal{O}(m_A^8/m_t^8)$. The IR divergences are regularized by giving a mass λ to the gluon, while the UV divergences are regularized by subtracting to any term a replica in which λ is replaced by M_{PV}. The final result is then obtained taking the limits $M_{PV} \to \infty$ and $\lambda \to 0$. We were able to reproduce in PVREG the known result for the top-gluon contributions obtained in DREG [4, 36] once the PVREG IR-divergent term $1/2 \log^2(-m_A^2/\lambda^2)$ is identified in DREG with $1/\epsilon^2$. This is quite non-trivial, because it is known that, in general, regularizing the IR divergences via a fictitious gluon mass does not respect the non-abelian symmetry of $SU(3)$. Thus, one expects to get the correct result only for the part proportional to C_F. However, we quantize the Lagrangian employing the Background Field Method (BFM) [60–64], so that the external background gluons satisfy QED-like Ward identities. Then it is not surprising that PVREG gives the correct results also for the C_A part. We also remark that within the BFM the renormalization of the strong gauge coupling is due only to the wave function renormalization of the external background gluons. Thus, the renormalization of α_s decouples completely from the rest of the calculation, and can be treated separately in the standard way. As a consequence, even if PVREG is used to regularize the loop integrals, the LO partonic cross section $\sigma^{(0)}$ can be directly expressed in terms of the running coupling $\alpha_s(\mu_R)$ as in eq. (3.3).

In the evaluation of the top-stop-gluino contributions to $\mathcal{H}_A^{2\ell}$, the two-loop integrals are regularized by subtracting from each of them the same expression with $m_{\tilde{t}_1}^2$ and $m_{\tilde{t}_2}^2$ replaced by M_{PV}^2. The top-stop-gluino contributions are then computed in two alternative ways: either by means of a Taylor expansion in the external momentum, retaining terms of $\mathcal{O}(m_A^2/m_t^2)$ and $\mathcal{O}(m_A^2/M^2)$, or by means of an asymptotic expansion in the superparticle masses, retaining terms up to $\mathcal{O}(m_A^2/M^2)$ and $\mathcal{O}(m_t^2/M^2)$. The bottom-sbottom-gluino contributions to $\mathcal{H}_A^{2\ell}$ can then be recovered from the top-stop-gluino contributions computed with the asymptotic expansion, by performing appropriate replacements and taking the limit $m_b \ll m_A$. Considering the hierarchy between m_b and the other masses, we retain only terms up to $\mathcal{O}(m_b^2/m_A^2)$ and $\mathcal{O}(m_b/M)$.

We conclude this section with a couple of observations concerning the use of PVREG in the computation of the virtual NLO contributions. First, we recall that in PVREG one obtains directly the correct result without the need of introducing a finite renormalization factor to restore the Ward identities (see sec. 4.1.1). Second, we note that in PVREG the evaluation of the leading term in the Taylor expansion (i.e., the term corresponding to $m_A = 0$) does not require the computation of counterterm diagrams. This seems natural, because the leading term in the one-loop expression, eq. (3.32), does not depend on the top mass. However, the same evaluation in DREG or DRED does require the computation

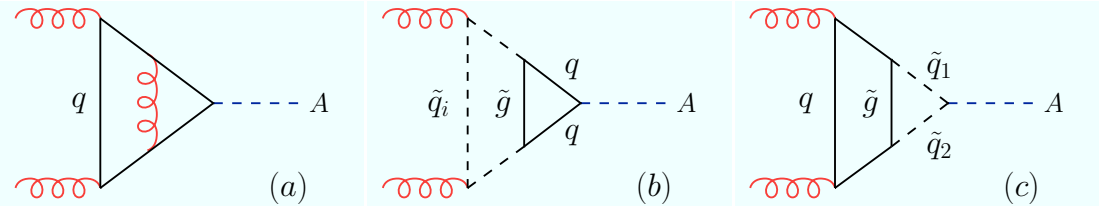

Figure 8.1: Examples of two-loop quark-gluon diagrams (a), and of two-loop quark-squark-gluino diagrams involving (b) the pseudoscalar-quark coupling or (c) the pseudoscalar-squark coupling. Here, $q = t, b$ and $i = 1, 2$.

of counterterm diagrams. Indeed, in d dimensions the one-loop leading term in the Taylor expansion contains an $\mathcal{O}(\epsilon)$ part that depends on the top mass, so that the counterterm diagrams give rise to a non-vanishing contribution.

8.3 Two-loop quark/squark contributions

The interactions of the CP-odd Higgs with quarks and squarks has been discussed in sec. 2.4. The fact that the pseudoscalar only couples to two different squark mass eigenstates, while gluons only couple to two equal eigenstates, implies that the form factor $\mathcal{H}_A$ receives neither one-loop contributions from diagrams with squarks nor two-loop contributions from diagrams with squarks and gluons. However, contributions to $\mathcal{H}_A^{2\ell}$ do arise from two-loop diagrams with quarks and gluons, as well as from two-loop diagrams with quarks, squarks and gluinos. Examples of such diagrams, involving either the pseudoscalar-quark coupling or the pseudoscalar-squark coupling, are given in figure 8.1.

The two-loop form factor for pseudoscalar production can be decomposed as

$$\mathcal{H}_A^{2\ell} \;=\; T_F \left[\cot\beta \left(\mathcal{K}_{tg}^{2\ell} + \mathcal{K}_{t\tilde{t}\tilde{g}}^{2\ell}\right) + \tan\beta \left(\mathcal{K}_{bg}^{2\ell} + \mathcal{K}_{b\tilde{b}\tilde{g}}^{2\ell}\right)\right] , \tag{8.3}$$

where $\mathcal{K}_{qg}^{2\ell}$ denotes the quark-gluon contributions ($q = t, b$), and $\mathcal{K}_{q\tilde{q}\tilde{g}}^{2\ell}$ denotes the quark-squark-gluino contributions. In the following we discuss separately the two-loop contributions arising from quark-gluon, top-stop-gluino and bottom-sbottom-gluino diagrams.

8.3.1 Quark-gluon contribution

We recall for completeness the results of refs. [4, 36] for the contributions to $\mathcal{H}_A^{2\ell}$ arising from diagrams with quarks and gluons (see figure 8.1a). If the corresponding contribution in the one-loop form factor $\mathcal{H}_A^{1\ell}$ is expressed in terms of the physical quark mass, the two-loop contribution for a given quark q reads

$$\mathcal{K}_{qg}^{2\ell} = C_F \left[\mathcal{F}_1(\tau_q) + \frac{4}{3}\mathcal{F}_2(\tau_q)\right] + C_A\,\mathcal{F}_3(\tau_q) , \tag{8.4}$$

where as usual $\tau_q \equiv 4m_q/m_A$. If the one-loop form factor is instead expressed in terms of the running quark mass, renormalized in the $\overline{\rm DR}$ scheme at the scale Q, the two-loop contribution becomes

$$\mathcal{K}_{qg}^{2\ell} = C_F \left[\mathcal{F}_1(\tau_q) + \mathcal{F}_2(\tau_q) \left(\ln\frac{m_q^2}{Q^2} - \frac{1}{3}\right)\right] + C_A\, \mathcal{F}_3(\tau_q) \ . \tag{8.5}$$

Expressions for the functions denoted here as $\mathcal{F}_1(\tau)$, $\mathcal{F}_2(\tau)$ and $\mathcal{F}_3(\tau)$, valid for arbitrary values of τ, can be found in ref. [36]. They correspond to the functions $\mathcal{E}_t^{(2\ell,a)}(4/\tau)$ in eq. (4.6), $\mathcal{E}_t^{(2\ell,b)}(4/\tau)$ in eq. (4.7), and $\mathcal{K}_t^{(2\ell,C_A)}(4/\tau)$ in eq. (4.12) of that paper, respectively. Their limiting behaviors for heavy and light quark are respectively

$$(\tau \gg 1): \ \mathcal{F}_1(\tau) \longrightarrow\ -\frac{4}{3\tau} \ +\ \mathcal{O}(\tau^{-2}) \ , \tag{8.6}$$

$$\mathcal{F}_2(\tau) \longrightarrow\ -\frac{1}{\tau} \ +\ \mathcal{O}(\tau^{-2}) \ , \tag{8.7}$$

$$\mathcal{F}_3(\tau) \longrightarrow\ -2 - \frac{1}{6\tau} \ +\ \mathcal{O}(\tau^{-2}) \ , \tag{8.8}$$

and

$$\begin{aligned}(\tau \ll 1): \ \mathcal{F}_1(\tau) \longrightarrow\ -\tau \Bigg[&\frac{9}{5}\,\zeta_2^2 - \zeta_3 + (2 - \zeta_2 - 4\,\zeta_3)\,\ln\left(\frac{-4}{\tau}\right) \\ &- (1-\zeta_2)\ln^2\left(\frac{-4}{\tau}\right) + \frac{1}{4}\,\ln^3\left(\frac{-4}{\tau}\right) + \frac{1}{48}\,\ln^4\left(\frac{-4}{\tau}\right)\Bigg] \\ &+\ \mathcal{O}(\tau^2) \ ,\end{aligned} \tag{8.9}$$

$$\mathcal{F}_2(\tau) \longrightarrow\ \frac{3\,\tau}{4}\left[2\,\ln\left(\frac{-4}{\tau}\right) - \ln^2\left(\frac{-4}{\tau}\right)\right] \ +\ \mathcal{O}(\tau^2) \ , \tag{8.10}$$

$$\begin{aligned}\mathcal{F}_3(\tau) \longrightarrow\ \tau \Bigg[&\frac{8}{5}\,\zeta_2^2 + 3\,\zeta_3 - 3\,\zeta_3\,\ln\left(\frac{-4}{\tau}\right) + \frac{1}{4}\,(1+2\,\zeta_2)\ln^2\left(\frac{-4}{\tau}\right) \\ &+ \frac{1}{48}\,\ln^4\left(\frac{-4}{\tau}\right)\Bigg] \ +\ \mathcal{O}(\tau^2) \ .\end{aligned} \tag{8.11}$$

8.3.2 Top-stop-gluino contribution

While a fully analytic computation of the top-stop-gluino contributions to $\mathcal{H}_A^{2\ell}$ valid for arbitrary values of all the relevant particle masses is currently beyond our reach, it is possible to derive approximate analytic results valid in different phenomenologically relevant limits.

To start with, we computed the term $\mathcal{K}_{t\tilde{t}\tilde{g}}^{2\ell}$ in eq. (8.3) via a Taylor expansion in the external Higgs momentum up to terms of $\mathcal{O}(m_A^2/m_t^2)$ and $\mathcal{O}(m_A^2/M^2)$, where M denotes

generically the stop and gluino masses. Such expansion should give a reasonable approximation to the full result when m_A is small compared to the other masses, and is anyway restricted to values of m_A below the lowest threshold encountered in the diagrams (this usually means $m_A < 2\,m_t$). In the limit of vanishing m_A we find that our result for $\mathcal{K}^{2\ell}_{t\tilde{t}\tilde{g}}$ can be cast in an extremely compact form:

$$\mathcal{K}^{2\ell}_{t\tilde{t}\tilde{g}} = \left(\frac{s_{2\theta_t}}{2} - \frac{m_t\,Y_t}{m^2_{\tilde{t}_1} - m^2_{\tilde{t}_2}}\right)\left[f(m^2_{\tilde{g}}, m^2_t, m^2_{\tilde{t}_1}) - f(m^2_{\tilde{g}}, m^2_t, m^2_{\tilde{t}_2})\right] , \tag{8.12}$$

where

$$\begin{aligned} f(m^2_{\tilde{g}}, m^2_t, m^2_{\tilde{t}_i}) &= C_F\,\frac{m_{\tilde{g}}}{m_t\,\Delta}\left[m^2_t\,(m^2_{\tilde{g}} - m^2_t + m^2_{\tilde{t}_i})\,\ln\frac{m^2_t}{m^2_{\tilde{g}}} + m^2_{\tilde{t}_i}\,(m^2_{\tilde{g}} + m^2_t - m^2_{\tilde{t}_i})\,\ln\frac{m^2_{\tilde{t}_i}}{m^2_{\tilde{g}}}\right. \\ &\qquad \left. +2\,m^2_{\tilde{g}}\,m^2_t\,\Phi(m^2_{\tilde{g}}, m^2_t, m^2_{\tilde{t}_i})\right] \\ &+ C_A\,\frac{m_t}{m_{\tilde{g}}\,\Delta}\left[m^2_{\tilde{t}_i}\,(m^2_{\tilde{t}_i} - m^2_t - m^2_{\tilde{g}})\,\ln\frac{m^2_t}{m^2_{\tilde{g}}} + m^2_{\tilde{t}_i}\,(m^2_t - m^2_{\tilde{t}_i} - m^2_{\tilde{g}})\,\ln\frac{m^2_{\tilde{t}_i}}{m^2_{\tilde{g}}}\right. \\ &\qquad \left. +m^2_{\tilde{g}}\,(m^2_t + m^2_{\tilde{t}_i} - m^2_{\tilde{g}})\,\Phi(m^2_{\tilde{g}}, m^2_t, m^2_{\tilde{t}_i})\right] , \end{aligned} \tag{8.13}$$

the function $\Phi(m^2_{\tilde{g}}, m^2_t, m^2_{\tilde{t}_i})$ is given, e.g., in appendix A of ref. [159], and we introduced the shortcut $\Delta = m^4_t + m^4_{\tilde{g}} + m^4_{\tilde{t}_i} - 2\,(m^2_t\,m^2_{\tilde{g}} + m^2_t\,m^2_{\tilde{t}_i} + m^2_{\tilde{g}}\,m^2_{\tilde{t}_i})$. As appears from eqs. (3.30) and (3.32), in the limit of vanishing m_A the one-loop top contribution to $\mathcal{H}_A$ reduces to $-\cot\beta$, i.e., it does not actually depend on any parameter subject to $\mathcal{O}(\alpha_s)$ corrections. Therefore, the results in eqs. 8.12 and 8.13 do not depend on the renormalization scheme in which the calculation is performed. The contributions to $\mathcal{K}^{2\ell}_{t\tilde{t}\tilde{g}}$ of the first order in the Taylor expansion in m^2_A are too lengthy to be printed here, but in section 8.5 we will discuss their relevance in a representative region of the MSSM parameter space.

The two terms between parentheses in eq. (8.12) come from the diagrams with pseudoscalar-top and pseudoscalar-stop couplings in figs. 8.1b and 8.1c, respectively. Inserting the explicit expressions for $s_{2\theta_t}$ and Y_t we find

$$\mathcal{K}^{2\ell}_{t\tilde{t}\tilde{g}} = \frac{m_t\,\mu}{m^2_{\tilde{t}_1} - m^2_{\tilde{t}_2}}\,(\cot\beta + \tan\beta)\,\left[f(m^2_{\tilde{g}}, m^2_t, m^2_{\tilde{t}_1}) - f(m^2_{\tilde{g}}, m^2_t, m^2_{\tilde{t}_2})\right] , \tag{8.14}$$

i.e., the explicit dependence of $\mathcal{K}^{2\ell}_{t\tilde{t}\tilde{g}}$ on A_t drops out, leaving only a dependence on μ. Ref. [51] points out that this happens because the μ term breaks the axial U(1) Peccei-Quinn symmetry of the MSSM potential, thus violating the Adler-Bardeen theorem [123] which would otherwise guarantee the cancellation of all contributions from irreducible diagrams beyond one loop.

We compared our result for $\mathcal{K}^{2\ell}_{t\tilde{t}\tilde{g}}$ in the limit of vanishing m_A, eqs. (8.12)–(8.13), with the result for the coefficient $\tilde{c}^{(1)}_1$ defined in ref. [51]. That result was deemed too voluminous

to be printed explicitly in ref. [51], and was made available in the fortran code `evalcsusy.f` [32, 33]. We find full numerical agreement with `evalcsusy.f`, after taking into account that $\tilde{c}_1^{(1)} = -T_F \cot\beta\, \mathcal{K}^{2\ell}_{t\tilde{t}\tilde{g}}$ and that ref. [51] employs the opposite convention for the sign of μ with respect to our (2.38).

Even when the superparticles are much heavier than the pseudoscalar, the validity of the result for $\mathcal{K}^{2\ell}_{t\tilde{t}\tilde{g}}$ obtained via a Taylor expansion in m_A^2 becomes questionable if m_A is close to or even larger than m_t. To cover this region of the parameter space we performed an asymptotic expansion of $\mathcal{K}^{2\ell}_{t\tilde{t}\tilde{g}}$ in the large superparticle masses. More specifically, we consider the case $(m_A, m_t) \ll M$ without assuming any hierarchy between m_A and m_t, and retain terms up to $\mathcal{O}(m_A^2/M^2)$ and $\mathcal{O}(m_t^2/M^2)$ in the expansion. Assuming that the top contribution to $\mathcal{H}_A^{1\ell}$ in eqs. (3.30) and (3.31) is expressed in terms of the pole top mass, we find

$$\begin{aligned}
\mathcal{K}^{2\ell}_{t\tilde{t}\tilde{g}} = & -\frac{C_F}{2}\,\mathcal{K}^{1\ell}(\tau_t)\,\frac{m_{\tilde{g}}}{m_t}\left(\frac{s_{2\theta_t}}{2} - \frac{m_t\,Y_t}{m_{\tilde{t}_1}^2 - m_{\tilde{t}_2}^2}\right)\left(\frac{x_1}{1-x_1}\ln x_1 - \frac{x_2}{1-x_2}\ln x_2\right) \\
& - \frac{m_t}{m_{\tilde{g}}}\,s_{2\theta_t}\,\mathcal{R}_1 \;+\; \frac{2\,m_t^2\,Y_t}{m_{\tilde{g}}\,(m_{\tilde{t}_1}^2 - m_{\tilde{t}_2}^2)}\,\mathcal{R}_2 \;+\; \frac{m_t^2}{m_{\tilde{g}}^2}\,\mathcal{R}_3 \;-\; \frac{1}{2}\,\mathcal{K}^{1\ell}(\tau_t)\,\frac{m_A^2}{m_{\tilde{t}_1}^2 - m_{\tilde{t}_2}^2}\,\mathcal{R}_4\;,
\end{aligned} \tag{8.15}$$

where $x_i = m_{\tilde{t}_i}^2/m_{\tilde{g}}^2$, the one-loop function $\mathcal{K}^{1\ell}(\tau)$ was defined in eq. (3.31), and the terms $\mathcal{R}_i$ collect contributions suppressed by m_t/M or m_t^2/M^2:

$$\begin{aligned}
\mathcal{R}_1 = & \frac{C_F}{4\,(1-x_1)^3}\left[(1-x_1^2+2\,x_1\,\ln x_1)\left(2\,\ln\frac{m_{\tilde{g}}^2}{m_t^2} - 3 - \frac{3}{2}\mathcal{K}^{1\ell}(\tau_t) + 2\,\mathcal{B}\right)\right. \\
& \qquad \left. - 8\,x_1\,\mathrm{Li}_2(1-x_1) - 2\,x_1\,(3+x_1)\,\ln x_1\right] \\
& + \frac{C_A}{2\,(1-x_1)^2}\left[(1-x_1+x_1\,\ln x_1)\left(\ln\frac{m_t^2}{m_{\tilde{g}}^2} + 1 + \frac{1}{2}\mathcal{K}^{1\ell}(\tau_t) - \mathcal{B}\right)\right. \\
& \qquad \left. + 2\,x_1\,\mathrm{Li}_2(1-x_1) + x_1\,(1+x_1)\,\ln x_1\right] \\
& + \frac{C_F}{(x_1-x_2)^2}\,\frac{Y_t}{m_{\tilde{g}}}\,\left(1 + \frac{1}{2}\mathcal{K}^{1\ell}(\tau_t)\right)\left[\frac{x_1^2\,(1-2\,x_2)}{2(1-x_1)(1-x_2)}\right. \\
& \qquad \left. + \frac{x_1}{2(1-x_1)^2}\,(x_1^2 - 2\,x_2 + x_1\,x_2)\,\ln x_1\right] \\
& - \Big(x_1 \longleftrightarrow x_2\Big)\;,
\end{aligned} \tag{8.16}$$

$$\mathcal{R}_2 = \frac{C_F}{4\,(1-x_1)^3}\,\Bigg[2\,(1-x_1^2+2\,x_1\,\ln x_1)\,\ln\frac{m_{\tilde{g}}^2}{m_t^2} - 8\,x_1\,\mathrm{Li}_2(1-x_1) + (1-x_1^2)\left(1+\frac{1}{2}\mathcal{K}^{1\ell}(\tau_t)\right) - 2\,x_1\left(2+x_1-\frac{1}{2}\mathcal{K}^{1\ell}(\tau_t)\right)\ln x_1\Bigg] + \frac{C_A}{2\,(1-x_1)^2}\,\Bigg[(1-x_1+x_1\,\ln x_1)\,\ln\frac{m_t^2}{m_{\tilde{g}}^2} + 2\,x_1\,\mathrm{Li}_2(1-x_1) + x_1\,(1+x_1)\,\ln x_1\Bigg] - \Big(x_1 \longleftrightarrow x_2\Big)\,, \tag{8.17}$$

$$\mathcal{R}_3 = \frac{C_F}{6\,(1-x_1)^4}\,(-2-3\,x_1+6\,x_1^2-x_1^3-6\,x_1\,\ln x_1)\Big(2+\mathcal{K}^{1\ell}(\tau_t)-\mathcal{B}\Big) + \frac{C_A}{8\,(1-x_1)^3}\,(1-x_1^2+2\,x_1\,\ln x_1)\left(2+\mathcal{K}^{1\ell}(\tau_t)-2\,\mathcal{B}\right) + \Big(x_1 \longleftrightarrow x_2\Big)\,, \tag{8.18}$$

$$\mathcal{R}_4 = \frac{C_F}{(x_1-x_2)^2}\,\frac{Y_t}{m_{\tilde{g}}}\,\Bigg[\frac{x_1^2\,(1-2\,x_2)}{2(1-x_1)(1-x_2)} + \frac{x_1}{2(1-x_1)^2}\,(x_1^2-2\,x_2+x_1\,x_2)\,\ln x_1\Bigg] - \Big(x_1 \longleftrightarrow x_2\Big)\,. \tag{8.19}$$

In the equations above, $\mathcal{B}$ denotes the finite part of the Passarino-Veltman function $B_0(m_A^2, m_t^2, m_t^2)$ computed at the renormalization scale $Q^2 = m_t^2$. The comparison between the result for $\mathcal{K}^{2\ell}_{t\tilde{t}\tilde{g}}$ obtained via a Taylor expansion in m_A^2 and the corresponding result obtained via an asymptotic expansion in M will be discussed in section 8.5.

8.3.3 Bottom-sbottom-gluino contribution

A result for the bottom-sbottom-gluino contribution $\mathcal{K}^{2\ell}_{b\tilde{b}\tilde{g}}$ can be obtained by performing the obvious replacement $t \to b$ in the result for $\mathcal{K}^{2\ell}_{t\tilde{t}\tilde{g}}$ obtained via the asymptotic expansion in M, eqs. (8.15)–(8.19). Considering that $m_b \ll m_A$, and that we are assuming $m_A \ll M$, we retain only the terms up to $\mathcal{O}(m_b/M)$ and $\mathcal{O}(m_b^2/m_A^2)$. In particular, the terms $\mathcal{R}_2$, $\mathcal{R}_3$ and $\mathcal{R}_4$ in eq. (8.15) give contributions of higher order in m_b and can be neglected, while in the expression for $\mathcal{R}_1$, eq. (8.16), we drop the occurrences of $\mathcal{K}^{1\ell}(\tau_b)$ and use $\mathcal{B} = 2 - \ln(-m_A^2/m_b^2)$. As a result, assuming that the bottom contribution to $\mathcal{H}_A^{1\ell}$ in eqs. (3.30) and (3.33) is fully expressed in terms of the pole bottom mass, we again find a rather compact expression for the term $\mathcal{K}^{2\ell}_{b\tilde{b}\tilde{g}}$ in eq. (8.3):

$$\mathcal{K}^{2\ell}_{b\tilde{b}\tilde{g}} \;=\; -\frac{C_F}{2}\,\mathcal{K}^{1\ell}(\tau_b)\,\frac{m_{\tilde{g}}}{m_b}\left(\frac{s_{2\theta_b}}{2} - \frac{m_b\,Y_b}{m_{\tilde{b}_1}^2 - m_{\tilde{b}_2}^2}\right)\left(\frac{x_1}{1-x_1}\ln x_1 - \frac{x_2}{1-x_2}\ln x_2\right) - \frac{m_b}{m_{\tilde{g}}}\;s_{2\theta_b}\,\mathcal{R}_1\,. \tag{8.20}$$

Here $x_i = m^2_{\tilde{b}_i}/m^2_{\tilde{g}}$, and $\mathcal{R}_1$ collects the contributions suppressed by m_b/M:

$$\begin{aligned}\mathcal{R}_1 = {} & \frac{C_F}{4\,(1-x_1)^3}\left[(1-x_1^2+2\,x_1\,\ln x_1)\left(1-2\,\ln(\frac{-m_A^2}{m^2_{\tilde{g}}})\right)-8\,x_1\,\mathrm{Li}_2(1-x_1)\right. \\ & \left.\qquad -2\,x_1\,(3+x_1)\,\ln x_1\right] \\ & + \frac{C_A}{2\,(1-x_1)^2}\left[(1-x_1+x_1\,\ln x_1)\left(\ln(\frac{-m_A^2}{m^2_{\tilde{g}}})-1\right)+2\,x_1\,\mathrm{Li}_2(1-x_1)\right. \\ & \left.\qquad +x_1\,(1+x_1)\,\ln x_1\right] \\ & + \frac{C_F}{(x_1-x_2)^2}\,\frac{Y_b}{m_{\tilde{g}}}\left[\frac{x_1^2\,(1-2\,x_2)}{2(1-x_1)(1-x_2)}+\frac{x_1}{2(1-x_1)^2}\,(x_1^2-2\,x_2+x_1\,x_2)\,\ln x_1\right] \\ & -\left(x_1 \longleftrightarrow x_2\right)\,. \end{aligned} \tag{8.21}$$

As in the case of the top-stop-gluino contribution, the terms proportional to Y_b originate from the diagrams that involve the pseudoscalar-sbottom coupling, while the other terms originate from the diagrams that involve the pseudoscalar-bottom coupling. Inserting the expressions for $s_{2\theta_b}$ and Y_b in the first term in the right-hand side of eq. (8.20) we obtain

$$\mathcal{K}^{2\ell}_{b\tilde{b}\tilde{g}} \;=\; -\frac{C_F}{2}\,\mathcal{K}^{1\ell}(\tau_b)\,\frac{m_{\tilde{g}}\,\mu}{m^2_{\tilde{b}_1}-m^2_{\tilde{b}_2}}\,(\tan\beta+\cot\beta)\,\left(\frac{x_1}{1-x_1}\ln x_1-\frac{x_2}{1-x_2}\ln x_2\right)-\frac{m_b}{m_{\tilde{g}}}\;s_{2\theta_b}\,\mathcal{R}_1\,. \tag{8.22}$$

Similarly to what found in ref. [42] for the production of CP-even Higgs bosons, if the one-loop contribution to $\mathcal{H}_A$ is expressed in terms of the pole bottom mass the bottom-sbottom-gluino diagrams induce potentially large two-loop contributions. According to whether or not we insert the explicit expression for $s_{2\theta_b}$ in our formulae, such contributions manifest themselves either as terms enhanced by the ratio $m_{\tilde{g}}/m_b$, as in eq. (8.20), or as terms enhanced by $\tan\beta$, as in eq. (8.22). However, such terms cancel out if the pseudoscalar-bottom coupling entering the one-loop contribution to $\mathcal{H}_A$ is identified with the $\overline{\mathrm{DR}}$-renormalized mass $\widehat{m}_b$, while the mass of the bottom quark running in the loop is identified with the pole mass M_b (this amounts to rescaling by $\widehat{m}_b/M_b$ the one-loop result fully computed in terms of M_b). As a result, the two-loop form factor in eq. (8.3) is shifted as

$$\mathcal{H}_A^{2\ell} \;\longrightarrow\; \mathcal{H}_A^{2\ell} \;-\; \tan\beta\,\mathcal{K}^{1\ell}(\tau_b)\,T_F\,C_F\left[\frac{3}{4}\,\ln\frac{m_b^2}{Q^2}-\frac{5}{4}+\frac{(\delta m_b)^{SUSY}}{m_b}\right] \tag{8.23}$$

with respect to the result obtained when the one-loop bottom contribution is fully expressed in terms of M_b. Here Q is the scale at which the running mass $\widehat{m}_b$ is renormalized, and $(\delta m_b)^{SUSY}$ denotes the SUSY contribution to the bottom self-energy, in units of $C_F\,\alpha_s/\pi$

and in the limit of vanishing m_b:

$$\frac{(\delta m_b)^{SUSY}}{m_b} = -\frac{1}{4}\left[\ln\frac{m_{\tilde{g}}^2}{Q^2} + f(x_1) + f(x_2) + \frac{m_{\tilde{g}}}{m_b}\, s_{2\theta_b}\left(\frac{x_1}{1-x_1}\ln x_1 - \frac{x_2}{1-x_2}\ln x_2\right)\right], \tag{8.24}$$

where

$$f(x) = \frac{x-3}{4\,(1-x)} + \frac{x\,(x-2)}{2\,(1-x)^2}\,\ln x\,. \tag{8.25}$$

While the shift in eq. (8.23) removes the contributions enhanced by $m_{\tilde{g}}/m_b$ (or $\tan\beta$), it does introduce potentially large logarithms of the ratio between the renormalization scale Q and the masses of the particles running in the loop. Such logarithms cannot be eliminated by a specific scale choice for $\widehat{m_b}$, unless Q is set to a value much smaller than the bottom mass itself. Therefore, as already found in ref. [42] for the CP-even Higgs bosons, the bottom contributions to $\mathcal{H}_A^{2\ell}$ may turn out to be sizable even in the "mixed" renormalization scheme in which the $\tan\beta$-enhanced contributions are absorbed in a redefinition of the pseudoscalar-bottom coupling entering $\mathcal{H}_A^{1\ell}$.

Finally, if the bottom contribution to $\mathcal{H}_A^{1\ell}$ is fully expressed in terms of the running bottom mass $\widehat{m_b}$ the bottom-sbottom-gluino contribution to the form factor in eq. (8.20) is shifted as

$$\mathcal{K}_{b\tilde{b}\tilde{g}}^{2\ell} \longrightarrow \mathcal{K}_{b\tilde{b}\tilde{g}}^{2\ell} + \frac{4}{3}\,C_F\,\mathcal{F}_2(\tau_b)\,\frac{(\delta m_b)^{SUSY}}{m_b}\,. \tag{8.26}$$

In this case $\mathcal{H}_A^{2\ell}$ contains both terms enhanced by $m_{\tilde{g}}/m_b$ and potentially large logarithms, the latter arising from $(\delta m_b)^{SUSY}$ in eq. (8.26) as well as from the two-loop bottom-gluon contribution in eq. (8.5).

8.4 Comparison with the effective-Lagrangian approximation

It is well known that, in the MSSM, loop diagrams involving superparticles induce interactions between the quarks and the "wrong" Higgs doublets, i.e., interactions that are absent from the tree-level Lagrangian due to the requirement that the superpotential be a holomorphic function of the superfields [160]. Such non-holomorphic, loop-induced Higgs-quark interactions result in $\tan\beta$-enhanced (or $\tan\beta$-suppressed) corrections to the MSSM predictions for various physical observables. If all superparticles are considerably heavier than the Higgs bosons they can be integrated out of the Lagrangian, in which case the loop-induced corrections are *resummed* in effective Higgs-quark couplings. In particular, if g_b^ϕ denote the tree-level couplings of a neutral Higgs $\phi = (h, H, A)$ to bottom quarks

(normalized to the SM value), the corresponding effective couplings $\tilde{g}_b^\phi$ read [52, 53]

$$\tilde{g}_b^h = \frac{g_b^h}{1+\Delta_b}\left(1 - \Delta_b \frac{\cot\alpha}{\tan\beta}\right) , \tag{8.27}$$

$$\tilde{g}_b^H = \frac{g_b^H}{1+\Delta_b}\left(1 + \Delta_b \frac{\tan\alpha}{\tan\beta}\right) , \tag{8.28}$$

$$\tilde{g}_b^A = \frac{g_b^A}{1+\Delta_b}\left(1 - \Delta_b \cot^2\beta\right) , \tag{8.29}$$

where α is the mixing angle in the CP-even Higgs sector and, to $\mathcal{O}(\alpha_s)$,

$$\Delta_b \;=\; \frac{\alpha_s C_F}{2\pi} \frac{m_{\tilde{g}}\,\mu\,\tan\beta}{m^2_{\tilde{b}_1} - m^2_{\tilde{b}_2}} \left(\frac{x_1}{1-x_1}\ln x_1 - \frac{x_2}{1-x_2}\ln x_2\right) . \tag{8.30}$$

In the calculation of processes involving the Higgs-bottom couplings, it is often found that the $\tan\beta$-enhanced corrections can be included to all orders in an expansion in powers of $\alpha_s \tan\beta$ by inserting the effective couplings of eq. (8.27) in the lowest-order result. A comparison with our explicit results for the two-loop form factors allows us to test the validity of that procedure in the case of the production of both CP-even [42] and CP-odd Higgs bosons in gluon fusion.*

We recall that the bottom-quark contributions $\mathcal{H}_\phi^{1\ell,b}$ to the one-loop form factors for the production of the Higgs boson $\phi = (h, H, A)$ read

$$\mathcal{H}_h^{1\ell,b} \;=\; -T_F \frac{\sin\alpha}{\cos\beta}\,\mathcal{G}_{1/2}^{1\ell}(\tau_b) , \quad \mathcal{H}_H^{1\ell,b} \;=\; T_F \frac{\cos\alpha}{\cos\beta}\,\mathcal{G}_{1/2}^{1\ell}(\tau_b) , \quad \mathcal{H}_A^{1\ell,b} \;=\; T_F \tan\beta\,\mathcal{K}^{1\ell}(\tau_b) , \tag{8.31}$$

where the function $\mathcal{G}_{1/2}^{1\ell}(\tau)$ is given, e.g., in eq. (12) of ref. [42]. Assuming that $\mathcal{H}_\phi^{1\ell,b}$ are expressed in terms of the pole bottom mass, and that the Higgs-sbottom couplings are renormalized in a way that avoids the introduction of additional $\tan\beta$-enhanced corrections (see ref. [42]), we find that the two-loop form factors read

$$\mathcal{H}_h^{2\ell} \;=\; \mathcal{H}_h^{1\ell,b}\left[-\frac{\pi}{\alpha_s}\Delta_b\left(1 + \frac{\cot\alpha}{\tan\beta}\right) + \frac{C_F}{4}\frac{A_b - \mu\cot\alpha}{m_{\tilde{g}}}\, s^2_{2\theta_b}\, g(x_1,x_2)\right] \;+\; \ldots \tag{8.32}$$

$$\mathcal{H}_H^{2\ell} \;=\; \mathcal{H}_H^{1\ell,b}\left[-\frac{\pi}{\alpha_s}\Delta_b\left(1 - \frac{\tan\alpha}{\tan\beta}\right) + \frac{C_F}{4}\frac{A_b + \mu\tan\alpha}{m_{\tilde{g}}}\, s^2_{2\theta_b}\, g(x_1,x_2)\right] \;+\; \ldots \tag{8.33}$$

$$\mathcal{H}_A^{2\ell} \;=\; -\mathcal{H}_A^{1\ell,b}\;\; \frac{\pi}{\alpha_s}\Delta_b\left(1 + \cot^2\beta\right) + \;\ldots\; , \tag{8.34}$$

where the ellipses denote contributions suppressed by m_b/M or m_Z^2/M^2, as well as all of

*A comparison for the light scalar h in the limit of vanishing sbottom mixing was discussed in ref. [43], and a numerical comparison for the heavy scalar H was shown, without a detailed discussion, in ref. [41].

the contributions from diagrams involving top and stop, and

$$g(x_1,x_2) = \frac{1}{1-x_1}\left(1+\frac{\ln x_1}{1-x_1}\right) + \frac{1}{1-x_2}\left(1+\frac{\ln x_2}{1-x_2}\right) - \frac{2}{x_1-x_2}\left(\frac{x_1}{1-x_1}\ln x_1 - \frac{x_2}{1-x_2}\ln x_2\right) . \tag{8.35}$$

In practice, the effective-Lagrangian approximation consists in rescaling the one-loop bottom contributions $\mathcal{H}_\phi^{1\ell,b}$ by the same factors that rescale the Higgs-bottom couplings g_b^ϕ in eq. (8.27). Expanding the rescaling factors to the first order in Δ_b it is easy to see that the effective-Lagrangian approximation does indeed reproduce the two-loop terms proportional to Δ_b in eqs. (8.32)–(8.34).

It is also interesting to consider the so-called decoupling limit of the MSSM, $m_A \gg m_Z$, in which $\cot\alpha \to -\tan\beta$ and the light scalar h has SM-like couplings to fermions and gauge bosons.[†] Eq. (8.27) shows that in this limit the effective coupling of h to bottom quarks is equal to the tree-level coupling, therefore in the effective-Lagrangian approximation there are no $\tan\beta$-enhanced contributions to $\mathcal{H}_h^{2\ell}$. Indeed, for $\cot\alpha \to -\tan\beta$ the terms proportional to Δ_b drop out of the two-loop form factor in eq. (8.32). However, eq. (8.32) also shows that in the decoupling limit $\mathcal{H}_h^{2\ell}$ contains additional $\tan\beta$-enhanced contributions, controlled by the left-right sbottom mixing $X_b = (A_b + \mu\tan\beta)$, which are not reproduced by the effective-Lagrangian approximation. However, when the implicit dependence of the sbottom masses and mixing on the bottom mass is taken into account, such contributions turn out to be partially suppressed by powers of m_b. Indeed, taking for illustrative purposes the limit in which the diagonal entries of the sbottom mass matrix as well as the squared gluino mass are all equal to M^2, and expanding the form factor in powers of m_b, we find

$$\mathcal{H}_h^{2\ell} \;\supset\; -\mathcal{H}_h^{1\ell,b}\;\frac{C_F}{12}\,\frac{m_b^2\,X_b^3}{M^5} \;+\; T_F\,\frac{2\,C_A+25\,C_F}{18}\,\frac{m_b^2\,X_b^2}{M^4} \;+\; \ldots\,, \tag{8.36}$$

where the ellipses denote terms further suppressed by powers of m_b or m_Z, as well as all of the contributions from diagrams involving top and stop. The first term in eq. (8.36) comes from the expansion of the terms proportional to $s^2_{2\theta_b}$ in eq. (8.32), while the second comes from the expansion of terms not shown in eq. (8.32). The contributions neglected by the effective-Lagrangian approximation can be relevant for values of X_b large enough to compensate for the suppression due to m_b. It should however be recalled that in the decoupling limit $\mathcal{H}_h^{1\ell,b}$ is not further enhanced by $\tan\beta$, therefore – differently from what happens in the case of the heavy Higgs bosons – the total form factor for h production can still be dominated by the top/stop contributions even for large values of $\tan\beta$.

[†]The validity of the effective-Lagrangian approximation for the light scalar h in the decoupling limit was already discussed in ref. [53] in the context of Higgs boson decays to bottom quark pairs.

8.5 Numerical examples

We will now illustrate the effect of the two-loop quark-squark-gluino contributions to the form factor for pseudoscalar Higgs production in a representative region of the MSSM parameter space.

The SM parameters entering our calculation include the Z boson mass $m_Z = 91.1876$ GeV, the W boson mass $m_W = 80.399$ GeV and the strong coupling constant $\alpha_s(m_Z) = 0.118$ [161]. For the pole masses of the top and bottom quarks we take $M_t = 173.3$ GeV [162] and $M_b = 4.49$ GeV, the latter corresponding to the SM running mass (in the $\overline{\rm MS}$ scheme) $\overline{m_b}(m_b) = 4.16$ GeV [163–165].

Since the squarks do not contribute to the one-loop amplitude for pseudoscalar production, the only parameters entering $\mathcal{H}_A^{1\ell}$ in addition to the quark masses are $\tan\beta$ and m_A. Neither of those parameters is subject to one-loop $\mathcal{O}(\alpha_s)$ corrections, therefore we need not specify a renormalization scheme for them (although it is natural to consider m_A as the pole pseudoscalar mass). The remaining input parameters are $m_{\tilde{g}}$, μ, A_t, A_b and the soft SUSY-breaking mass terms for stop and sbottom squarks, m_Q, m_U and m_D. Since these parameters only enter the two-loop part of the form factor we need not specify a renormalization scheme for them either. For simplicity, in our numerical examples we will set all the SUSY-breaking parameters, as well as the supersymmetric mass parameter μ, to a common value M. Note however that the squark mass eigenstates will differ from M, because of the supersymmetric (F-term and D-term) contributions to the squark mass matrices as well as of the left-right mixing terms.

In figure 8.2 we show the top-stop-gluino contribution to the two-loop form factor for pseudoscalar production, i.e., the term $\mathcal{K}_{t\tilde{t}\tilde{g}}^{2\ell}$ entering eq. (8.3), as a function of the common SUSY mass M, for $m_A = 150$ GeV and $\tan\beta = 2$. Even for the lowest value of M considered in the plot, $M = 100$ GeV, the stop and sbottom masses are above the threshold for real-particle production. The dashed line represents the result obtained in the limit of vanishing m_A, shown explicitly in eqs. (8.12) and (8.13), while the solid line represents the result computed at the the first order of the Taylor expansion in the pseudoscalar mass, i.e. it includes the effect of terms of $\mathcal{O}(m_A^2/m_t^2)$ and $\mathcal{O}(m_A^2/M^2)$ which are too long to be presented in analytic form. In the computation of these additional terms we assumed that the $\mathcal{O}(m_A^2/m_t^2)$ part of the one-loop top contribution, see eq. (3.32), is expressed in terms of the pole top mass.

It can be seen in figure 8.2 that the two-loop top-stop-gluino contribution $\mathcal{K}_{t\tilde{t}\tilde{g}}^{2\ell}$ is of non-decoupling nature, i.e., it does not tend to zero when all the superparticle masses become large (note that the superpotential parameter μ increases together with the SUSY-breaking parameters). In addition, the comparison between the solid and dashed lines shows that when the common SUSY mass M is close to m_A the combined effect of the terms of $\mathcal{O}(m_A^2/m_t^2)$ and $\mathcal{O}(m_A^2/M^2)$ can be as large as 20%–25% with respect to the result obtained for vanishing m_A. However, when M increases the effect of the terms of $\mathcal{O}(m_A^2/M^2)$ becomes quickly negligible. The remaining discrepancy between the solid and dashed lines for moderate to large values of M is due to the terms of $\mathcal{O}(m_A^2/m_t^2)$, and it amounts to a modest 6% for the value of m_A considered in this example.

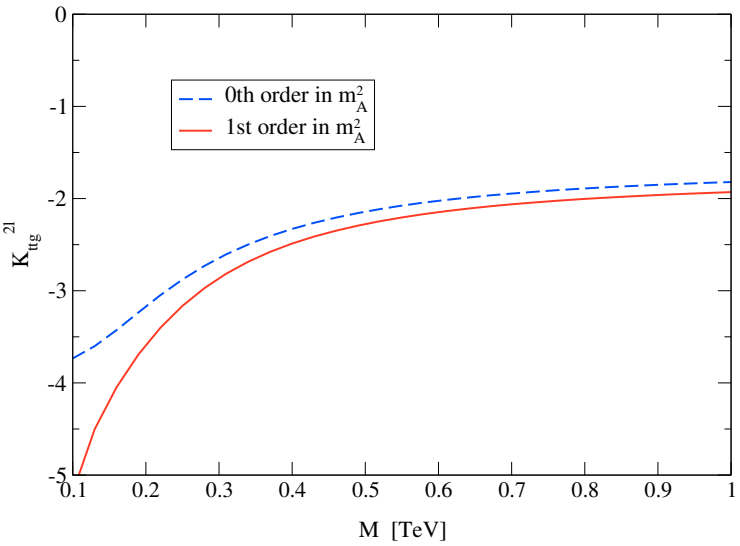

Figure 8.2: Top-stop-gluino contribution $\mathcal{K}^{2\ell}_{t\tilde{t}\tilde{g}}$ as a function of a common SUSY mass M, for $m_A = 150$ GeV and $\tan\beta = 2$. The dashed line is the result in the limit of vanishing m_A, while the solid line includes the first-order term of a Taylor expansion in m_A^2.

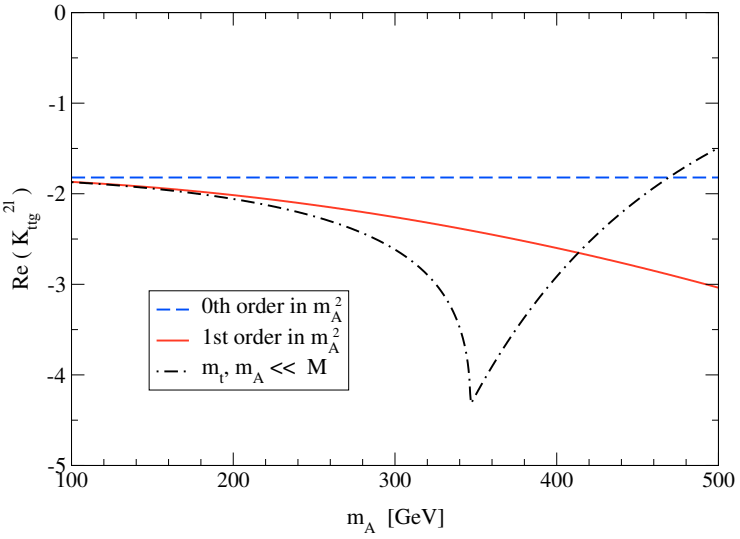

Figure 8.3: Real part of $\mathcal{K}^{2\ell}_{t\tilde{t}\tilde{g}}$ as a function of m_A, for a common SUSY mass $M = 1$ TeV and $\tan\beta = 2$. The solid and dashed lines are as in figure 8.2 above, while the dot-dashed line is the result of an asymptotic expansion in M which does not assume a specific hierarchy between m_t and m_A.

To assess the importance of the terms of $\mathcal{O}(m_A^2/m_t^2)$ for larger values of m_A, we plot in figure 8.3 the real part of $\mathcal{K}^{2\ell}_{t\tilde{t}\tilde{g}}$ as a function of the pseudoscalar mass, up to a value $m_A = 500$ GeV well above the threshold for real top-quark production. The common SUSY mass is set to the relatively large value $M = 1$ TeV, and $\tan\beta = 2$. As in figure 8.3, the dashed and solid lines represent the results obtained at the zeroth and first order of the Taylor expansion in m_A^2, respectively. The comparison between those lines shows that when m_A approaches $2\,m_t$ the effect of the terms of $\mathcal{O}(m_A^2/m_t^2)$ gets as large as 30% with respect to the result obtained for vanishing m_A. However, it is natural to wonder whether a Taylor expansion in m_A^2 can give an accurate approximation to $\mathcal{K}^{2\ell}_{t\tilde{t}\tilde{g}}$ for values of m_A close to or larger than m_t. To address this question, we show in figure 8.3 as a dot-dashed line the result of the asymptotic expansion in M, given explicitly in eqs. (8.15)–(8.19). This result was derived under the assumption that both m_A and m_t are much smaller than M, which is indeed the case for $M = 1$ TeV, but it does not require any specific hierarchy between m_A and m_t. The comparison between the dot-dashed and solid lines shows that the Taylor expansion at the first order in m_A^2 provides a good description of the dependence of $\mathcal{K}^{2\ell}_{t\tilde{t}\tilde{g}}$ on the ratio m_A/m_t up to values of m_A of the order of 250 GeV. On the other hand, when m_A reaches the threshold for real top production (i.e., at the cusp of the dot-dashed line) the result of the asymptotic expansion in M is roughly 80% larger in absolute value than the result at the first order of the Taylor expansion in m_A^2, and a full 140% larger than the result obtained for vanishing m_A.

In summary, it appears that the compact result for $\mathcal{K}^{2\ell}_{t\tilde{t}\tilde{g}}$ given in eqs. (8.12) and (8.13), which was derived for $m_A = 0$, can be safely applied only to scenarios in which m_A is smaller than m_t. While the inclusion of the terms proportional to m_A^2 pushes the validity of the Taylor expansion up to larger values of m_A, the expansion fails when m_A gets close to the threshold for real top production. In that case one can use the result of the asymptotic expansion in M, provided that the latter is still considerably larger than m_A.

We are now ready to discuss the relative importance of the various two-loop contributions to the form factor for pseudoscalar production. We will see that, at least in the region of the parameter space that we consider in this example, the results are qualitatively similar to what we found in ref. [42] for the case of the heavy scalar H.

A precise NLO determination of the cross section for pseudoscalar production would require us to take into account the contribution of one-loop diagrams with real parton emission, and to perform an integration over the phase space (see section 3.2.3). However, for the purpose of illustrating the relative importance of the various two-loop contributions, we can just define a factor K_A that contains the ratio of two-loop to one-loop form factors appearing in eq. (3.7):

$$K_A \;=\; 1 \,+\, 2\,\frac{\alpha_s}{\pi}\,\mathrm{Re}\left(\frac{\mathcal{H}_A^{2\ell}}{\mathcal{H}_A^{1\ell}}\right) \;. \tag{8.37}$$

In the left panel of figure 8.4 we plot K_A as a function of $\tan\beta$, for $m_A = 150$ GeV and all SUSY mass parameters equal to $M = 500$ GeV. The one-loop form factor $\mathcal{H}_A^{1\ell}$ in eq. (8.37) contains both the top and bottom contributions, computed under the approximations of eqs. (3.32) and (3.33), respectively. We identify the quark masses in the one-loop form

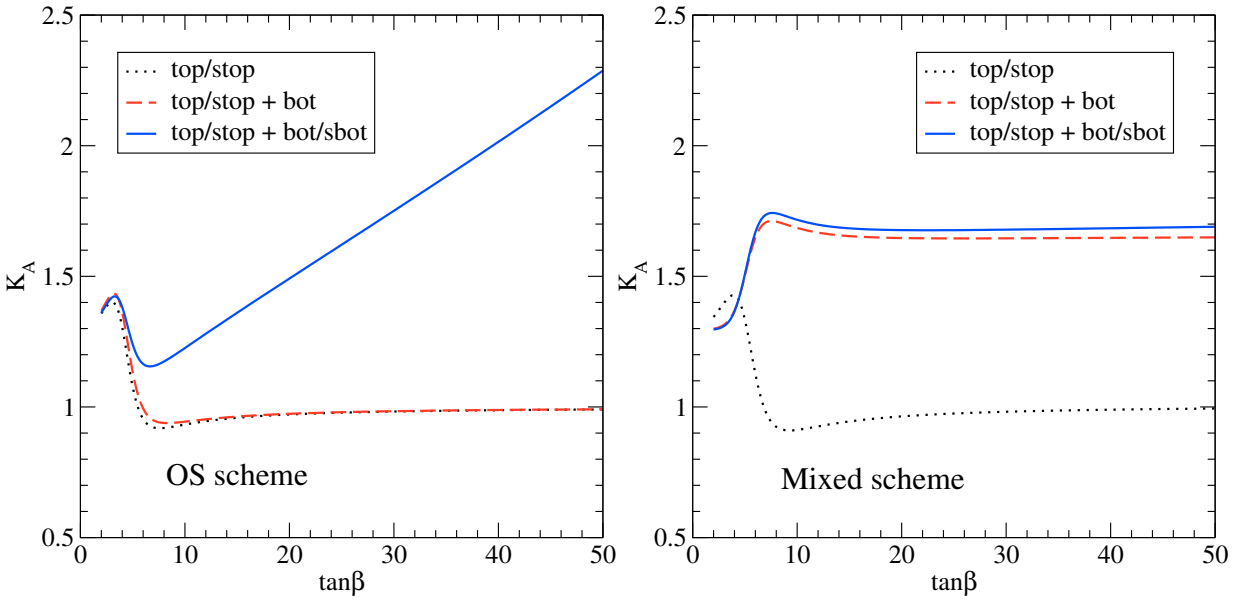

Figure 8.4: K factor for the production of a pseudoscalar Higgs A as a function of $\tan\beta$, for $m_A = 150$ GeV and all SUSY mass parameters equal to $M = 500$ GeV. The three lines show the effect of the different two-loop contributions, in the OS scheme (left panel) and in the "mixed" scheme (right panel).

factor with the pole masses, and refer to this choice as "on-shell" (OS) scheme. The lines in the plot correspond to different computations of the two-loop form factor $\mathcal{H}_A^{2\ell}$: the dotted line includes only the contributions of the top/stop sector (both those involving top quarks and gluons and those involving top, stop and gluinos) computed at the first order of the Taylor expansion in m_A^2; the dashed line includes also the contributions of two-loop diagrams with bottom quarks and gluons; finally, the solid line includes the full contributions of the bottom/sbottom sector.

Comparing the three lines in the left panel of figure 8.4 it can be seen that the top/stop contributions dominate the two-loop form factor up to values of $\tan\beta$ around 5. For larger values of $\tan\beta$ the contribution of the bottom-sbottom-gluino diagrams (included in the solid line) becomes the dominant one, and K_A grows linearly with $\tan\beta$. This behavior can be understood by recalling that, as discussed in sec. A.2, the Yukawa coupling of the pseudoscalar to bottom quarks is enhanced by $\tan\beta$ with respect to the coupling of the SM Higgs, while the coupling to top quarks is suppressed by $\tan\beta$. Consequently, for moderate to large values of $\tan\beta$ both the one-loop and the two-loop form factors in K_A are dominated by the contribution of the diagrams controlled by the pseudoscalar-bottom coupling, with the result that the coupling itself cancels out in the ratio. However, the dominant contribution from the bottom-sbottom-gluino diagrams in the OS scheme, see eq. (8.22), contains an additional $\tan\beta$-enhancement, which explains the linear rise of K_A. On the other hand, the proximity between the dotted and dashed lines shows that, in the OS scheme, the contribution to $\mathcal{H}_A^{2\ell}$ of the two-loop diagrams with bottom quarks and

gluons is very small. This is due to a partial cancellation among the three terms entering $\mathcal{K}_{bg}^{2\ell}$ in eq. (8.4), and to the fact that, in this scheme, the term $\mathcal{F}_2(\tau_b)$ is not enhanced by the potentially large logarithm of the ratio between the bottom mass and the renormalization scale, as can be seen by comparing eqs. (8.4) and (8.5).

As discussed in section 8.3.3, all $\tan\beta$-enhanced terms cancel out in a "mixed" renormalization scheme in which the pseudoscalar-bottom Yukawa coupling in the one-loop part of the result is identified with the $\overline{\rm DR}$-renormalized MSSM bottom mass $\widehat{m}_b(Q)$, where Q is a reference scale that we take equal to m_A, while the mass of the bottom quark running in the loop is identified with the pole mass M_b. To determine $\widehat{m}_b(m_A)$, we first evolve the $\overline{\rm MS}$-renormalized SM mass $\overline{m_b}(m_b)$ up to the scale m_A via the NLO-QCD renormalization group equations, then we convert it to the $\overline{\rm DR}$-renormalized SM mass $\widehat{m}_b^{\rm SM}(m_A)$ via the appropriate shift, and finally we convert it to the MSSM running mass according to

$$\widehat{m_b}(m_A) \;=\; \widehat{m_b}^{\rm SM}(m_A)\,\frac{1+\delta_b}{1+\Delta_b}\;, \tag{8.38}$$

where Δ_b is given in eq. (8.30), and δ_b is proportional to the part of $(\delta m_b)^{SUSY}$ in eq. (8.24) that is not enhanced by $\tan\beta$:

$$\delta_b \;=\; -\frac{\alpha_s\,C_F}{4\pi}\,\left[\ln\frac{m_{\tilde g}^2}{m_A^2} + f(x_1) + f(x_2) + \frac{2\,m_{\tilde g}\,A_b}{m_{\tilde b_1}^2 - m_{\tilde b_2}^2}\,\left(\frac{x_1}{1-x_1}\ln x_1 - \frac{x_2}{1-x_2}\ln x_2\right)\right]\;. \tag{8.39}$$

The "mixed" renormalization prescription is realized by computing the one-loop bottom contribution $\mathcal{K}^{1\ell}(\tau_b)$ in eq. (3.30) in terms of the pole mass M_b, then rescaling it by a factor $\widehat{m}_b(m_A)/M_b$. The two-loop form factor $\mathcal{H}_A^{2\ell}$ must then be shifted as in eq. (8.23). In the right panel of fig. 8.4 we present the result of this manipulation. The input parameters and the meaning of the different lines are the same as for the plot in the left panel. The proximity between the dashed and solid lines, and the flatness of the lines for moderate to large values of $\tan\beta$, show that the contribution of the two-loop bottom-sbottom-gluino diagrams is rather small in this renormalization scheme, and it does not induce an additional $\tan\beta$-enhancement. However, the comparison between the dotted and dashed lines shows that there is a sizable contribution to K_A from the two-loop diagrams involving bottom quarks and gluons. This is due to the fact that the shift in eq. (8.23) brings back a large logarithm, $\ln(m_b^2/m_A^2)$, which compensates the scale dependence of the running mass $\widehat{m}_b$.

Chapter 9

Conclusions

The calculation of the gluon fusion production cross section for the MSSM Higgs bosons is not quite as advanced as in the SM. Indeed, despite valiant efforts [40, 41], a full computation of the two-loop quark-squark-gluino contributions, valid for arbitrary values of all the relevant particle masses, has not been made publicly available so far. Approximate analytic results, however, can be derived if the Higgs bosons are somewhat lighter than the squarks and the gluinos. In the MSSM this condition almost certainly applies to the lightest scalar h. Moreover, recent results from SUSY searches at the LHC (see e.g. ref. [166]) set preliminary lower bounds on the squark and gluino masses just below the TeV (albeit for specific models of SUSY breaking), suggesting that there might be wide regions of the MSSM parameter space in which the condition also applies to the heavy scalar H and to the pseudoscalar A.

In this thesis we presented an original calculation of the two-loop quark-squark-gluino contributions to the cross section for the gluon fusion processes $gg \to \phi$ (where ϕ is a CP-even or CP-odd Higgs) in the limit of large supersymmetric particles masses. We exploited the techniques developed for the computations of the MSSM CP-even Higgs boson production cross section in ref. [34, 42], where the cases $m_\phi^2 \ll m_t^2$ and $m_\phi^2 \gg m_b^2$ were considered, in order to compute the cross section for MSSM CP-odd Higgs production to the same accuracy. We also extended the above mentioned techniques in such a way that no specific hierarchy is assumed between m_ϕ^2 and m_t^2. This allowed us to obtain analytic formulae for CP-even and CP-odd Higgs production which are expected to give a better approximation of the full result when the Higgs mass is not too far from the top-pair production threshold.

Our computation relies on an extensive use of the last generation of symbolic manipulation software like `Mathematica` [57] and `FORM` [65]. We generated the relevant two-loop diagrams through `FeynArts` [58], using a modified version of the MSSM model file [59], which implements the Background Field Method [60–64]. Such a choice turns out to be important in the use of Pauli-Villars regularization (PVREG). The asymptotic expansions procedure requires the exact evaluation of two-loop disconnected diagrams, *i.e.* two loop integrals in which propagators involving *both* integration momenta are absent, while scalar products of the two integration momenta, raised to integer powers, can occur. For the

reduction in Dimensional Regularization (DREG) of this class of integrals we developed a `FORM` code which performs an Integration By Parts (IBP) reduction by efficiently importing and enforcing the IBP identities generated with the software `REDUZE` [66].

In the case of CP-odd Higgs production, we performed the computation by regularizing the loop integrals both in DREG and PVREG. While in the former inconsistencies are known to arise in connection with the definition of the Dirac matrix γ_5 in $d \neq 4$ dimensions, the latter allows to avoid such difficulties, at the price of a somehow greater computational effort. We obtained identical results in the two approaches. No such problems affect the computation of the contributions to CP-even Higgs productions, so in that case we adopted DREG only.

For what concerns the top-stop-gluino contributions to CP-even Higgs production, we provided an original result based on an asymptotic expansion in the superparticle masses (which we generically denote by M), up to and including terms of $\mathcal{O}(m_A^2/M^2)$, $\mathcal{O}(m_t^2/M^2)$ and $\mathcal{O}(m_Z^2/M^2)$, for which no results have been made available so far. A numerical study of the result of this asymptotic expansion based evaluation and its renormalization scheme dependence, as well as a quantitative comparison against the Taylor series based result, is underway and will be presented in a forthcoming publication.

Regarding the contributions to CP-odd Higgs production cross section, we provided both the result of a Taylor expansion in the pseudoscalar mass, up to and including terms of $\mathcal{O}(m_A^2/m_t^2)$ and $\mathcal{O}(m_A^2/M^2)$, and the result of an asymptotic expansion in the superparticle masses, up to and including terms of $\mathcal{O}(m_A^2/M^2)$ and $\mathcal{O}(m_t^2/M^2)$. The latter can be easily adapted to the case of the bottom-sbottom-gluino contributions, which allowed us to provide a result valid up to and including terms of $\mathcal{O}(m_b^2/m_A^2)$ and $\mathcal{O}(m_b/M)$. We discussed how the $\tan\beta$-enhanced terms in the bottom-sbottom-gluino contributions can be eliminated via an appropriate choice of renormalization scheme for the parameters entering the one-loop part of the calculation, and compared our results with those obtained in the effective-Lagrangian approximation.

In both cases we obtained explicit and compact analytic results based on asymptotic expansions. All of our results can be easily implemented in computer codes for an efficient and accurate determination of the cross section for scalar and pseudoscalar production at hadron colliders.

Finally, the results derived in this work for the production cross section can be straightforwardly adapted to the NLO computation of the gluonic and photonic decay widths of the pseudoscalar Higgs boson in the MSSM, in analogy to what described in sec. 5 of ref. [34] for the case of the CP-even bosons.

Part IV

Appendices

Appendix A

Higgs-squark-squark couplings

For completeness we collect here the explicit Higgs-squark-squark couplings for both the CP-even and the CP-odd cases.

A.1 CP-even ($\phi = h, H$)

The ϕ-$\tilde{q}$-$\tilde{q}$ ($\phi = h, H$) interaction Lagrangian can be arranged in the following way ($\tilde{u}$ and $\tilde{d}$ denote here a generic up-type and down-type squark e.g. $\tilde{t}$ and $\tilde{b}$):

$$\begin{aligned}\mathcal{L}_{\text{MSSM}} \supset & -\frac{1}{\sqrt{2}} \left(\tilde{u}_L, \tilde{u}_R\right) G^{\phi}_{\tilde{u}} \begin{pmatrix} \tilde{u}_L \\ \tilde{u}_R \end{pmatrix} \phi - \frac{1}{\sqrt{2}} \left(\tilde{d}_L, \tilde{d}_R\right) G^{\phi}_{\tilde{d}} \begin{pmatrix} \tilde{d}_L \\ \tilde{d}_R \end{pmatrix} \phi \\ = & -\frac{1}{\sqrt{2}} \left(\tilde{u}_1, \tilde{u}_2\right) \hat{G}^{\phi}_{\tilde{u}} \begin{pmatrix} \tilde{u}_1 \\ \tilde{u}_2 \end{pmatrix} \phi - \frac{1}{\sqrt{2}} \left(\tilde{d}_1, \tilde{d}_2\right) \hat{G}^{\phi}_{\tilde{d}} \begin{pmatrix} \tilde{d}_1 \\ \tilde{d}_2 \end{pmatrix} \phi \,. \end{aligned} \tag{A.1}$$

For concreteness we specialize to the light Higgs case. The heavy Higgs couplings can be obtained with the replacement ($s_\alpha \to -c_\alpha$, $c_\alpha \to s_\alpha$). The coupling matrix for up-type squarks reads

$$\hat{G}^{h}_{\tilde{u}} = \begin{pmatrix} \sqrt{2}\, c_\alpha\, h_u\, m_u - \frac{g\, m_Z}{c_W}\, D_{u,L}\, s_{\alpha+\beta} & \frac{h_u}{\sqrt{2}} \left(A_u c_\alpha - \mu s_\alpha\right) \\ \frac{h_u}{\sqrt{2}} \left(A_u c_\alpha - \mu s_\alpha\right) & \sqrt{2}\, c_\alpha\, h_u\, m_u - \frac{g\, m_Z}{c_W}\, D_{u,R}\, s_{\alpha+\beta} \end{pmatrix} , \tag{A.2}$$

where the up-type and down-type Yukawas are defined by (we also explicitly show our conventions for v and m_W)

$$h_u = \sqrt{2}\, \frac{m_u}{v_2} = \sqrt{2}\, \frac{m_u}{v\, s_\beta} = \frac{g}{\sqrt{2}\, m_W}\, \frac{m_u}{s_\beta} \,, \tag{A.3}$$

$$h_d = \sqrt{2}\, \frac{m_d}{v_1} = \sqrt{2}\, \frac{m_d}{v\, c_\beta} = \frac{g}{\sqrt{2}\, m_W}\, \frac{m_d}{c_\beta} \,. \tag{A.4}$$

For convenience we recall the definition (2.35) of the coefficients of the D-term induced interaction ($q = u, d$)

$$D_{q,L} = I_{3,q} - Q_q s^2_W \,, \quad D_{q,R} = Q_q s^2_W \,, \tag{A.5}$$

where $I_{3,q} = +1/2\,(-1/2)$ is the third component of the weak isospin for up-type (down-type) squarks, Q_q the q squark electric charge and s_W is the sine of the weak angle θ_W. The coupling for down-type squarks can be obtained from the one for up-type squarks with the replacements

$$\left(G^h_{\tilde{u}} \to G^h_{\tilde{d}}\right) = \left(u \to d, c_\alpha \to -s_\alpha, s_\alpha \to -c_\alpha\right) \tag{A.6}$$

The h-$\tilde{q}$-$\tilde{q}$ coupling matrix in the mass eigenstates basis is obtained by rotating $G^h_{\tilde{q}}$ of an angle θ_q.

$$\hat{G}^h_{\tilde{q}} = R(\theta_q) G^h_{\tilde{q}} R^T(\theta_q)\,, \quad R(\theta_q) = \begin{pmatrix} c_{\theta_q} & s_{\theta_q} \\ -s_{\theta_q} & c_{\theta_q} \end{pmatrix}\,, \tag{A.7}$$

where θ_q is defined by (2.38). Eventually one gets for up-type squarks

$$\begin{aligned} \left(\hat{G}^\phi_{\tilde{u}}\right)_{11} = -\left(\hat{G}^\phi_{\tilde{u}}\right)_{22} &= \frac{h_u}{\sqrt{2}}\left[2\,c_\alpha m_u + s_{2\theta_u}\left(A_u c_\alpha - \mu s_\alpha\right)\right] \\ &\quad - \frac{g m_Z}{c_W}\left[\frac{I_{3u}}{2} + c_{2\theta_u}\left(\frac{I_{3u}}{2} - Q_u s^2_W\right)\right] s_{\alpha+\beta} \end{aligned} \tag{A.8}$$

$$\left(\hat{G}^\phi_{\tilde{u}}\right)_{12} = \left(\hat{G}^\phi_{\tilde{u}}\right)_{21} = c_{2\theta_u}\frac{h_u}{\sqrt{2}}\left(A_u c_\alpha - \mu s_\alpha\right) + s_{2\theta_u}\frac{g m_Z}{c_W}\left(\frac{I_{3u}}{2} - Q_u s^2_W\right) s_{\alpha+\beta}\,, \tag{A.9}$$

while the corresponding result for down-type squarks can again be obtained through (A.6).

A.2 CP-odd ($\phi = A$)

The A-$\tilde{q}$-$\tilde{q}$ interaction Lagrangian can be arranged in the following way ($\tilde{u}$ and $\tilde{d}$ denote here a generic up-type and down-type squark e.g. $\tilde{t}$ and $\tilde{b}$):

$$\begin{aligned} \mathcal{L}_{\text{MSSM}} \supset\; & \frac{i}{\sqrt{2}} c_\beta \left(\tilde{u}_L, \tilde{u}_R\right)^* G^A_{\tilde{u}} \begin{pmatrix} \tilde{u}_L \\ \tilde{u}_R \end{pmatrix} A + \frac{i}{\sqrt{2}} s_\beta \left(\tilde{d}_L, \tilde{d}_R\right)^* G^A_{\tilde{d}} \begin{pmatrix} \tilde{d}_L \\ \tilde{d}_R \end{pmatrix} A \\ = & \frac{i}{\sqrt{2}} c_\beta \left(\tilde{u}_1, \tilde{u}_2\right)^* \hat{G}^A_{\tilde{u}} \begin{pmatrix} \tilde{u}_1 \\ \tilde{u}_2 \end{pmatrix} A + \frac{i}{\sqrt{2}} s_\beta \left(\tilde{d}_1, \tilde{d}_2\right)^* \hat{G}^A_{\tilde{d}} \begin{pmatrix} \tilde{d}_1 \\ \tilde{d}_2 \end{pmatrix} A\,, \end{aligned} \tag{A.10}$$

where (the upper part of $\{\}$ is for up-type squarks, the lower part for down-type squarks)

$$G^A_{\tilde{q}} = \begin{pmatrix} 0 & -h_q Y_{\tilde{q}} \\ h_q Y_{\tilde{q}} & 0 \end{pmatrix}\,, \quad Y_{\tilde{q}} = A_q - \begin{Bmatrix} \tan\beta \\ \cot\beta \end{Bmatrix} \mu\,, \tag{A.11}$$

and, due to the structure of the A-$\tilde{q}$-$\tilde{q}$ coupling, it turns out that

$$\hat{G}^A_{\tilde{q}} = R(\theta_q) G^A_{\tilde{q}} R^T(\theta_q) = G^A_{\tilde{q}}\,. \tag{A.12}$$

By defining the Yukawa couplings h_q in terms of m_q, one easily sees that the down-type contributions are $\tan\beta$ enhanced. Note also that the interaction Lagrangian is purely imaginary.

Appendix B

Loop integrals

In this appendix we collect some useful known results concerning the one-loop scalar integrals (sec. B.1) and the two-loop vacuum scalar integrals relevant to our calculation in DREG (sec. B.2).

B.1 One-loop scalar integrals in DREG

We have shown in chap. 6 that, by making use of the IBP identities, every one-loop scalar integral in d-dimensions can be expressed as a linear combination of three master integrals (MI). Here we collect for completeness some basic definitions and results concerning the one-loop MI.

The one-loop scalar one-point (tadpole diagram) and two-point (bubble diagram) functions are defined in $d = 4 - 2\epsilon$ dimensions by

$$\frac{i}{16\pi^2} A_0(m^2) \equiv \frac{\mu^{4-d}}{(2\pi)^d} \int \frac{\mathrm{d}^d p}{p^2 - m^2 + i\varepsilon}\,, \tag{B.1}$$

$$\frac{i}{16\pi^2} B_0(q^2, m_1^2, m_2^2) \equiv \frac{\mu^{4-d}}{(2\pi)^d} \int \frac{\mathrm{d}^d p}{[p^2 - m_1^2 + i\varepsilon][(p+q)^2 - m_2^2 + i\varepsilon]}\,. \tag{B.2}$$

The above integrals can be evaluated with the standard techniques of $d-$dimensional integration (for a systematic discussion see, e.g., ref.[120]) and their expressions as a Laurent series in ϵ, in the limit $\epsilon \to 0$, read*

$$A_0(m^2) = m^2 \left(\frac{1}{\epsilon} + 1 - \ln \frac{m^2}{Q^2} \right) + \mathcal{O}(\epsilon)\,, \tag{B.3}$$

$$B_0(q^2, m_0^2, m_1^2) = \frac{1}{\epsilon} - \mathcal{B}(q^2, m_0^2, m_1^2) + \mathcal{O}(\epsilon)\,. \tag{B.4}$$

* Note that, in order to avoid the clutter, we always suppress all the constants (γ_E and $\ln 4\pi$) that show up together with the pole: by writing ϵ^{-1} we actually mean $\epsilon^{-1} - \gamma_E + \ln 4\pi$.

The finite part of the two-point function is given by the integral over the Feynman parameter x

$$\mathcal{B}(q^2, m_0^2, m_1^2) \equiv \int_0^1 \mathrm{d}x \ln \frac{(1-x)m_0^2 + xm_1^2 - x(1-x)q^2 - i\varepsilon}{Q^2} \tag{B.5}$$

where $Q^2 = 4\pi\mu^2 \mathrm{e}^{-\gamma_E}$. The quantity γ_E is the Euler-Mascheroni constant,

$$\gamma_E = \lim_{n\to\infty} \left(\sum_{k=1}^{n} \frac{1}{k} - \ln n \right) \simeq 0.5772\,. \tag{B.6}$$

An explicit expression for the integral in (B.5) can be found, e.g., in ref. [167].

The scalar three-point function (vertex diagram) is defined in $d = 4-2\epsilon$ dimensions by

$$\frac{i}{16\pi^2} C_0(q_1^2, q_2^2, (q_1+q_2)^2, m_0^2, m_1^2, m_2^2) \equiv \frac{\mu^{4-d}}{(2\pi)^d} \int \frac{\mathrm{d}^d p}{D_0 D_1 D_2}\,, \tag{B.7}$$

where the denominators read

$$D_0 := p^2 - m_0^2 + i\varepsilon\,, \tag{B.8}$$
$$D_1 := (p+q_1)^2 - m_1^2 + i\varepsilon\,, \tag{B.9}$$
$$D_2 := (p+q_1+q_2)^2 - m_2^2 + i\varepsilon\,. \tag{B.10}$$

The general result for the scalar three-point function, valid for all real momenta and physical masses, was calculated in ref. [150]. In our calculation the kinematics is fixed by the assumption of on-shell external particles, that is $q_1^2 = q_2^2 = 0$ and $(q_1+q_2)^2 = s = m_\phi^2$ (where we generically denote with ϕ the produced Higgs boson). Concerning the masses of the particles running in the loop, in our computation of the Higgs boson amplitudes by means of asymptotic expansions in the large sparticle masses, the C_0 function enters only in two particular cases. The first is the case $s \ll m_0, m_1, m_2$, which allows for an approximate evaluation through an expansion in the small external momenta *under* the integration sign. In the second case $m_0 = m_1 = m_2 = m$, and an explicit, compact analytic expression for the finite part of the C_0 function is given by

$$C_0(0, 0, q^2, m^2, m^2, m^2) = \frac{1}{2q^2} \ln^2 \left(\frac{\sqrt{1 - \frac{4m^2}{q^2}} - 1}{\sqrt{1 - \frac{4m^2}{q^2}} + 1} \right)\,. \tag{B.11}$$

Concerning the terms of $\mathcal{O}(\epsilon)$ in the Laurent series for the three MI's A_0, B_0 and C_0, one remark is in order. As illustrated in chap. 5, in the asymptotic expansions approach one has to compute the product of two disconnected one-loop integrals. In case both the UV and the IR divergences are regulated withing DREG, the A_0 and B_0 functions will have just a simple UV pole in ϵ, while the vertex functions can in principle have single (double) poles, corresponding to collinear (collinear and soft) singularieties due to massless

particles[†]. Therefore, when the pole (double pole) of one integral hits the $\mathcal{O}(\epsilon)$ ($\mathcal{O}(\epsilon)$ and $\mathcal{O}(\epsilon^2)$) part of the other integral, this will generate a finite term (a simple pole and a finite term) which ends up in the final result.

B.2 Two-loop scalar integrals in DREG

The basic two-loop integrals are:

$$\frac{1}{(16\pi^2)^2}\,J(x,y) \equiv -\frac{\mu^{2(4-d)}}{(2\pi)^{2d}} \iint \frac{\mathrm{d}^d p\,\mathrm{d}^d k}{[p^2-x][k^2-y]}\,, \tag{B.12}$$

$$\frac{1}{(16\pi^2)^2}\,I(x,y,z) \equiv -\frac{\mu^{2(4-d)}}{(2\pi)^{2d}} \iint \frac{\mathrm{d}^d p\,\mathrm{d}^d k}{[p^2-x][k^2-y][(p-k)^2-z]}\,. \tag{B.13}$$

The functions $I(x,y)$ and $J(x,y,z)$ have been evaluated in ref.[147], and their expressions read

$$J(x,y) = \frac{xy}{\epsilon^2} - \frac{xy}{\epsilon}(\,\overline{\ln}x + \overline{\ln}y - 2) - xy\left[2\,\overline{\ln}x + 2\,\overline{\ln}y - \frac{1}{2}\,\overline{\ln}^2 xy - \left(3+\frac{\pi^2}{6}\right)\right]\,, \tag{B.14}$$

$$\begin{aligned} I(x,y,z) =& -\frac{x+y+z}{2\epsilon^2} + \frac{1}{\epsilon}\left[x\,\overline{\ln}x + y\,\overline{\ln}y + z\,\overline{\ln}z - \frac{3}{2}(x+y+z)\right] \\ &+ \frac{1}{2}(x\,\overline{\ln}y\,\overline{\ln}z + y\,\overline{\ln}x\,\overline{\ln}z + z\,\overline{\ln}x\,\overline{\ln}y) - \frac{x+y+z}{2}\left(7+\frac{\pi^2}{6}\right) \\ &- \frac{1}{2}(x\,\overline{\ln}x + y\,\overline{\ln}y + z\,\overline{\ln}z)(x\,\overline{\ln}x + y\,\overline{\ln}y + z\,\overline{\ln}z - 6) - \frac{\Delta(x,y,z)}{2z}\Phi(x,y,z)\,, \end{aligned} \tag{B.15}$$

where we use the compact notation $\overline{\ln}x \equiv \ln(x/Q^2)$, the function Δ is the triangular (or Källén) function ($\Delta(x,y,z) \equiv x^2+y^2+z^2-2(xy+xz+yz)$) and the function Φ is defined by

$$\Phi(x,y,z) = \frac{1}{\lambda}\left[2\ln x_+\,\ln x_- - \ln u\,\ln v - 2\left(\mathrm{Li}_2(x_+) + \mathrm{Li}_2(x_-)\right) + \frac{\pi^2}{3}\right]\,, \tag{B.16}$$

where

$$u = \frac{x}{z}\,,\quad v = \frac{y}{z}\,,\quad \lambda = \sqrt{(1-u-v)^2-4uv}\,,\quad x_\pm = \frac{1}{2}[1\pm(u-v)-\lambda]\,. \tag{B.17}$$

The definition of the Φ function given above is valid when $x, y < z$, while symmetry properties allow to obtain the other branches:

$$\Phi(x,y,z) = \Phi(y,x,z)\,,\quad x\,\Phi(x,y,z) = z\,\Phi(z,y,x)\,, \tag{B.18}$$

[†]In the MSSM, these singularities arise only in the diagrams for the virtual corrections due to gluons, which are already known in the literature.

and the limit for small x:

$$\lim_{x\to 0}\Phi(x,y,z)=\frac{1}{1-v}[\ln u\,\ln v+2\,\mathrm{Li}_2(1-v)]\,. \tag{B.19}$$

The function Φ has also the property that $\Phi(x,y,y)=y/x\,\phi\,(x/(4y))$, where

$$\phi(z)=\begin{cases}4\sqrt{\frac{z}{1-z}}\,\mathrm{Cl}_2\,(2\arcsin\sqrt{z}) & \text{if } 0<z<1\\ \frac{1}{\lambda}\left[-4\mathrm{Li}_2(\frac{1-\lambda}{2})+2\ln^2(\frac{1-\lambda}{2})-\ln^2(4z)+\frac{\pi^2}{3}\right] & \text{if } z>1\,.\end{cases} \tag{B.20}$$

In the above equation $\mathrm{Cl}_2(z)=\mathrm{Im}\,\mathrm{Li}_2(\mathrm{e}^{iz})$ is the Clausen function. For $z\to 1$ one has $\phi(z)\to 8\ln 2$ while for $z=1/4$ (corresponding to the case $\Phi(x,x,x)$) one gets

$$\phi(1/4)=4\sqrt{3}\int_0^{\pi/6}\mathrm{d}x\,\ln(2\cos x)\simeq 2.343907\,. \tag{B.21}$$

Finally, in the derivation of analytical formulae for the two-loop corrections valid in simplified cases (e.g. for given hierarchies between the mass scales involved), it is often necessary to perform Taylor expansions of the results around some specific value of one or more of its arguments. The Taylor expansion of the Φ function can be easily recovered by using the following expression for the partial derivative w.r.t x (the partial derivative w.r.t. y and z can be obtained by means of the symmetry properties of eq.(B.18):

$$\Delta(x,y,z)\frac{\Phi(x,y,z)}{x}=(y+z-x)\Phi(x,y,z)+\frac{z}{x}\left[(y-z)\ln\frac{z}{y}+x\left(\ln\frac{x}{y}+\ln\frac{x}{z}\right)\right]\,. \tag{B.22}$$

Appendix C

NLO contributions from real parton emission

In this appendix we present for completeness our results for the NLO contributions to pseudoscalar production from one-loop diagrams with emission of a real parton, i.e., the functions $\mathcal{R}^A_{gg}$, $\mathcal{R}^A_{q\bar{q}}$ and $\mathcal{R}^A_{qg}$ entering eqs. (3.7) and (3.8) in the case $\phi = A$. Such contributions were first computed in ref. [4] (see also ref. [116]).

C.1 Pseudoscalar Higgs

The contribution of the gluon-fusion channel, $gg \to Ag$, can be written as

$$\mathcal{R}^A_{gg} = \frac{1}{z(1-z)} \int_0^1 \frac{dv}{v(1-v)} \left\{ 8\, z^4\, \frac{\left|\mathcal{A}_{gg}(\hat{s},\hat{t},\hat{u})\right|^2}{\left|\mathcal{H}^{1\ell}_A\right|^2} - (1-z+z^2)^2 \right\} , \tag{C.1}$$

where $\hat{t} = -\hat{s}\,(1-z)(1-v)$, $\hat{u} = -\hat{s}\,(1-z)\,v$, and

$$|\mathcal{A}_{gg}(s,t,u)|^2 \;=\; T_F^2 \left[\cot^2\beta \left|\mathcal{A}^{tt}_{gg}(s,t,u)\right|^2 + \tan^2\beta \left|\mathcal{A}^{bb}_{gg}(s,t,u)\right|^2 + 2\left|\mathcal{A}^{tb}_{gg}(s,t,u)\right|^2\right] , \tag{C.2}$$

with

$$\left|\mathcal{A}^{ij}_{gg}(s,t,u)\right|^2 = |A^{ij}(s,t,u)|^2 + |A^{ij}(u,s,t)|^2 + |A^{ij}(t,u,s)|^2 \; . \tag{C.3}$$

Defining, for $i = t, b$,

$$y_i \equiv \frac{m_i^2}{m_A^2}, \qquad s_i \equiv \frac{s}{m_i^2}, \qquad t_i \equiv \frac{t}{m_i^2}, \qquad u_i \equiv \frac{u}{m_i^2}, \tag{C.4}$$

we find:

$$
\begin{aligned}
|A^{ij}(s,t,u)|^2 \;=\; \frac{y_i y_j}{4m_A^4}\Bigg\{\Bigg[\;& b_1(s,t,u)\,H_2(s_i,y_i)\,H_2^\dagger(s_j,y_j) + b_2(s,t,u)\,H_2(s_i,y_i)\,H_2^\dagger(t_j,y_j) \\
&+ b_3(s,t,u)\,H_3(s_i,t_i,u_i)\,H_3^\dagger(s_j,t_j,u_j) + b_4(s,t,u)\,H_3(s_i,t_i,u_i)\,H_3^\dagger(u_j,s_j,t_j) \\
&+ b_5(s,t,u)\,H_2(s_i,y_i)\,H_3^\dagger(s_j,t_j,u_j) + b_6(s,t,u)\,H_2(s_i,y_i)\,H_3^\dagger(t_j,u_j,s_j) \\
&+ b_7(s,t,u)\,H_2(s_i,y_i)\,H_3^\dagger(u_j,s_j,t_j)\Bigg] \;+\; (i\leftrightarrow j)\Bigg\} \;+\; \text{h.c.}\;, \qquad \text{(C.5)}
\end{aligned}
$$

where the function $H_3(s,t,u)$ is defined in eq. (2.28) of ref. [37], and

$$
H_2(s,y) = \frac{1}{2}\left[\log^2\left(\frac{\sqrt{1-4/s}-1}{\sqrt{1-4/s}+1}\right) - \log^2\left(\frac{\sqrt{1-4y}-1}{\sqrt{1-4y}+1}\right)\right]\;. \qquad \text{(C.6)}
$$

The coefficient functions $b_i(s,t,u)$ entering eq. (C.5) are

$$
\begin{aligned}
b_1(s,t,u) &= \frac{1}{2}\left[\frac{4t^2u^2}{(t+u)^2} + s^2 - 3tu + s(t+u) + (t+u)^2\right]\;, && \text{(C.7)}\\
b_2(s,t,u) &= s^2+t^2+u^2+st + \frac{2s^2tu}{(s-t)(s+u)} - \frac{2st^2u}{(s-t)(t+u)}\;, && \text{(C.8)}\\
b_3(s,t,u) &= \frac{1}{8}\left[s^2+t^2+u^2+tu+s(t+u)\right]\;, && \text{(C.9)}\\
b_4(s,t,u) &= \frac{1}{4}(s+t)(t+u)\;, && \text{(C.10)}\\
b_5(s,t,u) &= -\frac{1}{2}\left[t^2+u^2+s(t+u)\right]\;, && \text{(C.11)}\\
b_6(s,t,u) &= -\frac{1}{2}\left[s^2+(t+u)(s+u)+\frac{(t-u)ut}{(t+u)}\right]\;, && \text{(C.12)}\\
b_7(s,t,u) &= -\frac{1}{2}\left[s^2+(t+u)(s+t)+\frac{(u-t)ut}{(t+u)}\right]\;. && \text{(C.13)}
\end{aligned}
$$

The contribution of the quark-antiquark annihilation channel, $q\bar{q}\to Ag$, can be written as

$$
\mathcal{R}^A_{q\bar{q}} = \frac{512}{27}\frac{z\,(1-z)\;|\mathcal{A}_{q\bar{q}}(\hat{s})|^2}{|\mathcal{H}_A^{1\ell}|^2}\,, \qquad \text{(C.14)}
$$

with

$$
\mathcal{A}_{q\bar{q}}(s) = T_F\,\Big[\cot\beta\,y_t\,H_2(s_t,y_t) + \tan\beta\,y_b\,H_2(s_b,y_b)\Big]\;. \qquad \text{(C.15)}
$$

Finally, the contribution of the quark-gluon scattering channel, $qg\to Aq$, can be written as

$$
\mathcal{R}^A_{qg} \;=\; \frac{C_F}{2}z \;+\; C_F\int_0^1\frac{dv}{(1-v)}\left\{\frac{1+(1-z)^2v^2}{[1-(1-z)v]^2}\,\frac{8\,z\,\big|\mathcal{A}_{q\bar{q}}(\hat{t}\,)\big|^2}{|\mathcal{H}_A^{1\ell}|^2} \;-\; \frac{1+(1-z)^2}{2z}\right\}\;. \qquad \text{(C.16)}
$$

We compared our results for the functions $\mathcal{R}^A_{gg}$, $\mathcal{R}^A_{q\bar{q}}$ and $\mathcal{R}^A_{qg}$ with the corresponding results in ref. [4], and found full agreement.*

*Some misprints in ref. [4] must be taken into account in the comparison. In eq. (C.4) of that paper the term within square modulus in the definition of d_{gq} should be divided by 2. Also, the formulae in the Appendices B and C omit all occurrences of the MSSM Higgs-quark couplings, denoted in that paper as g^{Φ}_{Q}.

Appendix D

Explicit formulae for the $gg \to \phi$ ($\phi = h, H$) two-loop top-stop-gluino contributions

In this appendix we collect the explicit results for the two-loop top-stop-gluino contributions to the functions Y_x, in terms of which we express the functions $G_t^{2\ell}$, $F_t^{2\ell}$, $\widetilde{F}_t^{2\ell}$ and $\widetilde{G}_t^{2\ell}$ entering the two-loop part of the form factors $\mathcal{H}_1$ (7.9) and $\mathcal{H}_2$ (7.10) for CP-even Higgs production. In particular, we collect the formulae for the C_A and C_F parts of the expansion coefficients $Y_x^{(n,\tilde{g})}$ ($x = t, \tilde{t}_1, c^2_{2\theta_t}$) entering (7.30). We assume that the one-loop form factor $\mathcal{H}_2^{1\ell}$ is expressed in terms of the $\overline{\rm DR}$-renormalized parameters evaluated at the scale Q^2. For the definitions of the quantities entering the formulae below, see sec. 7.2.

D.1 Top-stop-gluino contributions to Y_t

The expansion coefficients of the C_A part are given by

$$Y_t^{(-1,\tilde{g},C_A)} = 0\,, \tag{D.1}$$

$$Y_t^{(0,\tilde{g},C_A)} = 0\,, \tag{D.2}$$

$$\begin{aligned} Y_t^{(1,\tilde{g},C_A)} = {} & \frac{1}{6\,(1-x_1)^2}\, s_{2\theta_t} \Bigg[3\,(1 - x_1 + x_1 \ln x_1) \left(\ln \frac{m_t^2}{m_{\tilde{g}}^2} - \mathcal{B} - \frac{\mathcal{K}_{1/2}^{1\ell}(\tau_t)}{2} + 2 \right) \\ & + 6x_1 \mathrm{Li}_2\,(1-x_1) + 2x_1 + 2x_1\,(1+x_1) \ln x_1 - 2 \Bigg] \\ & - \Big(x_1 \longrightarrow x_2 \Big)\,, \end{aligned} \tag{D.3}$$

and

$$Y_t^{(2,\tilde{g},C_A)} = -\frac{1}{12\,(1-x_1)^3}\Bigg[3\left(1-x_1^2+2x_1\ln x_1\right)\left(2\ln\frac{m_t^2}{m_{\tilde{g}}^2}-\mathcal{B}-\frac{\mathcal{K}_{1/2}^{1\ell}(\tau_t)}{2}+2\right) + 24x_1\mathrm{Li}_2\,(1-x_1)+1-x_1^2+2x_1\,(3x_1+10)\ln x_1\Bigg] + \Big(x_1 \longrightarrow x_2\Big), \tag{D.4}$$

while the expansion coefficients of the C_F part read

$$Y_t^{(-1,\tilde{g},C_F)} = -\frac{1}{4}s_{2\theta_t}\mathcal{G}_{1/2}^{1\ell}(\tau_t)\left(\frac{x_1}{1-x_1}\ln x_1-\frac{x_2}{1-x_2}\ln x_2\right), \tag{D.5}$$

$$Y_t^{(0,\tilde{g},C_F)} = \frac{4}{3}\mathcal{F}_{1/2}^{(2\ell,b)}\big(x(\tau_t)\big)\frac{(\delta m_t)^{(\mathrm{SUSY})}}{m_t}, \tag{D.6}$$

$$Y_t^{(1,\tilde{g},C_F)} = -\frac{s_{2\theta_t}}{6\,(1-x_1)^3\,x_1}\Bigg[-3\left(x_1^3-x_1-2x_1^2\ln x_1\right)\left(\ln\frac{m_t^2}{m_{\tilde{g}}^2}-\mathcal{B}-\frac{\mathcal{G}_{1/2}^{1\ell}(\tau_t)}{4}-\frac{\mathcal{K}_{1/2}^{1\ell}(\tau_t)}{2}+2\right) + (1-x_1)^3\ln\frac{m_{\tilde{g}}^2}{Q^2}+12\,x_1^2\,\mathrm{Li}_2\,(1-x_1)+5x_1^3-5x_1^2+x_1-1+2\left(x_1^3+2x_1^2\right)\ln x_1\Bigg] - \Big(x_1 \longleftrightarrow x_2\Big), \tag{D.7}$$

and

$$Y_t^{(2,\tilde{g},C_F)} = \frac{1}{18\,(1-x_1)^4\,x_1}\Bigg\{-3x_1\left[(1-x_1)\left(x_1^2-5x_1-2\right)-6x_1\ln x_1\right]\times \left(2\ln\frac{m_t^2}{m_{\tilde{g}}^2}-\mathcal{B}-\frac{\mathcal{G}_{1/2}^{1\ell}(\tau_t)}{2}-\frac{\mathcal{K}_{1/2}^{1\ell}(\tau_t)}{2}+2\right)+6\,(1-x_1)^4\ln\frac{m_{\tilde{g}}^2}{Q^2} + 72\,x_1^2\,\mathrm{Li}_2\,(1-x_1)-x_1\,(1-x_1)^2\,(11x_1-26)-6\,(1-x_1)+6x_1^2\,(2x_1+9)\ln x_1\Bigg\} + \Big(x_1 \longleftrightarrow x_2\Big), \tag{D.8}$$

where we recall that in (D.6) $x(\tau) \equiv \frac{\sqrt{1-\tau}-1}{\sqrt{1-\tau}+1}$.

D.2 Top-stop-gluino contributions to $Y_{\tilde{t}_1}$

The explicit expressions for expansion coefficients of the C_A part read

$$Y_{\tilde{t}_1}^{(-1,\tilde{g},C_A)} = 0\,, \tag{D.9}$$

$$Y_{\tilde{t}_1}^{(0,\tilde{g},C_A)} = -\frac{1}{12}\left[\frac{1}{1-x_1}+\frac{1}{(1-x_1)^2}\ln x_1\right], \tag{D.10}$$

$$\begin{aligned} Y_{\tilde{t}_1}^{(1,\tilde{g},C_A)} = {} & \frac{s_{2\theta_t}}{6\,(1-x_1)^3}\left\{3\left[2-2x_1+(x_1+1)\ln x_1\right]\left(\ln\frac{m_t^2}{m_{\tilde{g}}^2}+1\right)+6\,(x_1+1)\,\mathrm{Li}_2\,(1-x_1)\right. \\ & \left.+2x_1\,(1-x_1)+2\,(6x_1+1)\ln x_1\right\}, \end{aligned} \tag{D.11}$$

while for the C_F part we have

$$Y_{\tilde{t}_1}^{(-1,\tilde{g},C_F)} = \frac{1}{4}s_{2\theta_t}\,\mathcal{G}_{1/2}^{1\ell}(\tau_t)\left[\frac{1}{1-x_1}+\frac{1}{(1-x_1)^2}\ln x_1\right], \tag{D.12}$$

$$\begin{aligned} Y_{\tilde{t}_1}^{(0,\tilde{g},C_F)} = {} & -\frac{1}{6}\left[\frac{1}{1-x_1}+\frac{1}{(1-x_1)^2}\ln x_1-\frac{1}{x_1^2}+\frac{1}{x_1^2}\ln\frac{m_{\tilde{g}}^2}{Q^2}\right] \\ & -\mathcal{G}_{1/2}^{1\ell}(\tau_t)\frac{(1-x_1)\,(3-x_1)+2\ln x_1}{8\,(1-x_1)^3}\,, \end{aligned} \tag{D.13}$$

$$\begin{aligned} Y_{\tilde{t}_1}^{(1,\tilde{g},C_F)} = {} & \frac{s_{2\theta_t}}{12\,(1-x_1)^4\,x_1^2}\left\{6x_1^2\left((1-x_1)\,(x_1+5)+2\,(2x_1+1)\ln x_1\right)\left(\frac{\mathcal{G}_{1/2}^{1\ell}(\tau_t)}{4}-\ln\frac{m_t^2}{m_{\tilde{g}}^2}\right)\right. \\ & +2\,(1-x_1)^4\ln\frac{m_{\tilde{g}}^2}{Q^2}+\left(2+\frac{\mathcal{G}_{1/2}^{1\ell}(\tau_t)}{\tau_t}\right)x_1\left[(1-x_1)\left(x_1^2-5x_1-2\right)-6x_1\ln x_1\right] \\ & -24x_1^2\,(2x_1+1)\,\mathrm{Li}_2\,(1-x_1)-2\left(x_1^3+9x_1^2-5x_1+1\right)(1-x_1) \\ & \left.-4x_1^2\left(x_1^2+18x_1+2\right)\ln x_1\right\}, \end{aligned} \tag{D.14}$$

D.3 Top-stop-gluino contributions to $Y_{c_{2\theta_t}^2}$

The explicit results for expansion coefficients of the C_A part are given by

$$Y_{c_{2\theta_t}^2}^{(-1,\tilde{g},C_A)} = 0\,, \tag{D.15}$$

$$Y_{c_{2\theta_t}^2}^{(0,\tilde{g},C_A)} = 0\,, \tag{D.16}$$

and

$$Y^{(1,\tilde{g},C_A)}_{c^2_{2\theta_t}} = \frac{x_1}{12\,(1-x_1)^2\,s_{2\theta_t}}\left[(x_1-1-\ln x_1)\left(3\ln\frac{m_t^2}{m_{\tilde{g}}^2}+1\right)-6\mathrm{Li}_2\,(1-x_1)\right.$$
$$\left.-\,2\,(x_1+2)\ln x_1\right]$$
$$-\left(x_1 \longleftrightarrow x_2\right), \tag{D.17}$$

while the explicit results for the C_F part read

$$Y^{(-1,\tilde{g},C_F)}_{c^2_{2\theta_t}} = \; -\frac{1}{8\,s_{2\theta_t}}\mathcal{G}^{1\ell}_{1/2}(\tau_t)\left(\frac{x_1}{1-x_1}\ln x_1-\frac{x_2}{1-x_2}\ln x_2\right), \tag{D.18}$$

$$Y^{(0,\tilde{g},C_F)}_{c^2_{2\theta_t}} = 0\,, \tag{D.19}$$

$$Y^{(1,\tilde{g},C_F)}_{c^2_{2\theta_t}} = \frac{1}{24\,(1-x_1)^3\,x_1 s_{2\theta_t}}\left\{6x_1\left(x_1^2-2x_1\ln x_1-1\right)\left(\frac{\mathcal{G}^{1\ell}_{1/2}(\tau_t)}{4}-\ln\frac{m_t^2}{m_{\tilde{g}}^2}\right)\right.$$
$$+\,2\,(1-x_1)^3\ln\frac{m_{\tilde{g}}^2}{Q^2}+3x_1\,(1-x_1)\,\frac{\mathcal{G}^{1\ell}_{1/2}(\tau_t)}{\tau_t}\times$$
$$\times\left[\frac{(1-x_1)\,(x_1-2x_1x_2+x_2)}{(1-x_2)\,(x_1-x_2)}+\frac{2x_1\,(x_1^2+x_1x_2-2x_2)\ln x_1}{(x_1-x_2)^2}\right]$$
$$\left.+\,24x_1^2\mathrm{Li}_2\,(1-x_1)-2\,(1-2x_1)\,(1-x_1)^2+4x_1^2\,(x_1+5)\ln x_1\right\}$$
$$-\left(x_1 \longleftrightarrow x_2\right). \tag{D.20}$$

Bibliography

[1] H. Georgi, S. Glashow, M. Machacek, and D. V. Nanopoulos, "Higgs Bosons from Two Gluon Annihilation in Proton Proton Collisions," *Phys.Rev.Lett.* **40** (1978) 692.

[2] S. Dawson, "Radiative corrections to Higgs boson production," *Nucl.Phys.* **B359** (1991) 283–300.

[3] A. Djouadi, M. Spira, and P. Zerwas, "Production of Higgs bosons in proton colliders: QCD corrections," *Phys.Lett.* **B264** (1991) 440–446.

[4] M. Spira, A. Djouadi, D. Graudenz, and P. M. Zerwas, "Higgs boson production at the LHC," *Nucl. Phys.* **B453** (1995) 17–82, arXiv:hep-ph/9504378.

[5] R. Harlander and P. Kant, "Higgs production and decay: Analytic results at next-to-leading order QCD," *JHEP* **0512** (2005) 015, arXiv:hep-ph/0509189 [hep-ph].

[6] R. V. Harlander, "Virtual corrections to $gg \to H$ to two loops in the heavy top limit," *Phys.Lett.* **B492** (2000) 74–80, arXiv:hep-ph/0007289 [hep-ph].

[7] S. Catani, D. de Florian, and M. Grazzini, "Higgs production in hadron collisions: Soft and virtual QCD corrections at NNLO," *JHEP* **0105** (2001) 025, arXiv:hep-ph/0102227 [hep-ph].

[8] R. V. Harlander and W. B. Kilgore, "Soft and virtual corrections to proton proton $\to$ H + X at NNLO," *Phys.Rev.* **D64** (2001) 013015, arXiv:hep-ph/0102241 [hep-ph].

[9] R. V. Harlander and W. B. Kilgore, "Next-to-next-to-leading order Higgs production at hadron colliders," *Phys.Rev.Lett.* **88** (2002) 201801, arXiv:hep-ph/0201206 [hep-ph].

[10] C. Anastasiou and K. Melnikov, "Higgs boson production at hadron colliders in NNLO QCD," *Nucl.Phys.* **B646** (2002) 220–256, arXiv:hep-ph/0207004 [hep-ph].

[11] V. Ravindran, J. Smith, and W. L. van Neerven, "NNLO corrections to the total cross-section for Higgs boson production in hadron hadron collisions," *Nucl.Phys.* **B665** (2003) 325–366, arXiv:hep-ph/0302135 [hep-ph].

[12] R. V. Harlander, H. Mantler, S. Marzani, and K. J. Ozeren, "Higgs production in gluon fusion at next-to-next-to-leading order QCD for finite top mass," *Eur.Phys.J.* **C66** (2010) 359–372, arXiv:0912.2104 [hep-ph].

[13] S. Marzani, R. D. Ball, V. Del Duca, S. Forte, and A. Vicini, "Higgs production via gluon-gluon fusion with finite top mass beyond next-to-leading order," *Nucl.Phys.* **B800** (2008) 127–145, arXiv:0801.2544 [hep-ph].

[14] S. Marzani, R. D. Ball, V. Del Duca, S. Forte, and A. Vicini, "Finite-top-mass effects in NNLO Higgs production," *Nucl.Phys.Proc.Suppl.* **186** (2009) 98–101, arXiv:0809.4934 [hep-ph].

[15] R. V. Harlander and K. J. Ozeren, "Top mass effects in Higgs production at next-to-next-to-leading order QCD: Virtual corrections," *Phys.Lett.* **B679** (2009) 467–472, arXiv:0907.2997 [hep-ph].

[16] R. V. Harlander and K. J. Ozeren, "Finite top mass effects for hadronic Higgs production at next-to-next-to-leading order," *JHEP* **0911** (2009) 088, arXiv:0909.3420 [hep-ph].

[17] A. Pak, M. Rogal, and M. Steinhauser, "Virtual three-loop corrections to Higgs boson production in gluon fusion for finite top quark mass," *Phys.Lett.* **B679** (2009) 473–477, arXiv:0907.2998 [hep-ph].

[18] A. Pak, M. Rogal, and M. Steinhauser, "Finite top quark mass effects in NNLO Higgs boson production at LHC," *JHEP* **1002** (2010) 025, arXiv:0911.4662 [hep-ph].

[19] A. Pak, M. Rogal, and M. Steinhauser, "Production of scalar and pseudo-scalar Higgs bosons to next-to-next-to-leading order at hadron colliders," *JHEP* **1109** (2011) 088, arXiv:1107.3391 [hep-ph].

[20] S. Catani, D. de Florian, M. Grazzini, and P. Nason, "Soft gluon resummation for Higgs boson production at hadron colliders," *JHEP* **0307** (2003) 028, arXiv:hep-ph/0306211 [hep-ph].

[21] S. Moch and A. Vogt, "Higher-order soft corrections to lepton pair and Higgs boson production," *Phys.Lett.* **B631** (2005) 48–57, arXiv:hep-ph/0508265 [hep-ph].

[22] V. Ravindran, "Higher-order threshold effects to inclusive processes in QCD," *Nucl.Phys.* **B752** (2006) 173–196, arXiv:hep-ph/0603041 [hep-ph].

[23] A. Djouadi and P. Gambino, "Leading electroweak correction to Higgs boson production at proton colliders," *Phys.Rev.Lett.* **73** (1994) 2528–2531, arXiv:hep-ph/9406432 [hep-ph].

[24] A. Djouadi, P. Gambino, and B. A. Kniehl, "Two loop electroweak heavy fermion corrections to Higgs boson production and decay," *Nucl.Phys.* **B523** (1998) 17–39, arXiv:hep-ph/9712330 [hep-ph].

[25] U. Aglietti, R. Bonciani, G. Degrassi, and A. Vicini, "Two loop light fermion contribution to Higgs production and decays," *Phys.Lett.* **B595** (2004) 432–441, arXiv:hep-ph/0404071 [hep-ph].

[26] U. Aglietti, R. Bonciani, G. Degrassi, and A. Vicini, "Master integrals for the two-loop light fermion contributions to $gg \to H$ and $H \to \gamma\gamma$," *Phys.Lett.* **B600** (2004) 57–64, arXiv:hep-ph/0407162 [hep-ph].

[27] G. Degrassi and F. Maltoni, "Two-loop electroweak corrections to Higgs production at hadron colliders," *Phys.Lett.* **B600** (2004) 255–260, arXiv:hep-ph/0407249 [hep-ph].

[28] S. Actis, G. Passarino, C. Sturm, and S. Uccirati, "NLO Electroweak Corrections to Higgs Boson Production at Hadron Colliders," *Phys.Lett.* **B670** (2008) 12–17, arXiv:0809.1301 [hep-ph].

[29] S. Actis, G. Passarino, C. Sturm, and S. Uccirati, "NNLO Computational Techniques: The Cases $H \to \gamma\gamma$ and $H \to gg$," *Nucl.Phys.* **B811** (2009) 182–273, arXiv:0809.3667 [hep-ph].

[30] A. Pak, M. Steinhauser, and N. Zerf, "Towards Higgs boson production in gluon fusion to NNLO in the MSSM," *Eur.Phys.J.* **C71** (2011) 1602, arXiv:1012.0639 [hep-ph].

[31] S. Dawson, A. Djouadi, and M. Spira, "QCD corrections to SUSY Higgs production: The Role of squark loops," *Phys.Rev.Lett.* **77** (1996) 16–19, arXiv:hep-ph/9603423 [hep-ph].

[32] R. V. Harlander and M. Steinhauser, "Hadronic Higgs production and decay in supersymmetry at next-to-leading order," *Phys.Lett.* **B574** (2003) 258–268, arXiv:hep-ph/0307346 [hep-ph].

[33] R. V. Harlander and M. Steinhauser, "Supersymmetric Higgs production in gluon fusion at next-to-leading order," *JHEP* **0409** (2004) 066, arXiv:hep-ph/0409010 [hep-ph].

[34] G. Degrassi and P. Slavich, "On the NLO QCD corrections to Higgs production and decay in the MSSM," *Nucl.Phys.* **B805** (2008) 267–286, arXiv:0806.1495 [hep-ph].

[35] C. Anastasiou, S. Beerli, S. Bucherer, A. Daleo, and Z. Kunszt, "Two-loop amplitudes and master integrals for the production of a Higgs boson via a massive quark and a scalar-quark loop," *JHEP* **0701** (2007) 082, arXiv:hep-ph/0611236 [hep-ph].

[36] U. Aglietti, R. Bonciani, G. Degrassi, and A. Vicini, "Analytic Results for Virtual QCD Corrections to Higgs Production and Decay," *JHEP* **0701** (2007) 021, arXiv:hep-ph/0611266 [hep-ph].

[37] R. Bonciani, G. Degrassi, and A. Vicini, "Scalar particle contribution to Higgs production via gluon fusion at NLO," *JHEP* **0711** (2007) 095, arXiv:0709.4227 [hep-ph].

[38] M. Muhlleitner and M. Spira, "Higgs Boson Production via Gluon Fusion: Squark Loops at NLO QCD," *Nucl.Phys.* **B790** (2008) 1–27, arXiv:hep-ph/0612254 [hep-ph].

[39] M. Kramer, E. Laenen, and M. Spira, "Soft gluon radiation in Higgs boson production at the LHC," *Nucl.Phys.* **B511** (1998) 523–549, arXiv:hep-ph/9611272 [hep-ph].

[40] C. Anastasiou, S. Beerli, and A. Daleo, "The two-loop QCD amplitude $gg \to h, H$ in the Minimal Supersymmetric Standard Model," *Phys. Rev. Lett.* **100** (2008) 241806, arXiv:0803.3065 [hep-ph].

[41] M. Muhlleitner, H. Rzehak, and M. Spira, "SUSY-QCD corrections to MSSM Higgs boson production via gluon fusion," *PoS* **RADCOR2009** (2010) 043, arXiv:1001.3214 [hep-ph].

[42] G. Degrassi and P. Slavich, "NLO QCD bottom corrections to Higgs boson production in the MSSM," *JHEP* **1011** (2010) 044, arXiv:1007.3465 [hep-ph].

[43] R. V. Harlander, F. Hofmann, and H. Mantler, "Supersymmetric Higgs production in gluon fusion," *JHEP* **1102** (2011) 055, arXiv:1012.3361 [hep-ph].

[44] R. P. Kauffman and W. Schaffer, "QCD corrections to production of Higgs pseudoscalars," *Phys.Rev.* **D49** (1994) 551–554, arXiv:hep-ph/9305279 [hep-ph].

[45] M. Spira, A. Djouadi, D. Graudenz, and P. Zerwas, "SUSY Higgs production at proton colliders," *Phys.Lett.* **B318** (1993) 347–353.

[46] K. Chetyrkin, B. A. Kniehl, M. Steinhauser, and W. A. Bardeen, "Effective QCD interactions of CP odd Higgs bosons at three loops," *Nucl.Phys.* **B535** (1998) 3–18, arXiv:hep-ph/9807241 [hep-ph].

[47] R. V. Harlander and W. B. Kilgore, "Production of a pseudoscalar Higgs boson at hadron colliders at next-to-next-to leading order," *JHEP* **0210** (2002) 017, arXiv:hep-ph/0208096 [hep-ph].

[48] C. Anastasiou and K. Melnikov, "Pseudoscalar Higgs boson production at hadron colliders in NNLO QCD," *Phys.Rev.* **D67** (2003) 037501, arXiv:hep-ph/0208115 [hep-ph].

[49] F. Caola and S. Marzani, "Finite fermion mass effects in pseudoscalar Higgs production via gluon-gluon fusion," *Phys.Lett.* **B698** (2011) 275–283, arXiv:1101.3975 [hep-ph].

[50] J. Brod, F. Fugel, and B. A. Kniehl, "Two-Loop Electroweak Corrections to the $A^0\gamma\gamma$ and A^0gg Couplings of the CP-Odd Higgs Boson," *Nucl. Phys.* **B807** (2009) 188–209, arXiv:0807.1008 [hep-ph].

[51] R. V. Harlander and F. Hofmann, "Pseudo-scalar Higgs production at next-to-leading order SUSY-QCD," *JHEP* **0603** (2006) 050, arXiv:hep-ph/0507041 [hep-ph].

[52] M. S. Carena, D. Garcia, U. Nierste, and C. E. Wagner, "Effective Lagrangian for the $\bar{t}bH^+$ interaction in the MSSM and charged Higgs phenomenology," *Nucl.Phys.* **B577** (2000) 88–120, arXiv:hep-ph/9912516 [hep-ph].

[53] J. Guasch, P. Hafliger, and M. Spira, "MSSM Higgs decays to bottom quark pairs revisited," *Phys.Rev.* **D68** (2003) 115001, arXiv:hep-ph/0305101 [hep-ph].

[54] G. Degrassi, S. Di Vita, and P. Slavich, "NLO QCD corrections to pseudoscalar Higgs production in the MSSM," *JHEP* **1108** (2011) 128, arXiv:1107.0914 [hep-ph].

[55] G. 't Hooft and M. J. G. Veltman, "Regularization and Renormalization of Gauge Fields," *Nucl. Phys.* **B44** (1972) 189–213.

[56] S. Larin, "The Renormalization of the axial anomaly in dimensional regularization," *Phys.Lett.* **B303** (1993) 113–118, arXiv:hep-ph/9302240 [hep-ph].

[57] Wolfram Research, Inc., *Mathematica*. Wolfram Research, Inc., Champaign, Illinois, version 8.0 ed., 2010.

[58] T. Hahn, "Generating Feynman diagrams and amplitudes with FeynArts 3," *Comput.Phys.Commun.* **140** (2001) 418–431, arXiv:hep-ph/0012260 [hep-ph].

[59] T. Hahn and C. Schappacher, "The Implementation of the minimal supersymmetric standard model in FeynArts and FormCalc," *Comput.Phys.Commun.* **143** (2002) 54–68, arXiv:hep-ph/0105349 [hep-ph].

[60] B. S. DeWitt, "Quantum Theory of Gravity. 2. The Manifestly Covariant Theory," *Phys.Rev.* **162** (1967) 1195–1239.

[61] J. Honerkamp, "The Question of invariant renormalizability of the massless Yang-Mills theory in a manifest covariant approach," *Nucl.Phys.* **B48** (1972) 269–287.

[62] H. Kluberg-Stern and J. Zuber, "Renormalization of Nonabelian Gauge Theories in a Background Field Gauge. 1. Green Functions," *Phys.Rev.* **D12** (1975) 482–488.

[63] L. F. Abbott, "The Background Field Method Beyond One Loop," *Nucl. Phys.* **B185** (1981) 189.

[64] L. F. Abbott, M. T. Grisaru, and R. K. Schaefer, "The Background Field Method and the S Matrix," *Nucl. Phys.* **B229** (1983) 372.

[65] J. Vermaseren, "New features of FORM," `arXiv:math-ph/0010025 [math-ph]`.

[66] C. Studerus, "Reduze-Feynman Integral Reduction in C++," *Comput.Phys.Commun.* **181** (2010) 1293–1300, `arXiv:0912.2546 [physics.comp-ph]`.

[67] M. Gell-Mann, "A Schematic Model of Baryons and Mesons," *Phys.Lett.* **8** (1964) 214–215.

[68] G. Zweig, "An SU(3) model for strong interaction symmetry and its breaking,".

[69] H. Fritzsch, M. Gell-Mann, and H. Leutwyler, "Advantages of the Color Octet Gluon Picture," *Phys.Lett.* **B47** (1973) 365–368. Introduces the term 'color'.

[70] S. Weinberg, "Nonabelian Gauge Theories of the Strong Interactions," *Phys.Rev.Lett.* **31** (1973) 494–497.

[71] S. Glashow, "Partial Symmetries of Weak Interactions," *Nucl.Phys.* **22** (1961) 579–588.

[72] S. Weinberg, "A Model of Leptons," *Phys.Rev.Lett.* **19** (1967) 1264–1266.

[73] A. Salam, "Weak and electromagnetic interactions, edited by n. svartholm," *Proc. of the 8th Nobel Symposium on "Elementary particle theory, relativistic groups and analyticity" 1968, Stockholm, Sweden* (1969) 367–377.

[74] **LEP Working Group for Higgs boson searches, ALEPH Collaboration, DELPHI Collaboration, L3 Collaboration and OPAL Collaboration**, R. Barate *et al.*, "Search for the standard model Higgs boson at LEP," *Phys.Lett.* **B565** (2003) 61–75, `arXiv:hep-ex/0306033 [hep-ex]`.

[75] **TEVNPH (Tevatron New Phenomena and Higgs Working Group), CDF and D0 Collaboration**, "Combined CDF and D0 Upper Limits on Standard Model Higgs Boson Production with up to 8.6 fb-1 of Data," `arXiv:1107.5518 [hep-ex]`.

[76] **ATLAS Collaboration**, "Update of the Combination of Higgs Boson Searches in 1.0 to 2.3 fb^{-1} of pp Collisions Data Taken at $\sqrt{s} = 7$ TeV with the ATLAS Experiment at the LHC," *ATLAS-CONF-2011-135* (2011) .

[77] **CMS Collaboration**, "Combination of Higgs Searches (Lepton Photon 2011)," *CMS PAS HIG-11-022* (2011) .

[78] J. Erler and P. Langacker, "Implications of high precision experiments and the CDF top quark candidates," *Phys.Rev.* **D52** (1995) 441–450, `arXiv:hep-ph/9411203 [hep-ph]`.

[79] **ALEPH Collaboration, CDF Collaboration, D0 Collaboration, DELPHI Collaboration, L3 Collaboration, OPAL Collaboration, SLD Collaboration, LEP Electroweak Working Group, Tevatron Electroweak Working Group and SLD Electroweak Heavy Flavour Groups**, "Precision Electroweak Measurements and Constraints on the Standard Model," `arXiv:1012.2367 [hep-ex]`.

[80] **Particle Data Group**, J. Erler and P. L. in:, "Review of particle physics," *J.Phys.G* **G37** (2010) 075021.

[81] M. Baak, M. Goebel, J. Haller, A. Hoecker, D. Ludwig, *et al.*, "Updated Status of the Global Electroweak Fit and Constraints on New Physics," `arXiv:1107.0975 [hep-ph]`.

[82] A. Sakharov, "Violation of CP Invariance, c Asymmetry, and Baryon Asymmetry of the Universe," *Pisma Zh.Eksp.Teor.Fiz.* **5** (1967) 32–35. Reprinted in *Kolb, E.W. (ed.), Turner, M.S. (ed.): The early universe* 371-373, and in *Lindley, D. (ed.) et al.: Cosmology and particle physics* 106-109, and in Sov. Phys. Usp. 34 (1991) 392-393 [Usp. Fiz. Nauk 161 (1991) No. 5 61-64].

[83] B. W. Lee, C. Quigg, and H. Thacker, "Weak Interactions at Very High-Energies: The Role of the Higgs Boson Mass," *Phys.Rev.* **D16** (1977) 1519.

[84] M. E. Machacek and M. T. Vaughn, "Two Loop Renormalization Group Equations in a General Quantum Field Theory. 3. Scalar Quartic Couplings," *Nucl.Phys.* **B249** (1985) 70.

[85] H. Arason, D. Castano, B. Keszthelyi, S. Mikaelian, E. Piard, *et al.*, "Renormalization group study of the standard model and its extensions. 1. The Standard model," *Phys.Rev.* **D46** (1992) 3945–3965.

[86] N. Cabibbo, L. Maiani, G. Parisi, and R. Petronzio, "Bounds on the Fermions and Higgs Boson Masses in Grand Unified Theories," *Nucl.Phys.* **B158** (1979) 295–305.

[87] J. Casas, J. Espinosa, and M. Quiros, "Improved Higgs mass stability bound in the standard model and implications for supersymmetry," *Phys.Lett.* **B342** (1995) 171–179, arXiv:hep-ph/9409458 [hep-ph].

[88] T. Hambye and K. Riesselmann, "Matching conditions and Higgs mass upper bounds revisited," *Phys.Rev.* **D55** (1997) 7255–7262, arXiv:hep-ph/9610272 [hep-ph].

[89] K. Tobe and J. D. Wells, "Higgs boson mass limits in perturbative unification theories," *Phys.Rev.* **D66** (2002) 013010, arXiv:hep-ph/0204196 [hep-ph].

[90] M. Sher, "Electroweak Higgs Potentials and Vacuum Stability," *Phys.Rept.* **179** (1989) 273–418.

[91] G. Altarelli and G. Isidori, "Lower limit on the Higgs mass in the standard model: An Update," *Phys.Lett.* **B337** (1994) 141–144.

[92] J. Casas, J. Espinosa, and M. Quiros, "Standard model stability bounds for new physics within LHC reach," *Phys.Lett.* **B382** (1996) 374–382, arXiv:hep-ph/9603227 [hep-ph].

[93] J. Espinosa and M. Quiros, "Improved metastability bounds on the standard model Higgs mass," *Phys.Lett.* **B353** (1995) 257–266, arXiv:hep-ph/9504241 [hep-ph].

[94] G. Isidori, G. Ridolfi, and A. Strumia, "On the metastability of the standard model vacuum," *Nucl.Phys.* **B609** (2001) 387–409, arXiv:hep-ph/0104016 [hep-ph].

[95] R. Barbieri and A. Strumia, "The 'LEP paradox'," arXiv:hep-ph/0007265 [hep-ph].

[96] J. Wess and B. Zumino, "Supergauge Transformations in Four-Dimensions," *Nucl.Phys.* **B70** (1974) 39–50.

[97] J. Wess and B. Zumino, "Supergauge Invariant Extension of Quantum Electrodynamics," *Nucl.Phys.* **B78** (1974) 1.

[98] S. Ferrara and B. Zumino, "Supergauge Invariant Yang-Mills Theories," *Nucl.Phys.* **B79** (1974) 413.

[99] A. Salam and J. Strathdee, "Supergauge Transformations," *Nucl.Phys.* **B76** (1974) 477–482.

[100] A. Salam and J. Strathdee, "Supersymmetry and Nonabelian Gauges," *Phys.Lett.* **B51** (1974) 353–355.

[101] H. Baer and X. Tata, "Weak scale supersymmetry: From superfields to scattering events,".

[102] S. P. Martin, "A Supersymmetry primer," arXiv:hep-ph/9709356 [hep-ph].

[103] S. Dimopoulos and D. W. Sutter, "The Supersymmetric flavor problem," *Nucl.Phys.* **B452** (1995) 496–512, arXiv:hep-ph/9504415 [hep-ph].

[104] B. Allanach, A. Djouadi, J. Kneur, W. Porod, and P. Slavich, "Precise determination of the neutral Higgs boson masses in the MSSM," *JHEP* **0409** (2004) 044, arXiv:hep-ph/0406166 [hep-ph].

[105] R. Harlander, P. Kant, L. Mihaila, and M. Steinhauser, "Higgs boson mass in supersymmetry to three loops," *Phys.Rev.Lett.* **100** (2008) 191602, arXiv:0803.0672 [hep-ph].

[106] P. Kant, R. Harlander, L. Mihaila, and M. Steinhauser, "Light MSSM Higgs boson mass to three-loop accuracy," *JHEP* **1008** (2010) 104, arXiv:1005.5709 [hep-ph].

[107] H. E. Haber and G. L. Kane, "The Search for Supersymmetry: Probing Physics Beyond the Standard Model," *Phys.Rept.* **117** (1985) 75–263.

[108] J. R. Ellis and S. Rudaz, "Search for Supersymmetry in Toponium Decays," *Phys.Lett.* **B128** (1983) 248.

[109] D. Binosi and L. Theussl, "JaxoDraw: A Graphical user interface for drawing Feynman diagrams," *Comput.Phys.Commun.* **161** (2004) 76–86, arXiv:hep-ph/0309015 [hep-ph].

[110] **LHC Higgs Cross Section Working Group**, S. Dittmaier *et al.*, "Handbook of LHC Higgs Cross Sections: 1. Inclusive Observables," arXiv:1101.0593 [hep-ph].

[111] A. Djouadi, "The Anatomy of electro-weak symmetry breaking. I: The Higgs boson in the standard model," *Phys.Rept.* **457** (2008) 1–216, arXiv:hep-ph/0503172 [hep-ph].

[112] A. Djouadi, "The Anatomy of electro-weak symmetry breaking. II. The Higgs bosons in the minimal supersymmetric model," *Phys.Rept.* **459** (2008) 1–241, arXiv:hep-ph/0503173 [hep-ph].

[113] M. Gomez-Bock, M. Mondragon, M. Muhlleitner, M. Spira, and P. Zerwas, "Concepts of Electroweak Symmetry Breaking and Higgs Physics," arXiv:0712.2419 [hep-ph].

[114] R. Ellis, I. Hinchliffe, M. Soldate, and J. van der Bij, "Higgs Decay to $\tau^+\tau^-$: A Possible Signature of Intermediate Mass Higgs Bosons at the SSC," *Nucl.Phys.* **B297** (1988) 221.

[115] U. Baur and E. Glover, "Higgs Boson Production at Large Transverse Momentum in Hadronic Collisions," *Nucl.Phys.* **B339** (1990) 38–66.

[116] B. Field, S. Dawson, and J. Smith, "Scalar and pseudoscalar Higgs boson plus one jet production at the CERN LHC and Tevatron," *Phys.Rev.* **D69** (2004) 074013, arXiv:hep-ph/0311199 [hep-ph].

[117] C. G. Bollini and J. J. Giambiagi, "Dimensional Renormalization: The Number of Dimensions as a Regularizing Parameter," *Nuovo Cim.* **B12** (1972) 20–25.

[118] J. Ashmore, "On renormalization and complex space-time dimensions," *Commun.Math.Phys.* **29** (1973) 177–187.

[119] G. Cicuta and E. Montaldi, "Analytic renormalization via continuous space dimension," *Lett.Nuovo Cim.* **4** (1972) 329–332.

[120] J. C. Collins, "Renormalization. An Introduction To Renormalization, The Renormalization Group, And The Operator Product Expansion,".

[121] F. Jegerlehner, "Facts of life with γ_5," *Eur. Phys. J.* **C18** (2001) 673–679, arXiv:hep-th/0005255.

[122] P. Breitenlohner and D. Maison, "Dimensional Renormalization and the Action Principle," *Commun. Math. Phys.* **52** (1977) 11–38.

[123] S. L. Adler and W. A. Bardeen, "Absence of higher order corrections in the anomalous axial vector divergence equation," *Phys.Rev.* **182** (1969) 1517–1536.

[124] I. Jack and D. Jones, "Regularization of supersymmetric theories," arXiv:hep-ph/9707278 [hep-ph].

[125] W. Siegel, "Supersymmetric Dimensional Regularization via Dimensional Reduction," *Phys. Lett.* **B84** (1979) 193.

[126] D. M. Capper, D. R. T. Jones, and P. van Nieuwenhuizen, "Regularization by Dimensional Reduction of Supersymmetric and Nonsupersymmetric Gauge Theories," *Nucl. Phys.* **B167** (1980) 479.

[127] D. Stockinger, "Regularization by dimensional reduction: consistency, quantum action principle, and supersymmetry," *JHEP* **0503** (2005) 076, arXiv:hep-ph/0503129 [hep-ph].

[128] W. Siegel, "Inconsistency of Supersymmetric Dimensional Regularization," *Phys.Lett.* **B94** (1980) 37.

[129] S. P. Martin and M. T. Vaughn, "Regularization dependence of running couplings in softly broken supersymmetry," *Phys.Lett.* **B318** (1993) 331–337, arXiv:hep-ph/9308222 [hep-ph].

[130] W. Pauli and F. Villars, "On the Invariant regularization in relativistic quantum theory," *Rev.Mod.Phys.* **21** (1949) 434–444.

[131] S. Frolov and A. Slavnov, "An Invariant regularization of the Standard Model," *Phys.Lett.* **B309** (1993) 344–350.

[132] P. C. West, "Higher Derivative Regulation Of Supersymmetric Theories," *Nucl.Phys.* **B268** (1986) 113.

[133] M. K. Gaillard, "Pauli-Villars regularization of supergravity coupled to chiral and Yang-Mills matter," *Phys.Lett.* **B342** (1995) 125–131, `arXiv:hep-th/9408149 [hep-th]`.

[134] M. K. Gaillard, "Pauli-Villars regularization of globally supersymmetric theories," *Phys.Lett.* **B347** (1995) 284–290, `arXiv:hep-th/9412125 [hep-th]`.

[135] M. K. Gaillard, "BRST invariant PV regularization of SUSY Yang-Mills and SUGRA," `arXiv:1109.3221 [hep-th]`.

[136] L. Faddeev and V. Popov, "Feynman Diagrams for the Yang-Mills Field," *Phys.Lett.* **B25** (1967) 29–30.

[137] M. Srednicki, *Quantum field theory*. Cambridge University Press, 2007.

[138] A. Denner, G. Weiglein, and S. Dittmaier, "Application of the background field method to the electroweak standard model," *Nucl.Phys.* **B440** (1995) 95–128, `arXiv:hep-ph/9410338 [hep-ph]`.

[139] G. Degrassi, P. Slavich, and F. Zwirner, "On the neutral Higgs boson masses in the MSSM for arbitrary stop mixing," *Nucl.Phys.* **B611** (2001) 403–422, `arXiv:hep-ph/0105096 [hep-ph]`.

[140] A. Pilaftsis, "Resonant CP violation induced by particle mixing in transition amplitudes," *Nucl.Phys.* **B504** (1997) 61–107, `arXiv:hep-ph/9702393 [hep-ph]`.

[141] J. Guasch, J. Sola, and W. Hollik, "Yukawa coupling corrections to scalar quark decays," *Phys.Lett.* **B437** (1998) 88–99, `arXiv:hep-ph/9802329 [hep-ph]`.

[142] H. Eberl, S. Kraml, and W. Majerotto, "Yukawa coupling corrections to stop, sbottom, and stau production in e^+e^- annihilation," *JHEP* **9905** (1999) 016, `arXiv:hep-ph/9903413 [hep-ph]`.

[143] Y. Yamada, "Gauge dependence of the on-shell renormalized mixing matrices," *Phys.Rev.* **D64** (2001) 036008, `arXiv:hep-ph/0103046 [hep-ph]`.

[144] M. Argeri and P. Mastrolia, "Feynman Diagrams and Differential Equations," *Int.J.Mod.Phys.* **A22** (2007) 4375–4436, `arXiv:0707.4037 [hep-ph]`.

[145] R. Bonciani, "Analytical calculation of two-loop Feynman diagrams," *Acta Phys. Polon.* **B35** (2004) 2587–2600, arXiv:hep-ph/0410210.

[146] U. Aglietti, "The Evaluation of loop amplitudes via differential equations," arXiv:hep-ph/0408014 [hep-ph].

[147] A. I. Davydychev and J. Tausk, "Two loop selfenergy diagrams with different masses and the momentum expansion," *Nucl.Phys.* **B397** (1993) 123–142.

[148] V. A. Smirnov, "Applied asymptotic expansions in momenta and masses," *Springer Tracts Mod.Phys.* **177** (2002) 1–262.

[149] R. Harlander, "Asymptotic expansions: Methods and applications," *Acta Phys.Polon.* **B30** (1999) 3443–3462, arXiv:hep-ph/9910496 [hep-ph].

[150] G. 't Hooft and M. J. G. Veltman, "Scalar One Loop Integrals," *Nucl. Phys.* **B153** (1979) 365–401.

[151] K. Chetyrkin and F. Tkachov, "Integration by Parts: The Algorithm to Calculate beta Functions in 4 Loops," *Nucl.Phys.* **B192** (1981) 159–204.

[152] F. Tkachov, "A Theorem on Analytical Calculability of Four Loop Renormalization Group Functions," *Phys.Lett.* **B100** (1981) 65–68.

[153] S. Laporta, "High precision calculation of multiloop Feynman integrals by difference equations," *Int.J.Mod.Phys.* **A15** (2000) 5087–5159, arXiv:hep-ph/0102033 [hep-ph].

[154] C. Anastasiou and A. Lazopoulos, "Automatic integral reduction for higher order perturbative calculations," *JHEP* **0407** (2004) 046, arXiv:hep-ph/0404258 [hep-ph].

[155] A. Smirnov, "Algorithm FIRE – Feynman Integral REduction," *JHEP* **0810** (2008) 107, arXiv:0807.3243 [hep-ph].

[156] G. Passarino and M. Veltman, "One Loop Corrections for e+ e- Annihilation Into mu+ mu- in the Weinberg Model," *Nucl.Phys.* **B160** (1979) 151.

[157] A. Denner, "Techniques for calculation of electroweak radiative corrections at the one loop level and results for W physics at LEP-200," *Fortsch.Phys.* **41** (1993) 307–420, arXiv:0709.1075 [hep-ph].

[158] O. Tarasov, "An Algorithm for small momentum expansion of Feynman diagrams," arXiv:hep-ph/9505277 [hep-ph].

[159] A. Dedes and P. Slavich, "Two loop corrections to radiative electroweak symmetry breaking in the MSSM," *Nucl.Phys.* **B657** (2003) 333–354, arXiv:hep-ph/0212132 [hep-ph].

[160] L. J. Hall, R. Rattazzi, and U. Sarid, "The Top quark mass in supersymmetric SO(10) unification," *Phys.Rev.* **D50** (1994) 7048–7065, arXiv:hep-ph/9306309 [hep-ph].

[161] **Particle Data Group**, K. Nakamura *et al.*, "Review of particle physics," *J.Phys.G* **G37** (2010) 075021.

[162] **CDF Collaboration and D0 Collaboration**, The Tevatron Electroweak Working Group, "Combination of CDF and D0 Results on the Mass of the Top Quark using up to 5.6 fb^{-1} of data," arXiv:1007.3178 [hep-ex].

[163] J. H. Kuhn, M. Steinhauser, and C. Sturm, "Heavy Quark Masses from Sum Rules in Four-Loop Approximation," *Nucl.Phys.* **B778** (2007) 192–215, arXiv:hep-ph/0702103 [HEP-PH].

[164] K. Chetyrkin, J. Kuhn, A. Maier, P. Maierhofer, P. Marquard, *et al.*, "Charm and Bottom Quark Masses: An Update," *Phys.Rev.* **D80** (2009) 074010, arXiv:0907.2110 [hep-ph].

[165] J. H. Kuhn, "Precise Charm- and Bottom-Quark Masses: Recent Updates," *PoS* **RADCOR2009** (2010) 035, arXiv:1001.5173 [hep-ph].

[166] **ATLAS**, G. Aad *et al.*, "Search for squarks and gluinos using final states with jets and missing transverse momentum with the ATLAS detector in $\sqrt{s} = 7$ TeV proton-proton collisions," arXiv:1109.6572 [hep-ex].

[167] G. Degrassi and A. Sirlin, "Gauge invariant selfenergies and vertex parts of the Standard Model in the pinch technique framework," *Phys.Rev.* **D46** (1992) 3104–3116.